AFRICA CENTER OF EXCELLENCE FOR WATER MANAGEMENT

ADDIS ABABA UNIVERSITY SCHOOL OF GRADUATE STUDIES

COLLEGE OF NATURAL AND COMPUTATIONAL SCIENCES

Simultaneous Removal of Fluoride and Arsenic in Drinking Water by Electrocoagulation Technology using Hybrid Al-Fe Electrodes

By

Magori Jackson Nyangi

A PhD dissertation submitted to Africa Center of Excellence for Water Management, the School of Graduate Studies of Addis Ababa University in partial fulfilment of the requirements for The Degree of Doctor of Philosophy in Water Management (Water Science and Technology)

June, 2021

Addis Ababa, Ethiopia

Africa Center of Excellence for Water Management
Addis Ababa University School of
Graduate Studies

Simultaneous Removal of Fluoride and Arsenic in Drinking Water by Electrocoagulation Technology using Hybrid Al-Fe Electrodes

By

Magori Jackson Nyangi

A PhD dissertation submitted to Africa Center of Excellence for Water Management, the School of Graduate Studies of Addis Ababa University in partial fulfilment of the requirements for The Degree of Doctor of Philosophy in Water Management (Water Science and Technology)

Declaration

I, Magori Jackson Nyangi (GSR 9808/10), hereby declare that this thesis, "*Simultaneous Removal of Fluoride and Arsenic in Drinking Water by Electrocoagulation Technology using Hybrid Al-Fe Electrodes*" has been developed by me and has not been submitted, to this or any other University for any degree and is, except where otherwise stated the original work of the author. The content of the dissertation has not been plagiarized and where works of other researchers have been used, they have been appropriately cited.

Candidate Name	**Signature**	**Date**
……	……	……

AFRICA CENTER OF EXCELLENCE FOR WATER MANAGEMENT

ADDIS ABABA UNIVERSITY

Simultaneous Removal of Fluoride and Arsenic in Drinking Water by Electrocoagulation Technology using Hybrid Al-Fe Electrodes

By:

Magori Jackson Nyangi

A PhD DISSERTATION SUBMITTED

TO

AFRICA CENTER OF EXCELLENCE FOR WATER MANAGEMENT

ADDIS ABABA UNIVERSITY

APPROVED BY BOARD OF EXAMINERS

This is to certify that we have read this PhD research dissertation and that in our opinion; it is fully adequate, in scope and quality, as a PhD dissertation for The Degree of Doctor of Philosophy in Water Management (Water Science and Technology)

Advisor
Name _____Signature_____ Date_____

Co-Advisor
Name _____Signature_____ Date_____

Examiner
Name _____Signature_____ Date_____

Examiner
Name _____Signature_____ Date_____

Chairperson
Name _____Signature_____ Date_____

Dedication

This research work is dedicated to my wife, children, parents, brothers, sister and my supervisors

Acknowledgments

I would like to express my honest thankfulness to my supervisors Dr. Yonas Chebude and Dr. Kessy Fidel Kilulya for their advice and guidance over the course of this research work. They always provided me with positive support and trust during the entire course of programme. It would have been very hard to complete this PhD program without their guidance. I deeply escalate all the advice, encouragement, expertise, inspiration and commitment they accorded to me in the whole period of my research work. They used to be there for me and provided timely feedback on my work whenever I needed it. Particular thanks to Dr. Minu Andrew for his help, especially on report editing during the course of my study.

I wish to acknowledge the Africa Centre of Excellence for Water Management (ACEWM) through the World Bank ACEII project for funding this study. The ACEWM apart from funding my studies, they helped me to build a research network with scientists in different parts of Africa, particularly those who were part of the project. Also, my special and heartfelt thanks go to Dr. Feleke, Director, Africa Center of Excellence for Water Management who provided me with such scholarship opportunity.

I am extremely indebted to all the technical staff of the Department of Chemistry AAU, in particular Adunache for her willing to help and provided great research environment. A special mention is for Dr. Tesfaye for his help, support and inspiring discussions. A number of people have made my stay in Ethiopia an enjoyable experience. My friends in Water Science and Technology PhD students, Muluwork, Getachew, Adane and Admasu, for always making me comfortable and enjoy memorable Ethiopian culture, academic fruitful discussions, laughter and many other. I am also particularly grateful to Netsanet, Samuel and Sablewengel, the ACEWM staff for their remarkable welcoming me in Addis Ababa and support in social and academic needful.

To my parents Nyangi, and Ester, my brothers Chacha, John, Getera, Patrice and Christopher and my sister Neema for their encouragements, motivation, prayers, support and love. To my wife Roda Yohana, she has always stood by me and given support even during the hardest periods, my son Emmanuel and daughter Sharon for their prayers and patience when I was away.

Table of Contents

List of Figures

List of Tables

List of Abbreviations

ANOVA	Analysis of Variance
BBD	Box Behnken Design
BP-P	Bipolar Parallel arrangement
CCD	Central Composite Design
CEI	Co-existing ions
DOP	D-optimal design
EARV	East Africa Rift Valley
EC	Electrocoagulation
FFD	Full Factorial Design
FTIR	Fourier Transform Infrared spectroscopy
ICP-OES	Inductively Coupled Plasma- Optical Emission Spectroscopy
IHP	Inner Helmholtz Layer
ISE	Ion Selective Electrode
MP-P	Monopolar Parallel arrangement
MP-S	Monopolar Series arrangement
NF	Nano-Filtration
OHP	Outer Helmholtz Layer
PAF	Polymeric Anionic Flocculent
RO	Reverse Osmosis
ROS	Reactive Oxygen Species
RSM	Response Surface Methodology
SEM	Scanning Electron Microscopy
UF	Ultra-Filtration

UNESCO	United Nations Educational, Scientific and Cultural Organization
UNICEF	United Nations Children's Fund
WHO	World Health Organization
XRD	X-ray powder diffraction

Abstract

The coexisting fluoride and arsenic in the groundwater sources of drinking water has been threat to the general public health worldwide and in particular to the East African Rift Valley (EARV). The use of

bone char and Nalgonda technique for defluoridation face rejection by the users in the area due to cultural beliefs and foul smell they produce. New, cost-effective method for removal of fluoride and/ or arsenic is therefore required. In this study the electrocoagulation process using hybrid aluminum-iron electrode was optimized and evaluated for the removal of arsenic and fluoride from water. At the optimized operation parameter of 9.90 $mAcm^{-2}$, pH 7.5; the hybrid Al-Fe EC reduced 16 mg/L fluoride and 200 µg/L arsenic to 1.12 mg/L and 9.60 µg/L, respectively in 50 minutes with an operation cost estimated to 0.99 $\$/m^3$. Moreover, the study investigated the effects of co-existing ions in water on the performance of Al-Fe EC and found that Ca^{2+} (0.5-100 mg/L) enhanced F- removal, while SO_4^{2-} (> 80 mg/L) and NO_3^- (> 75 mg/L) suppressed F- removal. On the other hand, NO_3^- (0.5-100 mg/L), SO_4^{2-} (> 50 mg/L), Mg^{2+} (> 50 mg/L), and Ca^{2+} (> 50 mg/L) reduced As^{3+} removal. The combination of Mg^{2+} (< 70 mg/L) and Ca^{2+} appears to increase the fluoride removal, while the combination of other ions had antagonistic effects on the removal of both F^- and As^{3+}. Carbonates showed an insignificant influence on the removal of both pollutants. The effect of co-existing ions on the performance of hybrid Al-Fe EC was found to depend on the type and concentration of individual co-ion. The last objective reports on the adsorption isotherm and kinetic of arsenic and/or fluoride. Adsorption of fluoride and arsenic followed both Freundlich and Langmuir models. The adsorption processes for fluoride and arsenic were spontaneous and physical in nature with monolayer maximum adsorption capacities of 76.36 mg/g and 1.14 mg/g, respectively in single systems. In a binary mixture adsorption capacity of arsenic was 0.40 mg/g while that of fluoride was 75.60 mg/g. Moreover, the kinetic of fluoride and or arsenic removal followed pseudo second order model. The removal of fluoride and arsenic were through ionic exchange and electrostatic attraction, respectively. Meanwhile, a real groundwater (F^- = 22 mg/L) and simulated groundwater (As^{3+} = 0.22 mg/L and F^- = 7.6 mg/L), have also been treated successfully. The optimized Al-Fe EC upon scale up can be used for the remediation of fluoride and/or arsenic from contaminated groundwater in EARV.

CHAPTER ONE

Introduction and Literature Review

1.0 Introduction

Water quality has been a major focus on water analysis because of its significance in maintaining the health of ecosystems and human well-being. However, there are reports on the deterioration of water quality due to pollution from both anthropogenic activities and natural processes (Khatri & Tyagi, 2015). It's estimated that 748 million people do not have access to adequate and safe water and over 2.5 billion people have access to meagre water supply (UNESCO, 2019). Apart from microorganisms' contamination, there are a vast number of chemicals causing great risk to human health. The most notable at the global scale, according to the WHO, are arsenic and fluoride. The two elements have become the major challenge in ensuring access to quality water worldwide (Alarcón-Herrera et al., 2020).

One of the areas affected with elevated levels of chemicals in its groundwater due to natural activities is the East African Rift Valley zone. The Rift valley zone is characterized mostly by sedimentary and young volcanic rocks including flurospar (CaF_2), cryolite (Na_3AlF_6), native arsenic (As), arsenopyrite (FeAsS), arsenolite (As_2O), and scorodite ($FeAsO_4 \cdot 2H_2O$). The natural processes such as hydrolysis of the mineral rocks, water-rock interactions, desorption, dissolution and sedimentation are common in different rift-valley zones (Vithanage & Bhattacharya, 2015). These processes are responsible for the reported elevated level of fluoride (> 1.5 mg/L) in the Rift Valley groundwater. For example, the reported fluoride level in Tanzania of up to 13.6 mg/L (Thole, 2013), in Ethiopia 13 mg/L (Tekle-Haimanot et al., 2006) and the highest level being that in Nakuru Kenya reaching 72 mg/L, all of which occurring in the Rift valley zones (Gevera & Mouri, 2018).

On the other hand, the geochemical and occurrence of fluorine in volcanic rocks is anomaly associated with other potentially toxic chemicals including boron, silicon, lithium and arsenic (Rango et al., 2013). Arsenic is also released into water bodies from other primary rocks through biological catalyzed reduction, desorption and dissolution processes, in both redox conditions, making arsenic dominant oxyanion species in groundwater (Rango et al., 2013). The co-occurrence of fluoride and arsenic worldwide is reported in groundwater in various parts of the world such as China (Khair, Li, et al., 2014), Argentina (Alarcón-Herrera et al., 2013), Mexico (Alarcón-Herrera et al., 2013), India (Kumar et al., 2016) and Pakistan (Rasool et al., 2015)

among other countries. In Africa, the only cases are reported to occur in the main Rift valley area in Ethiopia (Rango et al., 2010) and Tanzania (Makoba & Muzuka, 2019).

The arsenic species are known to be top hazardous chemicals even at low concentration < 10 µg/L. They are associated with cancer, gastrointestinal problems, arsenicosis and non-cancerous diseases in a long-term exposure above a level > 10 µg/L (Limón-Pacheco et al., 2018). The report from UNICEF intimates the absence of proper medical cure for arsenicosis and the only solution to this problem is the prevention of exposure. On the other hand, at above threshold level of 1.5 mg/L, fluoride is known to cause skeletal fluorosis (above 4 mg/L) and crippling fluorosis above 10 mg/L (Mohammadi, Yousefi, Yaseri, Jalilzadeh, & Mahvi, 2017). Moreover, the high fluoride level thyroid function, glucose tolerance, neurological disorder (Mohammadi et al., 2017;Verma et al., 2018), and is associated with lower IQ level (Duan, Jiao, Chen, & Wang, 2018). The individual harmful effects of arsenic and fluoride to human are well documented; however, little is known on their co-exposure. Study by Rao & Tiwari, (2006) on rats showed synergetic effect upon co-exposure even at low concentration (Flora et al., 2009). At higher concentration, co-exposure can damage intelligence in children and their growth (Saeed et al., 2020). Thus, it becomes necessary to remove these toxicants from potable water.

The dental fluorosis, skeletal fluorosis, and bone crippling have been reported to affect 90% of the population living along the Rift Valley region especially in Kenya, Tanzania and Ethiopia because of long term exposure to high levels of fluoride (> 1.5 mg/L) in drinking water sources (Fawell et al., 2006). In Ethiopia, approximately 80% of people living in the Ethiopian Rift Valley are exposed to elevated concentration of fluoride (Kloos et al., 1999). More than 60 % of local population in Tanzania and in Kenya Rift Valley zone are affected by diseases such as mottled teeth and skeletal fluorosis (Gevera & Mouri, 2018). Despite the fact that the health burden of arsenic is not well studied in East African Rift Valley, studies in Bangladesh which is mostly affected show an estimated of 45 million people drinking water with arsenic concentrations > 10 µg/L and almost 24,000 adult deaths are attributed to arsenic exposure each year (Flanagan et al., 2012).

Regardless of the reported high level of arsenic and fluoride in groundwater sources, their remediation from groundwater is still a challenge, especially in developing countries. For many years, they have been removed individually from contaminated waters by chemical coagulation,

ion exchange, adsorption, membrane processes, nanofiltration, and electrochemical technologies (Sandoval et al., 2020). Notwithstanding, the issue of cost, sludge disposal, high chemical demand and materials availability have been a challenge for the applicability of these technologies in rural communities. Operating costs, skilled labor requirements, and concentrated sludge generation are major drawbacks associated with the membrane filtration technologies (Lacasa et al., 2011). Furthermore, adsorption process is pH dependent, it requires pre-treatment step, which is time consuming, and its contamination removal efficiency is reduced up to 30% after each regeneration cycle (Kobya et al., 2011). On the other hand, chemical coagulation method requires a large amount of chemical, large area for treatment and produces a secondary sludge (Kobya et al., 2011), thus making these methods questionable for arsenic and fluoride remediation especially in rural areas.

In spite of the challenges, coagulation-precipitation method is mostly used in rural areas, due to its low cost and availability of materials (Du et al., 2014). In East African Rift Valley (EARV) zone, people mainly use bone char and Nalgonda methods for defluoridation (Osterwalder et al., 2014). A high-quality bone char can reduce up to 23 mg/L of fluoride by 98% (WHO, 2008). Unfortunately, poor production of bone char is associated with odor and offensive taste of treated water and in some cases face rejection by the users due to cultural beliefs. On the other hand, Nalgonda treatment demands high chemical coagulants for effective fluoride removal (Dahi, 2016), trained personnel to operate the treatment plant, especially in ensuring a controlled pH and proper dosage ratio (Yami et al., 2018). These necessitate further research for acceptable and cost-effective technology to be used not only for fluoride but also for arsenic removal mainly in the EARV zone.

The use of chemical coagulants and adsorbents have been successful for individual removal of arsenic (Litter et al., 2019) and fluoride (Zewge, 2016) but facing the challenge of high sludge production and high chemical demands (Shrivastava & Vani, 2009). However, the electrocoagulation (EC) technology can overcome these challenges (Moussa et al., 2017). The electrocoagulation method allows in-situ production of the metal oxyhydroxide coagulant through electro-dissolution of electrodes. The most used sacrificial electrodes are aluminum and iron due to their availability, sharp affinity to hydrolyze in aqueous media, and efficiency (Amrose et al., 2013). The method is easy to operate, cost effective in terms of material

availability and possibility of complete automation of process (Emamjomeh & Sivakumar, 2009). In the EC, fluoride is removed through co-precipitation of fluoro-metal ion complexes by chemical substitution and attachment on the electrodes surface. On the other hand, the arsenic species tend, to adsorb on the metal flocs by charge neutralization for its removal (Flores et al., 2013).

The iron and aluminum electrodes have been proven effective on the removal of arsenic and fluoride in a separate set of reactors (Hashim et al., 2017). Moreover, various studies have reported aluminum electrode to be more effective for fluoride remediation (Takdastan et al., 2014) while iron is more effective for arsenic removal (Sandoval et al., 2021). Meanwhile, the combination of aluminum and iron in a single sacrificial electrode have shown to improve general performance of EC than individual electrode towards removal of individual pollutant (Gomes et al., 2007). Few researchers have reported on the simultaneous removal of fluoride and arsenic in a single EC set up (Chen et al., 2011; Sandoval et al., 2020; Guzmán et al., 2016; Zhao et al., 2011; Thakur & Mondal, 2017). Among them, only study by Chen et al., (2011) has reported on the use of hybrid electrode aluminum-iron EC for simultaneous removal of arsenic and fluoride. However, the electrodes were combined with titanium anode. The method was successful on treating low concentrated water (F^- = 4.5 mg/L, As^{3+} = 1 mg/L) after 40 minutes. But since titanium electrodes are costly (18 $/Kg), this makes their finding unreliable cost-effective method. Moreover, their finding could not be applicable to the groundwater in EARV as the majority of water wells are composed of fluoride > 5 mg/L. Therefore, investigation for optimal conditions for simultaneous removal of arsenic using a combined Fe-Al as the sacrificial electrode can be an attractive work toward access of fluoride and/or arsenic free water in EARV zone.

There is an understandable interest for a new cost-effective method to remove arsenic and fluoride from contaminated water, in terms of cost, efficiency, simplicity, power requirements, availability of materials, know-how and user acceptance. The areas in the Rift Valley zone region of Ethiopia and Tanzania with high geological sources of fluoride, have also high level of arsenic due to co-existence between arsenic and fluoride (Bianchini et al., 2020; Rango et al., 2010). To our knowledge, there was no reported work on the simultaneous removal of arsenic and fluoride using a combined Fe-Al electrocoagulation as the only active electrode. Therefore,

the aim of this research was to investigate for the optimal operational conditions, efficiency and mechanisms on simultaneous removal of fluoride and arsenic by a combined Fe-Al electrocoagulation. The performance of the optimized Al-Fe EC was then tested on the removal of fluoride and/or arsenic from groundwater water samples in the East African Rift valley zone collected in Arusha, Tanzania and Ziway, Ethiopia.

1.1 Statement of the problem

The groundwater sources in East African Rift valley zone such as in Arusha (Tanzania) and Ziway (Ethiopia) is associated with high fluoride level (Thole, 2013), and elevated arsenic (Rango et al., 2010; Alarcón-Herrera et al., 2013). People in these areas use bone-char and Nalgonda methods for defluoridation (Mjengera & Mkongo, 2003). However, bone-char faces rejection from some users because of local beliefs, intense odor of treated water, aesthetic and physiological problems. On the other hand, Nalgonda is associated with large sludge production that results into secondary hazard to the environment. This means that an alternative cost-effective method for remediation of arsenic and/or fluoride to a level recommended for human consumption is undeniable. Therefore, the focus of this study was to investigate for the optimal operational conditions, efficiency and removal mechanism of a combined Al-Fe electrode of electrocoagulation technology for simultaneous remediation of arsenic and/or fluoride from contaminated groundwater in EARV.

1.2 Objectives of the study

1.2.1 General objective

The main objective of this research was to investigate for the optimal operation conditions, efficiency and mechanism of a combined Al-Fe electrocoagulation for arsenic and/or fluoride removal from groundwater.

1.2.2 Specific objectives

i. To investigate the optimal operating current densities for individual Al-EC and Fe-EC through defluoridation efficiencies.
ii. To investigate the optimal conditions and efficiency of hybrid iron-aluminum electrodes in electrocoagulation for simultaneous removal of arsenic and fluoride.
iii. To assess the effect of common ions on the removal of arsenic and/ or fluoride from groundwater by combined Fe-Al electrodes in EC technology

iv. To elucidate the mechanism of the combined aluminum-iron electrodes of electrocoagulation during simultaneous removal of arsenic and fluoride in a batch reactor.

1.2.3 Research questions

1. What is the optimum operation current density and treatment time do the aluminum electrode and iron electrode release enough coagulant for defluoridation?
2. What are the optimal conditions in hybrid Al-Fe electrocoagulation technology effective for simultaneous removal of arsenic and fluoride from the groundwater?
3. Does the presence of common ions in the water affect removal efficiency of Al-Fe hybrid EC on arsenic and/or fluoride?
4. What removal mechanism is associated with fluoride and arsenic during electrolytic production of coagulants by a combined Al-Fe electrocoagulation setup?

1.3 Significance of the study

Arsenic and fluoride are now recognized as the most serious inorganic contaminants in drinking water on a worldwide basis. The World Health Organization has set standard levels of < 10µg/L and < 1.5 mg/L in drinking water for arsenic and fluoride, respectively. The groundwater containing arsenic and fluoride levels above 10 µg/L and 1.5 mg/L, respectively is reported in Ethiopia Rift-valley area, while in Tanzania the high level of fluoride is well known. Local people in these areas are using bone char and Nalgonda methods for fluoride treatment. Both methods are associated with high sludge disposal problem and treatment cost. This study was expected to provide an alternative method to Nalgonda and bone char for defluoridation and an additional advantage of removing arsenic from contaminated water sources in selected water wells in Arusha, Tanzania and Ziway, Ethiopia. The optimized hybrid Al-Fe electrocoagulation method targeted to remediate fluoride and/or arsenic to a level that comply with WHO standards for dinking purpose. Furthermore, in electrocoagulation, coagulant is produced in situ which reduces large production of hazardous sludge, making the method environmentally friendly. The results of this investigation also aimed at supporting Sustainable Development Goal 6 of ensuring access to universal improved water sources in rural areas mainly in Arusha, Tanzania and Ziway, Ethiopia located in East Africa Rift-valley zone.

1.4 Literature review

1.4.0 Co-occurrence of arsenic and fluoride in groundwater

The co-contamination of arsenic (As) and fluoride (F) in shallow and deep aquifers is frequently observed worldwide, and the correlation between these contaminants differs according to the redox conditions. The reasons for elevated co-occurrence of As (> 10 µg/L) and F (> 1.5 mg/L) in groundwater is reported to be both geogenic and anthropogenic. The major population exposure reported worldwide is mainly due to geogenic occurrences (Warren et al., 2005). In most cases, arsenic and fluoride are found to coexist in arid or semi-arid regions groundwater in oxidizing conditions and rarely under reducing conditions. The positive correlation between arsenic (µg/L) and fluoride (mg/L) have been reported in USA (i.e., Washington 18,000 and 8.9, Wisconsin 1500 and 7.6, West Virginia 10 and 4): China (i.e., Songnen Basin 250 and 9.2, 1550 and 10.4, 469 and 22 (Currell et al., 2011), Argentina (i.e., Cordoba province 760 and 8.3, 250 and 12, 535 and 14.2, and 5300 and 10) (Warren et al., 2005; Gomez et al., 2009), Mexico (i.e. Michoacan 24 & 17, Sonora 134 and 3.6, Durango 149 and 17.8, 39 & 4.5) (Hurtado-Jiménez & Gardea-Torresdey, 2006), South Korea (Mankyeong river 100 and 2.7; Geumsan county 113 and 7.54 (Kim et al., 2012), India (i.e Uttar Pradesh 12.8 and 3.8, West Bengal 25.1 and 14 (Kumar et al., 2016) and Pakistan (i.e. Mails 1900 and 21, Tharparkar 2400 and 22.3, Rahim Yar 4100 and 60.5, 683 and 35.6, 507 and 29.6, 107 and 26.4 (Farooqi et al., 2007).

In Africa, there are limited number of researches conducted on the co-occurrence of fluoride and arsenic. However, few studies have indicated the geogenic co-occurrence of arsenic and fluoride such as in the Main Rift Valley area of Ethiopia where 220 µg/L of As and 7.6 mg/L were found in the same groundwater sources (Rango et al., 2010). Another report showed that in semi-arid places of Ghana and Burkina Faso, the groundwaters are composed of As > 100 µg/L and F ~ 3.8 mg/L (Smedley et al., 2003).

1.4.1 Mobilization of arsenic and fluoride into groundwater

Several minerals including oxides and hydroxides of metals (Mn, Al, and Fe), elemental arsenic, sulfides (Arsenopyrite (FeAsS), Orpiment (As_2S_3) and Realgar (As_4S_4), arsenides, and arsenites are known to contain arsenic (Smedley & Edmunds, 2002). However, in the groundwater arsenic exists as oxyanion under different oxidation states, depending on existing pH and redox potential of the surrounding (Jonnalagadda & Nenzou, 1996). Thus, the release of arsenic from minerals bearing arsenic is influenced by the pH and redox potential of the water (Smedley & Edmunds, 2002). It is reported that under both reducing and oxidizing conditions arsenic can be released into water bodies from the rock bearing arsenic. The former is more common in arid to semi-arid

conditions (Alarcón-Herrera et al., 2013). Under reducing conditions (devoid of oxygen), arsenic is mainly released through desorption by reductive hydrolysis of metal hydroxides (reaction 1.0). On the other hand, under oxidizing conditions, arsenic is released in groundwater by the oxidation of As bearing sulfide minerals like arsenopyrite (FeAsS) at higher pH levels (Alarcón-Herrera et al., 2013). Some reports have shown that at neutral conditions of pH and in high dissolved oxygen, the reaction 1.1 to be taking place, releasing As into water (Walker et al., 2006). When the pH of groundwater increases, there is onset of the point of zero charge (PZC) on the surface of the metal hydroxides that lead to desorption of arsenic. The PZC is described as the pH at which the net charge of total particle surface is equal to zero (Birdi, 2015).

(1.0)

(1.1)

Meanwhile, fluoride is reported to be contained in the mineral rocks like fluorite CaF_2, apatite ($Ca_5(PO_4)_3F$ and micas (Brunt et al., 2004). Moreover, other minerals like topaz, biotites, and their analogous host rocks such as syenite, granite, basal, and shales also contain fluoride. Thus, dissolution of these minerals and rock-water interaction are the main pathways for fluoride release into water (Edmunds & Smedley, 1996). In the igneous and metamorphic rocks that also contain fluoride, the hydrolysis of fluoride of these minerals at higher acidic conditions is responsible for the desorption of fluoride from metal oxide leading to the release of fluoride into water (Edmunds & Smedley, 1996).

The co-occurrence of arsenic and fluoride in groundwater have been associated with factors such as desorption and solubility of rock bearing arsenic and fluoride as well as presence of precipitating or complexing agents (Figure 1.0, Levy et al., 1999). Under oxidizing conditions, the co-contamination between arsenic and fluoride is mainly observed in oxy-hydroxide of manganese or iron minerals aquifers (Smedley & Mike Edmunds, 2002). It must be noted that at a pH range (5-8), iron oxy-hydroxides possess more positive surfaces of 8.5 - 9.0, which tend to attract more anions including F^- and $H_2AsO_4^-$ on their surfaces (Appelo & Postma, 2004). As the water p*H* increases (pH > 8), the surface of the metal oxy-hydroxides become more negative leading to desorption of such anions from the surface of Mn/Fe-(hydr) oxides surface (Streat et al., 2008). Therefore, it is reasonable to infer that desorption of both fluoride and arsenic from Mn/Fe-hydroxides, due to the increase in pH is the main reason for the co-contamination of

arsenic and fluoride in the oxidizing aquifers minerals. This is always the case in the absence of other arsenic precipitation causing minerals like sulphide (Farooqi et al., 2007).

The co-contamination of arsenic and fluoride is rarely observed in reducing aquifers. Few literatures available have shown groundwater in the Huhhot Basin (Smedley et al., 2003) Hetao Basin (Guo et al., 2008) and Datong Basin (Guo & Wang, 2005) in China, and in Montana in the US (Nimick, 1998) to be examples for the co-contamination in reducing environments. The co-occurrence is suggested to occur through different mechanisms of the two ions. The reductive dissolution of Mn/Fe-oxy-hydroxides containing arsenic is the major process increasing arsenic concentrations in groundwater (Figure 1.0). While the weathering of fluoride bearing minerals such as fluorapatite ($Ca_5(PO_4)_3F$ and/or fluorite (CaF_2) is the main reason for elevated fluoride in groundwaters (Das et al., 2003) the co-contamination of arsenic and fluoride exist rarely under reducing conditions of higher sulphide minerals, due to co-precipitation of orpiment (As_2S_3) and realgar (As_4S_4) (Levy et al., 1999).

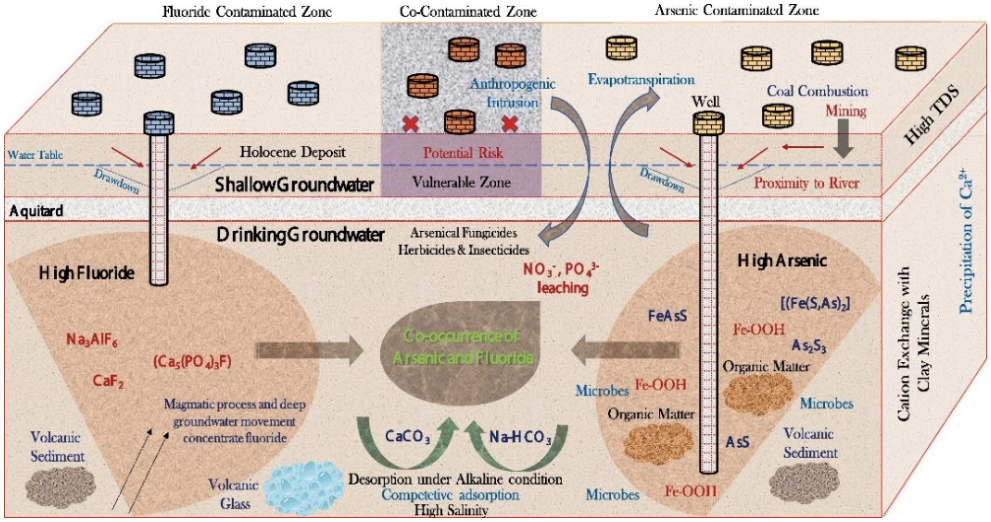

Figure 1.0: Conceptual model depicting the source, process, and conducive environment of arsenic and/or fluoride mobilization into groundwater (Kumar et al., 2020).

1.4.2 The chemistry of arsenic and fluoride species in groundwater

Arsenic is a metalloid that can be found in both inorganic form and organic form. It exists in four different oxidation states, As^{5+} (arsenate), As^{3+} (arsenite), As (arsenic), As^{3-} (arsine), and their methylated derivatives (Mandal & Suzuki, 2002). Organic arsenic forms is either produced by biological activities, mostly in surface waters, or occur where waters are significantly impacted by industrial pollution (Zhang et al., 2007). In natural waters, arsenic is mostly found in

inorganic forms as oxyanions of trivalent or pentavalent arsenate (Smedley & Edmunds, 2002). Among the four forms, As^{5+} is most stable in aerobic condition while As^{3+} is stable in anaerobic condition (Zhao et al., 2010). The speciation of arsenic in groundwater is controlled by sorption processes of metal oxy-hydroxides, the source of arsenic and mainly the redox potential (Eh) and pH of the groundwater (Figure 1.1) (Huq et al., 2020). Under oxidising conditions, $H_2AsO_4^-$ is dominant at low pH < 6.9, whilst at higher pH > 8, $HAsO_4^{2-}$ becomes dominant. The H_3AsO_4 and AsO_4^{3-} may be present in extremely acidic (pH < 3) and alkaline (pH > 10) conditions, respectively. However, in deficiency of oxygen at pH < 9.2, the uncharged arsenite species H_3AsO_3 dominate (Huq et al., 2020).

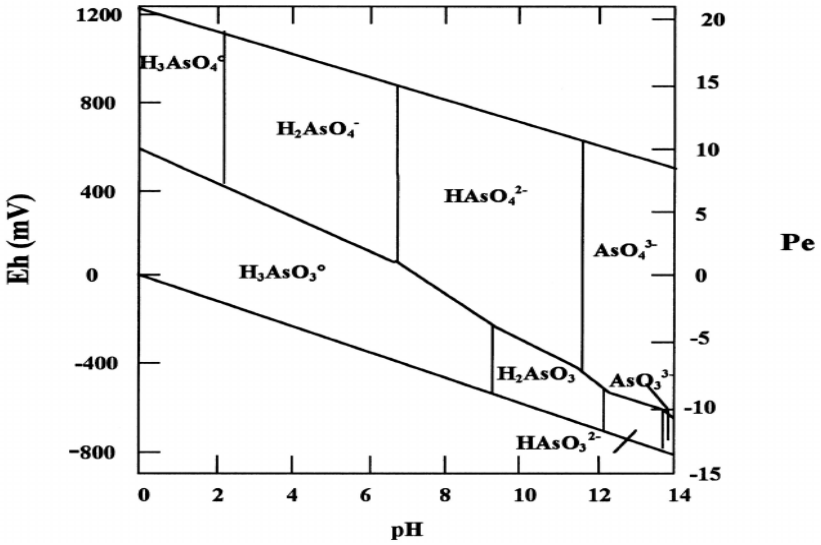

Figure 1.1: Redox potential (Eh)–pH diagram for aqueous arsenic species in the system at 25°C and 1 bar total pressure (Smedley & Edmunds, 2002)

On the other hand, fluoride forms soluble complexes with metal ions in water including magnesium, calcium, aluminum and iron making it different from other halides in water (Nordstrom & Jenne, 1977). These soluble fluoride salts react slowly with water to form hydrofluoric acid which behaves in a slightly different way compared to other hydrogen halide acids owing to the higher reactivity of fluoride ion. However, in groundwater, due to the lower percentage of other cations fluoride ions tend to form aqua complexes. In aprotic solvents, fluorides are fairly unsolvated and named as "naked" fluorides and easily react with Lewis's acid to form strong bond. Due to this low binding affinity of fluoride with other ions in water, these ions exist as free fluoride ions in groundwater and very few exist as major cation complexes (Edmunds & Smedley, 2013).

1.4.3 Toxicity and health implications of arsenic and fluoride

Once ingested in the human body arsenic get absorbed by the gastrointestinal track at a rate of 40-60 %. Thus, the detoxification process here involves oxidation of As^{3+} to As^{5+} followed by methylation process. The methyl arsenate is not reactive with the body cell and easily eliminated from the body through urination (Chatterjee et al., 1995). However, long exposure to above threshold level (As > 10 µg/L) detoxification become ineffective and can lead to various adverse effect. Regardless of the form ingested, both As^{5+} and As^{3+} can cause similar effects, this is because once entered in a body system, As^{5+} can also be reduced to As^{3+}. Moreover, the two forms have different mode of action. As^{5+} reduces phosphates during a normal cell reaction, while As^{3+} reacts with thiol (SH^-) group of various enzymes and deactivating them. The actual toxicity of arsenic depends on the frequency and severity of chronic arsenic intoxication leading to skin cancer and other arsenicosis diseases (Figure 1.2a). The burden is reported in various countries like Thailand and Bangladesh where groundwater is highly contaminated with arsenic many cases of skin cancer have been reported (Karim, 2000). Other common health consequences linked to As exposure include the development of children, skin disorders, hypertension, gangrene, intestinal cancers, tangential vascular disease, ischemic heart disorder, cardiovascular disease, restrictive pulmonary infection, problems with respiration, hypertension, as well as diabetes mellitus (Agusa et al., 2014).

On the other hand, fluoride in water normally exists as fluoride (F^-). It's the most electronegative element and has highest affinity to positively charged ions like Ca^{2+}. Meanwhile, the human tissues such as bones and teeth are made up of hydroxyapatite ($Ca_{10}(PO_4)_6(OH)_2$), its approximated that the adult human body contains around 1 kg calcium on average, 99 % of it being located in bones and teeth (Quelch et al., 1983). Calcium plays a key role in preventing bone loss and osteoporotic fractures in later life. Likewise, fluoride is very important to prevent dental caries/tooth decay when consumed in a low concentration in a range of 0.5 – 1.0 mg/L (Srivastava & Flora, 2020). However, when fluoride is present in excess (F^- > 1.5 mg/L), the consumed F^- tend to incorporate into hydroxyapatite during its formation by substituting the hydroxyl as shown in Equation 1.2 (Fawell et al., 2006). The formation of cause the imbalance in the bone mineral metabolism leading to a condition known as fluorosis (Figure 1.2b) (Srivastava & Flora, 2020). This condition takes place especially during the first eight years of

life since at this time is when permanent tissues are being formed. Depending on the amount of fluoride consumed it can lead to dental or skeletal fluorosis (Figure 1.2b).

(1.2)

It is reported that long-term exposure to individual arsenic and fluoride, mainly through drinking water, can lead to several human health complications including arsenicosis and fluorosis. However, several studies conducted *in-vitro* show that combination of arsenic and fluoride may lead to some health complications (Indu et al., 2007; Flora et al., 2009; Rao & Tiwari, 2006; Nair et al., 2004; Yao & Wang, 1988; Jhala et al, 2008). For example, Rao & Tiwari (2006) found the destruction to enzymatic activities, chromosomal breakages, and inhibition to DNA replication to be potentiated when the two co-exist than the individual effect. Similarly, Jhala, Chinoy, & Rao (2008) reported that the combination of arsenic and fluoride could destruct production of free radicals, scavengers and antioxidants of the body which is not the case when they are administered individually. Another *in-vitro* study conducted on mice found the damage on the brain neurones caused by excessive generation of reactive oxygen species (ROS) that lead to a decreased levels of brain activities when the two administered together (Flora et al., 2009). On the other hand, the combined exposure to arsenic and fluoride was found to exhibit some antagonistic effects in mouse blood, liver and kidney (Mittal & Flora, 2006). Therefore, the effect of co-exposure to arsenic and fluoride may lead to both antagonism and potentiation of some health complications.

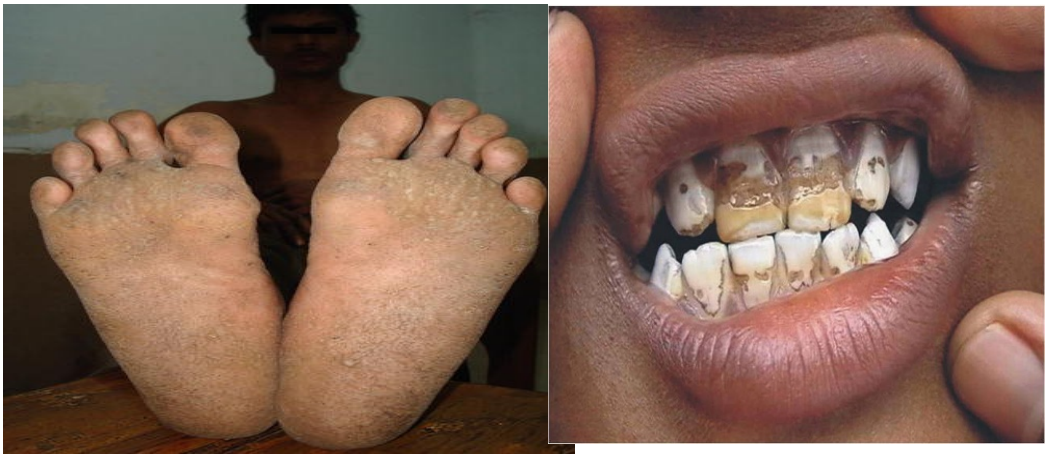

Figure 1.2: Severe variety of (a) arsenical keratosis (Sengupta et al., 2008), (b) dental fluorosis of a young boy

1.5 Fluoride and arsenic remediation technologies from water

Arsenic and fluoride have been removed from drinking water using various separation technologies. The technologies that allow the simultaneous removal of fluoride and arsenic are essentially similar to the individual removal using adsorption. However, each of them presents several benefits and shortcomings. The research review reveals that the conventional precipitation-coagulation, adsorption, ion exchange, membrane processes to be the most highly researched and applied methods in the removal of fluoride and arsenic (Alka et al., 2021; Hering et al., 2017).

1.5.1 Chemical precipitation or coagulation

Chemical precipitation or coagulation followed by filtration method using chemicals such as alum, magnesium and iron salts have demonstrated to be effective to remove arsenic and fluoride as a single and or in combination (Davis & Edwards, 2014). The reagents convert dissolved fluoride and arsenic to solid phase which can then be allowed to settle or easily filtered out. The removal capacity of coagulant is largely dependent on the adsorption site density making the salts of iron effective on arsenic removal and alumina salts effective in fluoride removal (Fan et al., 2003). For the simultaneous removal (Piñón-Miramontes et al., 2003) reported 99% and 77% removal of initial As (0.134 mg/L) and F (5.9 mg/L), respectively in groundwater, when they used cake and polymeric anionic flocculent (PAF) with an estimated cost of $38 cents/$m^3$. Similar results is reported when aluminum sulphate, and cationic polyelectrolyte were used as coagulant, however, this study required 12 hours run time to effectively treat F^- (3.2 mg/L) and As^{3+} (90 µg/L) (Ingallinella et al., 2011). Another study reported effective removal of both arsenic (190 µg/L) and fluoride (6 mg/L) using aluminum sulphate to a recommended level by WHO (Camacho et al., 2011). Moreover, the arsenic and fluoride at initial concentration of 150-200 µg/L and 1.8-2 mg/L was successfully lowered using aluminum polychloride (100 mg/L) to 20 µg/L and 1.5 mg/L with operating costs of 3.36 USD/m^3 (Litter et al., 2019).

1.5.2 Membrane technologies

The membrane technology utilizes reverse technology for separation of components from water. Reverse osmosis uses pressure to force concentrated water through a semipermeable membrane leaving behind solute on one side based on particle size to achieve separation (Qasim et al., 2019). The membranes have well-proven their potential use in the simultaneous removal of arsenic and fluoride (Jadhav et al., 2015). For example, ultra-filtration followed by nanofiltration

and reverse osmosis as a pilot study using synthetic water F^- (10 mg/L) and As^{3+} (6 mg/L) in Australia was reported to remove 88% and 78%, regardless of the water pH. The same study, but this time using real groundwater having initial concentration of F^- (1.1 mg/L) and As (5 µg/L) in UF-NF/RO membrane system found a rejection level of 98.5% and 79.0%, respectively (Richards et al., 2009) in the presence of other ions such as sulphate and nitrate. Starting with initial concentrations at a range of arsenic (100-200 µg/L) and F^- (10-20 mg/L) the membrane managed to lower simultaneously arsenic and fluoride to a lower level recommended by WHO (Jadhav et al., 2016). Similarly, rejection of 93% arsenic and 89% fluoride were found in a NF operating pilot plant using synthetic water having initial arsenic concentration of 180 µg/L and fluoride 5 mg/L. Another study has reported to remove more > 95% of the both F^- and As^{3+} at a wider range of initial pH (3-11) (Katsoyiannis & Zouboulis, 2006). However, the technology suffers some major setback, almost 35-60% water that was to be treated is lost during treatment (Alarcón-Herrera et al., 2013). The presence of other ions and organic matters in water also appear to reduce the removal performance by blocking the membrane pores (Shon et al., 2009). Furthermore, the method is the most expensive and requires power supply and become impractical especially for rural communities (Ingallinella et al., 2011). One study has reported that it can cost 0.52 $/m^3$ to produce water that save 20,000 inhabitant using RO system (Abejón et al., 2015).

1.5.3 Adsorption

This technology relies on the attachment of the species on the surface of solid material to achieve separation. It's most popular due to simplicity, better efficiency and suitability in small scale treatment. Few researches have been carried out using various adsorbents for simultaneous removal of arsenic and fluoride. The range of adsorbent has been prepared and tested such as activated carbon or metals impregnated activated carbon has achieved limited success (Jing et al., 2012), activated alumina (Li et al., 2011), ferric hydroxides (Streat et al., 2008), iron-aluminum doped (Kumar et al., 2011), volcanic ash (Chen et al., 2011), modified cellulose (Tian et al., 2011) and many others. Doped material appeared to be the most effective, for example one study achieved 99% of (100 µg/L) of arsenic and adsorption of 450 mg/g of fluoride at pH 7 using a 1 g of calcium-doped alumina (Li et al., 2011). Similarly doped activated micro and nano sized Al-Fe, exhibited significant removal of fluoride and arsenic reaching adsorption capacity of 100 mg/g and 40 mg/g, respectively (Kumar et al., 2011).

Adsorption and coagulation appear to be cost-effective, simple to use and material are cheaply available. However, the removal process consumes almost 50% of the counter ions producing high volume of sludge that become the major constraint for their disposal. Meanwhile, there is a loss of nearly 50% of the treated water and very costly in membrane treatment. Most of these methods are more efficient for removal of fluoride and arsenate rather than arsenite, affecting total arsenic removal. This is because arsenite is uncharged at near neutral water pH, making it less available for precipitation, adsorption, membrane or ion exchange. Therefore, for total removal of arsenic, most of these technologies are coupled to oxidation process using oxidants such as Cl_2, NaOCl, or H_2O_2 to convert all arsenite to arsenate. Following the above notable shortfalls of the widely and recognisable treatment methods, there is a need of researching for the inexpensive but effective method for removal of both arsenic and fluoride from contaminated water. One of the effective methods that has recently received considerable attention for remediating organic and inorganic pollutants from water is electrocoagulation with negligible or almost no generation of by-product wastes.

1.6. Electrocoagulation method in arsenic and fluoride removal

1.6.1 The basic principle of electrocoagulation technology

The electrocoagulation is a method that involves electricity for in-situ generation of coagulant that destabilizes chemical pollutants in water (Figure 1.3). The common electrodes include aluminum, titanium, zinc, copper, and iron, aluminum and iron electrodes being superior than other due to their efficiency and easy availability (Moussa et al., 2017). In the EC process, the metal ion dissociates from the anode (Equation 1.4 and 1.6) while the water reaction occurring at the surface of cathode dissociate into H^+ ions and OH^- (Equation 1.3). The hydroxide and metal ions react to form metal hydroxide that act as a coagulant (Equation 1.5 and 1.7) (Behbahani et al., 2011a). In addition to these hydroxide species, Fe^{2+} and Al^{3+} ions also form monomeric, hydroxo complexes with hydroxide ions and polymeric species, depending on the pH range (Bazrafshan et al., 2015). The coagulant then provides surface sites for charge neutralization, adsorption, coagulation or co-precipitation in removing pollutants by forming floc (Kobya et al, 2016). The amount of the metal dissolved by anodic dissolution can be calculated using Faraday's (Equation 1.8). This amount of coagulant produced is the one that will determine the amount of pollutant to be removed, which is a function of the electrolysis time t (sec) and of the electric current I (A):

- Reaction at the cathode

(1.3)

- Reactions at the anode

Aluminum electrode

(1.4)

(1.5)

Iron electrode

(1.6)

(1.7)

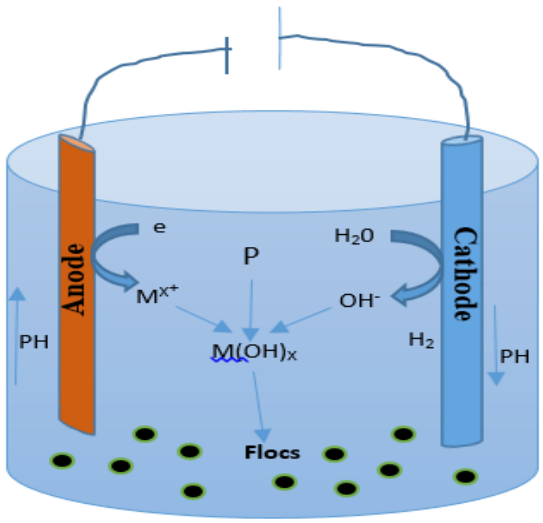

Figure 1.3: The basic principle involved in EC process

1.6.2 Coagulation theory

The pollutant removal by coagulation consists of destabilising the particle surface charge, suspending them by coagulant before they can stick together to form flocs. The interaction between the coagulant and the pollutant in the solution is described by coagulation theory. This is achieved by reducing the energy barrier between the pollutant and the coagulant. In most cases

the pollutants in the water are characterized by surface charges acquired by the preferential adsorption of ions from solution or their parent group dissociation. For the pollutant to be stabilized their charges must be neutralized by another counter charge from the coagulant. This leads to the formation of electrical double layer during the neutralization process. Normally the coagulant surface acquires two layers during the process of coagulation. The first layer is of ion adsorbed to the interface (called stern layer) which also have sub-layers, inner (IHP) and outer Helmholtz (OHP) regions, and the second is a diffuse layer (Figure 1.4). The inner layer (IHP) has static net electric potential (zeta potential) that tend to decrease with distance from the interface towards the diffuse layer. Thus, because of the higher electric potential of the inner layer, the stability of suspension depends on the potential between inner-sphere and the bulk solution (Svarovsky, 2000). However, when the concentration of the counter ion is increased there is decrease in the zeta-potential of the surface layer and double electric layer between the two is compressed and particles stick together.

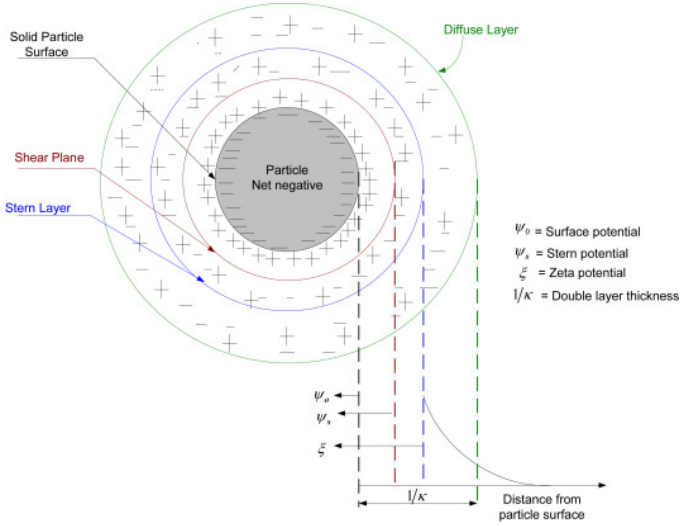

Figure 1.4: Electric double layer formation during coagulation process (Moussa et al.,2017)

1.6.3 Operational factors affecting electrocoagulation performance

1.6.3.1 Effect of initial pH on fluoride and arsenic removal

The key factor that controls the arsenic and fluoride removal by EC method involving aluminum and iron electrode is the solution initial pH. During dissolution of iron and aluminum electrodes, the ionic species of ferric and aluminum (Fe^{3+}, $Fe(OH)^{2+}$, $Fe(OH)_2^+$ $Fe(OH)_3$ and (Al^{3+}, $Al(OH)^{2+}$, $Al(OH)_2^+$ $Al(OH)_3$ and $Al(OH)_4^-$), are formed respectively depending on the water pH and redox

(Figure 1.4) (Khairul et al., 2016). The minimum pH range for the precipitation of the most important flocs (Kobya et al., 2006), ferric hydroxide and aluminum hydroxides are 4.5-10 and 4-7, respectively while at pH > 8, there is formation of unfavourable ions $Fe(OH)_4^-$ & $Al(OH)_4^-$ (Kobya et al., 2011). Likewise, in aqueous solution arsenite As(III) species are present in the form of H_3AsO_3, $H_2AsO_3^-$, $HAsO_3^{2-}$, while fluoride is present in HF and F^- form as the pH increases. At pH > 8, the negative $HAsO_3^{2-}$ and F^- species dominate. Therefore, there is an increase in repulsion forces between the species and the dominant flocs $Fe(OH)_4^-$ and $Al(OH)_4^-$ at pH > 9 (Figure 1.5). This will tend to lower arsenic and fluoride removal from the solution, suggesting that the optimal pH range for arsenic and fluoride removal is 4-9 (Thakur & Mondal, 2017).

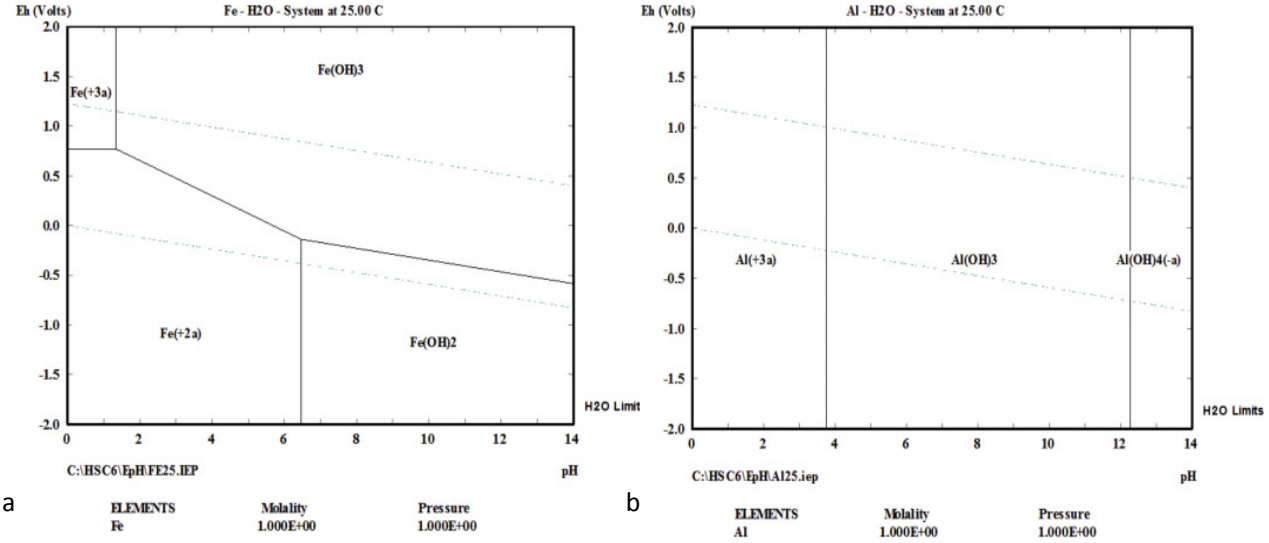

Figure 1.5: The Eh-PH diagram of (a) iron electrode (b) aluminum electrode (Moussa et al.,2017)

1.6.3.2 Effect of current density

Current density plays an important role for the removal of arsenic and fluoride during electrocoagulation process, as it determines the rate of coagulant dosage, bubble production, size and growth of flocs (Kobya et al., 2016).The bubble production control hydrodynamic of the system and mass transfer of the particles that in turn dictate collision rate between coagulant and pollutant and efficiency of the EC in general (Holt, et al., 2002). The current density is a measure of the amount of current passed through unit total cross section area of electrode (Harif & Adin, 2007). Here dissolution of a metal ion is proportional to the quantity of the electricity passed in solution, and the molecular weight of the ion dissoluted as theoretically predicted by Faradays

Law Equation 1.8. For Al^{3+} and Fe^{2+}, the electrochemical equivalent mass 335.6 mg/(Ah) and 1041 mg/(Ah). The values of the current density may widely vary according to the other water and operation features and the amount of pollutants to be removed from water, for instance from 0.001 $mAcm^{-2}$ (Gosh et al., 2008) to 88 $mAcm^{-2}$ (Mansoorian et al., 2014). However, at higher current the ohmic potential between the electrodes drops, leading to more secondary reactions and over dissolution of metal anode that lower anode lifetime. Furthermore, it would increase the cost of treatment process. Thus, to operate EC system utilizing Al or Fe for a long period, the current density is suggested to be between 2 and 3 $mA \cdot cm^{-2}$ (Moussa et al., 2017). However, it must be noted that the selection of an optimum value for current density is also affected by other parameters such as pH, temperature and water conductivity (Khandegar & Saroha, 2013).

Where; I is the current (A), t is the time of operation (s), M_w is the molecular weight (g/mol), F is Faraday's constant (96,485 C/mol), N_T is the number of electrons involved in the reaction and *m* is the mass of anode dissolved (g).

1.6.3.3 Distance between electrodes

As the distance between electrodes increases the collision between the particles tend to decrease as well. This means that at a lower electrode distance the hydrodynamic of generated ions and gas bubbles is higher leading to a high mass transfer and shorter distance for particles collision. It lead to a higher reaction rate between pollutant and coagulant which also tend to decrease energy consumption (Canizares et al., 2009). Furthermore, as the distance between electrodes increases the IR drop also tend to increase affecting efficiency of EC. In addition, inter-electrode gap defines the residence time between the anode and the cathode for a continuous system and the time of treatment for a batch reactor for reaching a desirable EC efficiency. Thus, the suggested range for the inter-distance between electrodes is 0.5-3 cm in a simple EC system. At higher distance than 3 cm the mass transfer between pollutant and coagulant will be low this in turn will reduce hydrodynamic of the reaction. On the other hand at a too short inter-distance (< 0.5 cm), the hydrodynamic of particles becomes too high and may cause short circuit resulting into EC failure (Mameri et al., 1998).

1.6.3.4 Supporting electrolyte

The electrolyte mainly affects EC by determining the free flow of charges within the solution. The increase in electrolytic conductivity of the solution tend to decrease resistance to mass flow of particles. An increase of conductivity on the other hand, reduces the treatment time required and energy consumption as well. Electrolytes of phosphate, sulphates, carbonates, and chloride have been tested in various experiments but chloride have merged superior. The existence of the carbonate or sulphate ions would lead to the precipitation of Ca^{2+} or Mg^{2+} ions that forms an insulating layer on the surface of the electrodes. But chloride anions apart from increasing the conductivity it also takes part in the reduction of the adverse effects in the system by reducing formation of insulating layer on the surface of the electrodes (Chen, 2004). In order to ensure a normal operation of EC in water treatment, it is recommended that 20% of the anions present should be chloride (Chen, 2004). However, conductivity increase during drinking water treatment by EC is highly limited in accordance with the standard norms that define the maximum chloride concentration in industrial effluents at 250 mg/L (WHO 1993).

1.6.3.5 The type of electrode

The type of electrode mainly iron and aluminum have different influence on the removal of arsenic and fluoride. In an EC the Al electrode undergoes electrolysis to form trivalent aluminum ions, and other complex compounds depending on the pH of the solution. When initial pH is acidic or basic there is a raise or fall of the pH to neutralize the changes occurred. This is attributed to the fact that the vicinity of anode becomes acidic during dissolution while the surface of cathode become basic due to water hydrolysis, this tends to neutralize the pH of the solution in the reactor. At pH < 3.5, Al^{3+} is the major specie present which is soluble and cannot permit pollutants removal, for pH values in a range 4 – 9, $Al(OH)_3$ predominates and when the pH > 10, $Al(OH)_4^-$ dominates that also results to a higher repulsive force with the pollutants (Linares-Hernández et al., 2009). Thus, the higher removal of arsenic and fluoride by aluminum electrode are reportedly to be higher at a pH range of 6-8 (Moussa et al., 2017).

On the other hand, iron can dissolve as Fe^{2+} or Fe^{3+} which can then form several precipitates into iron complex depending on the pH. However, there is contradiction on the dissolution nature of iron, because of lack of experimental evidence on which species is exactly produced. Several authors reported the formation of Fe^{2+} as a result of electrolysis followed by hydrolysis to produce $Fe(OH)_2$ (Parga et al., 2005; Cañizares et al., 2007). Other have reported the oxidation of

Fe^{2+} to Fe^{3+} during EC (Linares-Hernández et al., 2009; Lakshmanan et al., 2010) and few have shown direct production of Fe^{3+} and forming $Fe(OH)_3$ or FeOOH (Mollah et al., 2004).

Therefore, selection of the proper electrode material is critical since it will determine the nature of reaction that takes place and removal efficiency of metal ions. For example the arsenate As(V) has adsorption capacity which is 3-20 times than arsenite As(III) (Lakshmanan et al., 2010) which means that pre-oxidation of As (III) and subsequent adsorption of As(V) are the best way to remove As(III) by electrocoagulation (Lakshmanan et al., 2010). The rate of arsenite oxidation can be activated by the Fe(IV) intermediates formed during oxidation of Fe(II) at pH above 7.5 making iron a better electrode choice for arsenic removal (Lacasa et al., 2011). On the other hand, Al has better affinity to fluoride than Fe which is attributed to the more positive charge on its surface. Hence fluoride can be removed better by Al-electrode (Vepsäläinen & Sillanpää, 2020). Moreover, this is believed to be due to the reaction between aluminum hydroxide generated and fluoride that yield aluminum fluoride hydroxide complexes [AlF(OH)]. This complex compound stabilizes fluoride rapidly.

Meanwhile, combination involving iron electrode such as Al-Fe and Fe-Fe is reported to be more effective than those of Al-Al in arsenic remediation (Gomez et al., 2009). One research has found 99.5% arsenic removal by Al-Fe electrodes, higher than in a single electrode system. Similar results were also reported by other researchers for Fe-Fe combination (Ucar et al., 2013). This was attributed to the co-precipitation between iron and arsenic (Ratna K. et al., 2006). Moreover, arsenic removal of only 85% (Can et al., 2014) and 95.7% (Kobya et al., 2014) was found for Al-Al indicating low efficiency of aluminum in arsenic removal. Generally, the higher adsorption capacity and ability to oxidize arsenate favour iron electrode in arsenic removal than aluminum electrode (Lacasa et al., 2011).

1.6.3.6 The effects of co-existing ions on electrocoagulation performance

The presence of naturally occurring ions in groundwater such as calcium, magnesium phosphate, carbonate sulphate and nitrates are reportedly to affect the performance of EC. They affect EC removal efficiency by either interfering with the current density, competing with pollutant for adsorbent or on electrodynamics of pollutant in the reactor (Lacasa et al., 2011). One study has reported 100 % current efficiency during fluoride removal by Al-EC in the absence of co ions. However, efficiency declined to 80-90% and 20-60% in the presence of (Cl^- + NO_3^-) and (F^- +

SO_4^{2-}), respectively. This reduction was attributed to the pitting corrosion phenomenon, where ions such as chloride and nitrate tend to adsorb on the oxide film of electrode or react with the metal ion and reduce formation of adsorbent (Hu et al., 2003). Meanwhile, sulphate is reported to slow down removal rate of arsenic (You & Han, 2015) and fluoride (Hu et al., 2003) at concentration ≥ 100 mg/L. However, at < 10 mg/L the removal was higher. The decrease in the removal was due to the inhibition of the dissolution of electrodes caused by a buildup of an inert film on the electrode surface that prevent current from crossing the cell leading to a lower efficiency (Hu et al., 2003). Another study has also reported that the presence of sulphate in the solution does not influence the arsenic removal, because it does not adsorb as strongly on metal oxyhydroxide as arsenic (Song et al., 2014). On the other hand, it has been shown that the presence of fluoride above 5 mg/L can lower the arsenic removal Fe-EC (Lacasa et al., 2011). This is because fluoride tends to replace hydroxide and is preferably adsorbed on the coagulant and thereby reducing adsorption sites for arsenic. Nevertheless, the removal reduction rate of arsenic in the presence of fluoride is insignificant to the overall performance, due to the same reason (Joao F. et al., 2018). Therefore, the affinity of co-ions, concentration level, and ability to form inert layer on electrode are found to be the main reasons for co-ions affecting performance of electrocoagulation.

1.6.3.7 Reactor design

The design of the reactor depends on the arrangement of electrodes in the cell. The electrodes provide coagulant for the pollutant removal. They are in contact with water and therefore the arrangement of electrodes in the reactor is essential for the performance of EC. The electrodes can either be monopolar or bipolar, where they can also be arranged in parallel or series combination. In a series monopolar design, the sacrificial electrodes are positioned in parallel and inter linked without being connected to the outer electrode (Figure 1.6c). Due to the absence of direct connection between electrodes there is high resistance to mass transfer in series connected cells, thus requiring higher potential difference to derive the charge flow. In monopolar parallel connection (Figure 1.6a) the sacrificial electrodes are interconnected to the outer electrodes allowing equal distribution of electric current (Mollah et al., 2004). Meanwhile, the sacrificial electrodes are located between the two parallel electrodes without electrical interconnection between them in a bipolar design (Figure 1.6b) (Nasrullah et al., 2018). The outer two monopolar electrodes are only linked to the electric current without being electrically

connected to the sacrificial electrodes. The study conducted to compare efficiency of the different design MP-P, MP-S and BP-P found the MP-P to be the most cost effective, which is due to the low potential difference required to derive the electric charge (Demirci et al., 2015). However, the bipolar electrodes are found to be negligibly higher efficient than monopolar which is attributed to the higher surface area exhibited by bipolar connection. This results in a more anodic oxidation compared to that of monopolar connection (Mansouri et al., 2011).

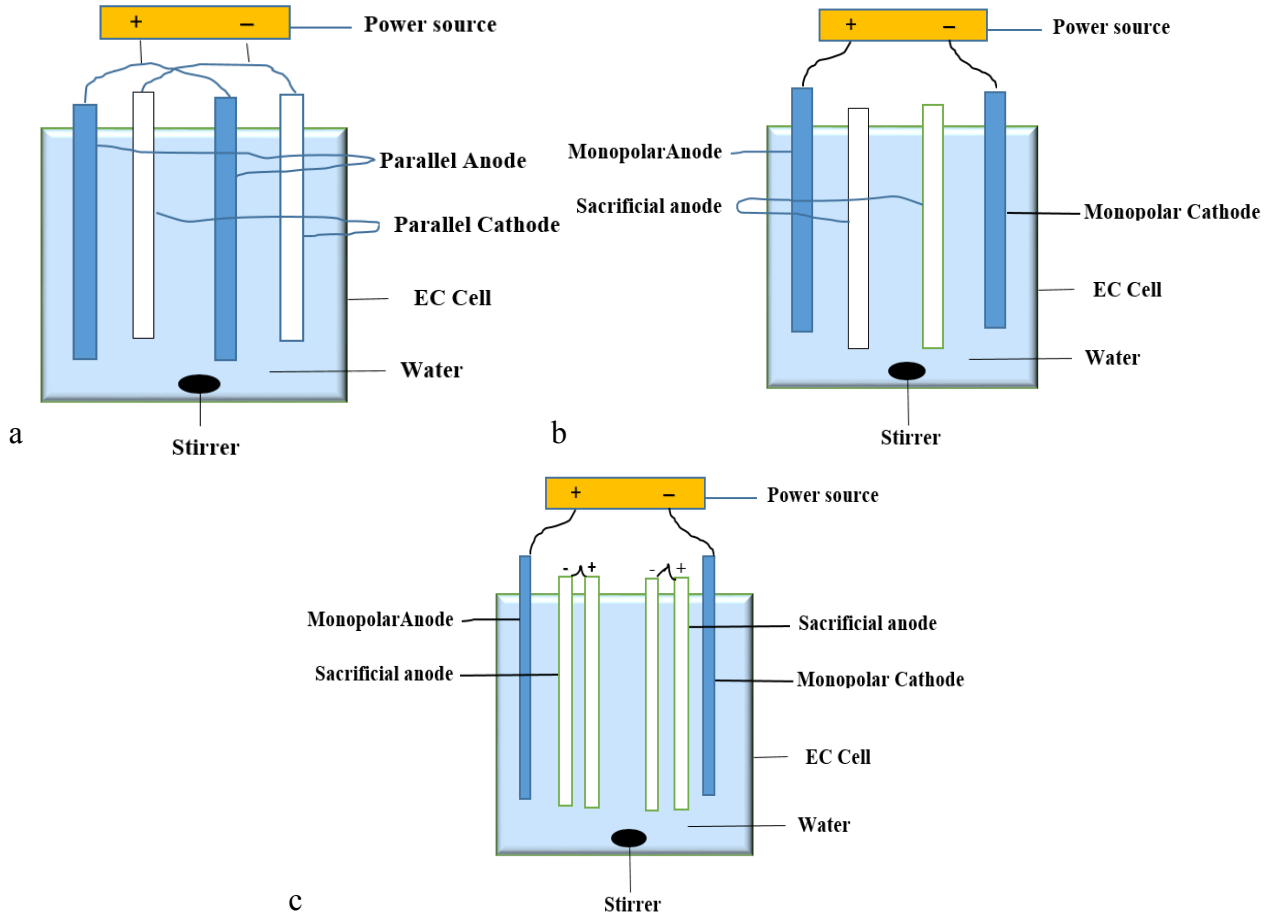

Figure 1.6: Schematic diagram of a bench-scale EC reactor with (a) monopolar electrodes in parallel connection (b) bipolar electrodes in parallel connection (c) monopolar electrodes in series connection

1.7 Process optimization of operational factors in electrocoagulation

The efficiency of EC technology depends on interaction among several independent factors, namely, the current density applied, initial pH, treatment time, conductivity of the sample and initial pollutant concentration (Moussa et al., 2017). Recently, optimization of EC operation factors has been performed by varying a single factor, while keeping other factors fixed at a

specific set of conditions. This process requires many experimental sets that leads in many cases poor optimization due to disregarding of some interaction and even resources wastage (Tir & Moulai-Mostefa, 2008). The poor optimization and reduction of number of runs can be easily solved by response surface methodology, (RSM). RSM is basically a collection of mathematical and statistical methods that is useful for designing the experiments, developing models by considering the interactions of parameters and process optimization (Behbahani, 2011b). RSM is based on fitting the mathematical models (linear, square polynomial functions, quadratic and others) to the experimental results from the designed set of experiments and verification of the model obtained by the statistical inbuilt techniques (Witek-Krowiak et al., 2014).

RSM uses various designs, such as full factorial design (FFD) (Daghrir et al., 2013), central composite design (CCD) (Garg and Prasad, 2016), D-optimal design (DOP) (Tir & Moulai-Mostefa, 2008), and Box-Behnken design (BBD) (Behbahani et al., 2011a). FFD, CCD, DOP and BBD are widely used to estimate the optimum operating conditions and to generate the statistical model represented by a second order polynomial regression model. However, FFD, CCD and DOP face the challenge of higher number of experiments required, thus becoming costly in terms of time and materials (Amani-Ghadim et al., 2013). BBD provides the same information as the above mentioned design methods, but with the advantage of less number of experiments (Box & Behnken, 1960). BBD also doesn't contain combinations for which all factors are simultaneously at their highest or lowest levels, which is important in avoiding experiments performed under extreme conditions that may cause unsatisfactory results. (Nasrullah et al., 2012).

1.8 Thesis overview

This thesis is based on five papers: four published papers and one submitted manuscript, of the specific objectives outlined in 1.2.2. Each of the paper and manuscript reported here comprises of an abstract, introduction, methodology, results, discussion and conclusions. The papers citations are as follows:

1. Nyangi, M. J., Chebude, Y., & Kilulya, K. F. (2020). Fluoride removal efficiencies of Al-EC and Fe-EC reactors: process optimization using Box–Behnken design of the surface response methodology. Applied Water Science, 10(9), 1-11. https://doi.org/10.1007/s13201-020-01297-x

2. Nyangi, M. J., Chebude, Y., Kilulya, K. F., & Salim, C. J. (2021). Comparative Study on Adsorption Isotherm and Kinetics of Defluoridation Using Aluminum and Iron Electrodes in Electrocoagulation. Chemistry Africa, 1-8. https://doi.org/10.1007/s42250-021-00228-w
3. Nyangi, M. J., Chebude, Y., Kilulya, K. F., & Andrew, M. (2020). Simultaneous removal of fluoride and arsenic from water by hybrid Al-Fe electrocoagulation: process optimization through surface response method. Separation Science and Technology, 1-11. 10.1080/01496395.2020.1837877
4. Nyangi, M. J., Chebude, Y., Kilulya, K. F., & Andrew, M. Effects of co-existing ions on simultaneous removal of fluoride and arsenic from water by hybrid Al-Fe electrocoagulation (under review)
5. Nyangi, M. J., Chebude, Y., Kilulya, K. F., & Minu, A. (2021). Removal of fluoride and arsenic from groundwater by hybrid Al–Fe electrocoagulation: Adsorption isotherm and kinetics study of single and binary component systems. Remediation, 1–13. https://doi.org/10.1002/rem.21677

This thesis report consists of six chapters, CHAPTER ONE gives a background and literature survey of the research work. It gives the context of the study and presents the overview about threat from arsenic and fluoride to human health as well as some of the available treatment options with their shortfalls. Furthermore, it elaborates on the importance of the use of combined Al and Fe electrodes in electrocoagulation technology for simultaneous remediation of As and F from groundwater.

CHAPTER TWO presents the individual Al and Fe EC performance on electrocoagulation. It justifies the optimum operation current density and treatment time for individual aluminum and iron electrodes where there is an effective dissolution of ions and production of adequate coagulant for defluoridation. Such parameters are important for optimization of the combined Al-Fe EC.

CHAPTER THREE reports optimum operation parameters and efficiency of the hybrid Al-Fe EC for simultaneous removal of fluoride and arsenic. Furthermore, it describes the effects of each operation parameters and identifies the significant factors affecting performance of the

hybrid Al-Fe EC. This chapter also evaluates the costs associated with simultaneous removal of fluoride and arsenic by hybrid Al-Fe EC at the optimum conditions.

CHAPTER FOUR assesses the effects of co-existing ions such as carbonates, sulphates, nitrates, calcium and magnesium on the performance of the optimized hybrid Al-Fe EC during simultaneous removal of fluoride and arsenic from water. This is important to identify the tolerance levels of the hybrid Al-Fe EC where it can achieve maximum performance in the presence of co-existing ions. The chapter also reports performance of the hybrid Al-Fe EC on the removal of fluoride and/or arsenic from real groundwater.

CHAPTER FIVE evaluates the fluoride and arsenic removal mechanisms by the hybrid Al-Fe EC in single and binary component mixture. It assesses adsorption isotherm models as well as adsorption kinetic models to which the removal of fluoride and arsenic follow during adsorption on the electrogenerated Al-Fe oxyhydroxide.

CHAPTER SIX concludes the study, by summarizing the key findings, and sets forth, the recommendations for policy and further studies.

References

Abejón, A., Garea, A., & Irabien, A. (2015). Arsenic removal from drinking water by reverse osmosis: Minimization of costs and energy consumption. Separation and Purification Technology, 144, 46–53. https://doi.org/10.1016/j.seppur.2015.02.017

Agusa, T., Thi, P., Trang, K., Mai, V., Hong, D., Tanabe, S., … Berg, M. (2014). Science of the Total Environment Human exposure to arsenic from drinking water in Vietnam. Science of the Total Environment, The, 488–489, 562–569. https://doi.org/10.1016/j.scitotenv.2013.10.039

Alarcón-Herrera, María T, Martin-Alarcon, D. A., Gutiérrez, M., Reynoso-Cuevas, L., Martín-Domínguez, A., Olmos-Márquez, M. A., & Bundschuh, J. (2020). Co-occurrence, possible origin, and health-risk assessment of arsenic and fluoride in drinking water sources in Mexico: Geographical data visualization. Science of the Total Environment, 698, 134168.

Alarcón-Herrera, María Teresa, Bundschuh, J., Nath, B., Nicolli, H. B., Gutierrez, M., Reyes-Gomez, V. M., … Sracek, O. (2013). Co-occurrence of arsenic and fluoride in groundwater

of semi-arid regions in Latin America: Genesis, mobility and remediation. Journal of Hazardous Materials, 262, 960–969. https://doi.org/10.1016/j.jhazmat.2012.08.005

Alka, S., Ibrahim, N., Jibrin, M., Vo, D. N., & Abd, F. (2021). Arsenic removal technologies and future trends : A mini review. 278. https://doi.org/10.1016/j.jclepro.2020.123805

Amani-Ghadim, A. R., Aber, S., Olad, A., & Ashassi-Sorkhabi, H. (2013). Optimization of electrocoagulation process for removal of an azo dye using response surface methodology and investigation on the occurrence of destructive side reactions. Chemical Engineering and Processing: Process Intensification. https://doi.org/10.1016/j.cep.2012.10.012

Amrose, S., Gadgil, A., Srinivasan, V., Kowolik, K., Muller, M., Huang, J., & Kostecki, R. (2013). Arsenic removal from groundwater using iron electrocoagulation: effect of charge dosage rate. Journal of Environmental Science and Health, Part A, 48(9), 1019–1030.

Appelo, C. A. J., & Postma, D. (2004). Geochemistry, groundwater and pollution. CRC press.

Bazrafshan, E., Mohammadi, L., Ansari-moghaddam, A., & Mahvi, A. H. (2015). Environmental health heavy metals removal from aqueous environments by electrocoagulation process – a systematic review. Journal of Environmental Health Science and Engineering. https://doi.org/10.1186/s40201-015-0233-8

Behbahani, M., Moghaddam, M. R. A., & Arami, M. (2011a). Techno-economical evaluation of fluoride removal by electrocoagulation process: Optimization through response surface methodology. Desalination, 271(1–3), 209–218. https://doi.org/10.1016/j.desal.2010.12.033

Behbahani, M., Moghaddam, M. R. A., & Arami, M. (2011b). Techno-economical evaluation of fluoride removal by electrocoagulation process: Optimization through response surface methodology. Desalination, 271(1–3), 209–218. https://doi.org/10.1016/j.desal.2010.12.033

Bianchini, G., Brombin, V., Marchina, C., Natali, C., Godebo, T. R., Rasini, A., & Salani, G. M. (2020). Origin of Fluoride and Arsenic in the Main Ethiopian Rift Waters. *Minerals*. 2020; 10(5):453. https://doi.org/10.3390/min10050453

Birdi, K. and S. (2015). Handbook of surface and colloid chemistry. CRC press.

Box, G. E. P., & Behnken, D. W. (1960). Some New Three Level Designs for the Study of

Quantitative Variables. Technometrics. https://doi.org/10.1080/00401706.1960.10489912

Brunt, R., Vasak, L., & Griffioen, J. (2004). Fluoride in groundwater: probability of occurrence of excessive concentration on global scale. Igrac: international groundwater resources assessment Centre. *SP*, *2*, 1-12.

Camacho, L. M., Gutiérrez, M., Alarcón-Herrera, M. T., de Lourdes Villalba, M., & Deng, S. (2011). Occurrence and treatment of arsenic in groundwater and soil in northern Mexico and southwestern USA. Chemosphere, 83(3), 211–225.

Canizares, P., Jiménez, C., Martínez, F., Rodrigo, M. A., & Sáez, C. (2009). The pH as a key parameter in the choice between coagulation and electrocoagulation for the treatment of wastewaters. Journal of Hazardous Materials, 163(1), 158–164.

Cañizares, P., Jiménez, C., Martínez, F., Sáez, C., & Rodrigo, M. A. (2007). Study of the electrocoagulation process using aluminum and iron electrodes. Industrial and Engineering Chemistry Research, 46(19), 6189–6195. https://doi.org/10.1021/ie070059f

Chowdhury, T. (1995). Arsenic in groundwater in six districts of West Bengal, India: the biggest arsenic calamity in the world. Part I. Arsenic species in drinking water and urine of the affected people. *Analyst*, *120*(3), 643-650.

Chen, G. (2004). Electrochemical technologies in wastewater treatment. Separation and Purification Technology, 38(1), 11–41.

Chen, R., Zhang, Z., Yang, Y., Lei, Z., Chen, N., Guo, X., … Sugiura, N. (2011). Use of ferric-impregnated volcanic ash for arsenate (V) adsorption from contaminated water with various mineralization degrees. Journal of Colloid and Interface Science, 353(2), 542–548.

Currell, M., Cartwright, I., Raveggi, M., & Han, D. (2011). Controls on elevated fluoride and arsenic concentrations in groundwater from the Yuncheng Basin, China. Applied Geochemistry, 26(4), 540–552. https://doi.org/10.1016/j.apgeochem.2011.01.012

Daghrir, R., Drogui, P., & Zaviska, F. (2013). Effectiveness of a hybrid process combining electro-coagulation and electro-oxidation for the treatment of domestic wastewaters using response surface methodology. Journal of Environmental Science and Health - Part A Toxic/Hazardous Substances and Environmental Engineering.

https://doi.org/10.1080/10934529.2013.726840

Dahi, E. (2016). Africa's U-Turn in defluoridation policy: From the Nalgonda technique to bone char. Fluoride, 49(4), 401.

Das, B., Talukdar, J., Sarma, S., Gohain, B., Dutta, R. K., Das, H. B., & Das, S. C. (2003). Fluoride and other inorganic constituents in groundwater of Guwahati, Assam, India. Current Science, 657–661.

Davis, C. C., & Edwards, M. (2014). Coagulation with hydrolyzing metal salts: mechanisms and water quality impacts. Critical Reviews in Environmental Science and Technology, 44(4), 303–347.

Demirci, Y., Pekel, L. C., & Alpbaz, M. (2015). Investigation of different electrode connections in electrocoagulation of textile wastewater treatment. International Journal of Electrochemical Science, 10(3), 2685–2693.

Du, J., Jing, C., Duan, J., Zhang, Y., & Hu, S. (2014). Removal of arsenate with hydrous ferric oxide coprecipitation: effect of humic acid. Journal of Environmental Sciences, 26(2), 240–247.

Duan, Q., Jiao, J., Chen, X., & Wang, X. (2018). Association between water fluoride and the level of children's intelligence: a dose–response meta-analysis. Public Health, 154, 87–97.

Edmunds, W M, & Smedley, P. L. (1996). Groundwater geochemistry and health: an overview. Geological Society, London, Special Publications, 113(1), 91–105.

Edmunds, W Mike, & Smedley, P. L. (2013). Fluoride in natural waters. In Essentials of medical geology (pp. 311–336).

Emamjomeh, M. M., & Sivakumar, M. (2009). Fluoride removal by a continuous flow electrocoagulation reactor. Journal of Environmental Management. https://doi.org/10.1016/j.jenvman.2008.06.001

Farooqi, A., Masuda, H., & Firdous, N. (2007). Toxic fluoride and arsenic contaminated groundwater in the Lahore and Kasur districts, Punjab, Pakistan and possible contaminant sources. Environmental Pollution, 145(3), 839–849.

https://doi.org/10.1016/j.envpol.2006.05.007

Fawell, J., Bailey, K., Chilton, J., Dahi, E., & Magara, Y. (2006). Fluoride in drinking-water. IWA publishing.

Flanagan, S. V, Johnston, R. B., & Zheng, Y. (2012). Arsenic in tube well water in Bangladesh: health and economic impacts and implications for arsenic mitigation. Bulletin of the World Health Organization, 90, 839–846.

Flora, S. J. S., Mittal, M., & Mishra, D. (2009). Co-exposure to arsenic and fluoride on oxidative stress, glutathione linked enzymes, biogenic amines and DNA damage in mouse brain. Journal of the Neurological Sciences, 285(1–2), 198–205.

Flores, O. J., Nava, J. L., Carreño, G., Elorza, E., & Martínez, F. (2013). Arsenic removal from groundwater by electrocoagulation in a pre-pilot-scale continuous filter press reactor. Chemical Engineering Science, 97, 1–6. https://doi.org/10.1016/j.ces.2013.04.029

Garg, K. K., & Prasad, B. (2016). Treatment of multicomponent aqueous solution of purified terephthalic acid wastewater by electrocoagulation process: Optimization of process and analysis of sludge. Journal of the Taiwan Institute of Chemical Engineers. https://doi.org/10.1016/j.jtice.2015.10.038

Gevera, P., & Mouri, H. (2018). Natural occurrence of potentially harmful fluoride contamination in groundwater: an example from Nakuru County, the Kenyan Rift Valley. Environmental Earth Sciences, 77(10), 365.

Gomes, J. A. G., Daida, P., Kesmez, M., Weir, M., Moreno, H., Parga, J. R., … Peterson, E. (2007). Arsenic removal by electrocoagulation using combined Al–Fe electrode system and characterization of products. Journal of Hazardous Materials, 139(2), 220–231.

Gomez, M. L., Blarasin, M. T., & Martínez, D. E. (2009). Arsenic and fluoride in a loess aquifer in the central area of Argentina. Environmental Geology, 57(1), 143–155.

Guo, H., & Wang, Y. (2005). Geochemical characteristics of shallow groundwater in Datong basin, northwestern China. J Geochem Explor, 87(3), 109–120. https://doi.org/10.1016/j.gexplo.2005.08.002

Guo, H., Yang, S., Tang, X., Li, Y., & Shen, Z. (2008). Groundwater geochemistry and its implications for arsenic mobilization in shallow aquifers of the Hetao Basin, Inner Mongolia. Science of the Total Environment, 393(1), 131–144.

Guzmán, A., Nava, J. L., Coreño, O., Rodríguez, I., & Gutiérrez, S. (2016). Arsenic and fluoride removal from groundwater by electrocoagulation using a continuous filter-press reactor. Chemosphere, 144, 2113–2120. https://doi.org/10.1016/j.chemosphere.2015.10.108

Harif, T., & Adin, A. (2007). Characteristics of aggregates formed by electroflocculation of a colloidal suspension. Water Research, 41(13), 2951–2961.

Hashim, K. S., Shaw, A., Al Khaddar, R., Pedrola, M. O., & Phipps, D. (2017). Iron removal, energy consumption and operating cost of electrocoagulation of drinking water using a new flow column reactor. Journal of Environmental Management, 189, 98–108.

Hering, J. G., Katsoyiannis, I. A., Theoduloz, G. A., Berg, M., & Hug, S. J. (2017). Arsenic removal from drinking water: Experiences with technologies and constraints in practice. American Society of Civil Engineers.

Holt, P. K., Barton, G. W., Wark, M., & Mitchell, C. A. (2002). A quantitative comparison between chemical dosing and electrocoagulation. Colloids and Surfaces A: Physicochemical and Engineering Aspects, 211(2–3), 233–248.

Hu, C. Y., Lo, S. L., & Kuan, W. H. (2003). Effects of co-existing anions on fluoride removal in electrocoagulation (EC) process using aluminum electrodes. Water Research, 37(18), 4513–4523.

Huq, E., Fahad, S., Shao, Z., Sinthia, M., Ali, I., Alam, M., … Ullah, W. (2020). Arsenic in a groundwater environment in Bangladesh : Occurrence and mobilization. Journal of Environmental Management, 262(March), 110318. https://doi.org/10.1016/j.jenvman.2020.110318

Hurtado-Jiménez, R., & Gardea-Torresdey, J. L. (2006). Arsenic in drinking water in the Los Altos de Jalisco region of Mexico. Revista Panamericana de Salud Pública, 20, 236–247.

Indu, R., Krishnan, S., & Shah, T. (2007). Impacts of groundwater contamination with fluoride and arsenic: affliction severity, medical cost and wage loss in some villages of India.

International Journal of Rural Management, 3(1), 69–93.

Ingallinella, A. M., Pacini, V. A., Fernández, R. G., Vidoni, R. M., & Sanguinetti, G. (2011). Simultaneous removal of arsenic and fluoride from groundwater by coagulation-adsorption with polyaluminum chloride. Journal of Environmental Science and Health, Part A, 46(11), 1288–1296.

Jadhav, S. V, Bringas, E., Yadav, G. D., Rathod, V. K., Ortiz, I., & Marathe, K. V. (2015). Arsenic and fl uoride contaminated groundwaters : A review of current technologies for contaminants removal. Journal of Environmental Management, 162, 306–325. https://doi.org/10.1016/j.jenvman.2015.07.020

Jadhav, S. V, Marathe, K. V, & Rathod, V. K. (2016). Journal of Water Process Engineering A pilot scale concurrent removal of fluoride , arsenic , sulfate and nitrate by using nanofiltration : Competing ion interaction and modelling approach. Journal of Water Process Engineering, 13, 153–167. https://doi.org/10.1016/j.jwpe.2016.04.008

Jhala, D. D., Chinoy, N. J., & Rao, M. V. (2008). Mitigating effects of some antidotes on fluoride and arsenic induced free radical toxicity in mice ovary. Food and Chemical Toxicology, 46(3), 1138–1142.

Jing, C., Cui, J., Huang, Y., & Li, A. (2012). Fabrication, characterization, and application of a composite adsorbent for simultaneous removal of arsenic and fluoride. ACS Applied Materials & Interfaces, 4(2), 714–720.

Jonnalagadda, S. B., & Nenzou, G. (1996). Studies on arsenic rich mine dumps: I. Effect on the surface soil. Journal of Environmental Science & Health Part A, 31(8), 1909–1915.

Karim, M. D. M. (2000). Arsenic in groundwater and health problems in Bangladesh. Water Research, 34(1), 304–310.

Katsoyiannis, I. A., & Zouboulis, A. I. (2006). Comparative evaluation of conventional and alternative methods for the removal of arsenic from contaminated groundwaters. Reviews on environmental health, 21(1), 25.

Khair, A. M., Li, C., Hu, Q., Gao, X., & Wanga, Y. (2014). Fluoride and Arsenic Hydrogeochemistry of Groundwater at Yuncheng Basin , Northern China 1. 52(10),

868–881. https://doi.org/10.1134/S0016702914100024

Khairul, M., Mahmad, N., Remy, M., Rozainy, M. A. Z., & Abustan, I. (2016). Electrocoagulation Process by Using Aluminum and Stainless Steel Electrodes to Treat Total Chromium , Colour and Turbidity. Procedia Chemistry, 19, 681–686. https://doi.org/10.1016/j.proche.2016.03.070

Khandegar, V., & Saroha, A. K. (2013). Electrocoagulation for the treatment of textile industry effluent–a review. Journal of Environmental Management, 128, 949–963.

Khatri, N., & Tyagi, S. (2015). Influences of natural and anthropogenic factors on surface and groundwater quality in rural and urban areas. Frontiers in Life Science, 8(1), 23–39.

Kim, S. H., Kim, K., Ko, K. S., Kim, Y., & Lee, K. S. (2012). Co-contamination of arsenic and fluoride in the groundwater of unconsolidated aquifers under reducing environments. Chemosphere, 87(8), 851–856. https://doi.org/10.1016/j.chemosphere.2012.01.025

Kim, Y., Kim, C., Choi, I., Rengaraj, S., & Yi, J. (2004). Arsenic removal using mesoporous alumina prepared via a templating method. Environmental Science & Technology, 38(3), 924–931.

Kloos, H., & Tekle Haimanot, R. (1999). Distribution of fluoride and fluorosis in Ethiopia and prospects for control. Tropical Medicine and International Health, 4(5), 355–364. https://doi.org/10.1046/j.1365-3156.1999.00405.x

Kobya, M, Demirbas, E., & Ulu, F. (2016). Journal of Environmental Chemical Engineering Evaluation of operating parameters with respect to charge loading on the removal ef fi ciency of arsenic from potable water by electrocoagulation. Biochemical Pharmacology, 4(2), 1484–1494. https://doi.org/10.1016/j.jece.2016.02.016

Kobya, M, Gebologlu, U., Ulu, F., Oncel, S., & Demirbas, E. (2011). Electrochimica Acta Removal of arsenic from drinking water by the electrocoagulation using Fe and Al electrodes. Electrochimica Acta, 56(14), 5060–5070. https://doi.org/10.1016/j.electacta.2011.03.086

Kobya, M, Hiz, H., Senturk, E., Aydiner, C., & Demirbas, E. (2006). Treatment of potato chips manufacturing wastewater by electrocoagulation. Desalination, 190(1–3), 201–211.

Kobya, Mehmet, Ulu, F., Gebologlu, U., Demirbas, E., & Oncel, M. S. (2011). Treatment of potable water containing low concentration of arsenic with electrocoagulation: Different connection modes and Fe–Al electrodes. Separation and Purification Technology, 77(3), 283–293.

Kumar, M., Das, A., Das, N., Goswami, R., & Singh, U. K. (2016). Co-occurrence perspective of arsenic and fluoride in the groundwater of Diphu, Assam, Northeastern India. Chemosphere, 150, 227–238.

Kumar, M., Goswami, R., Patel, A. K., Srivastava, M., & Das, N. (2020). Scenario, perspectives and mechanism of arsenic and fluoride Co-occurrence in the groundwater: A review. Chemosphere, 249, 126126.

Kumar, V., Talreja, N., Deva, D., Sankararamakrishnan, N., Sharma, A., & Verma, N. (2011). Development of bi-metal doped micro-and nano multi-functional polymeric adsorbents for the removal of fluoride and arsenic (V) from wastewater. Desalination, 282, 27–38.

Lacasa, E., Ca, P., Sáez, C., Fernández, F. J., & Rodrigo, M. A. (2011). Removal of arsenic by iron and Aluminum electrochemically assisted coagulation. 79, 15–19. https://doi.org/10.1016/j.seppur.2011.03.005

Lakshmanan, D., Clifford, D. A., & Samanta, G. (2010). Comparative study of arsenic removal by iron using electrocoagulation and chemical coagulation. Water Research, 44(19), 5641–5652. https://doi.org/10.1016/j.watres.2010.06.018

Levy, D. B., Schramke, J. A., Esposito, K. J., Erickson, T. A., & Moore, J. C. (1999). The shallow groundwater chemistry of arsenic, fluorine, and major elements: Eastern Owens Lake, California. Applied Geochemistry, 14(1), 53–65.

Li, W., Cao, C.-Y., Wu, L.-Y., Ge, M.-F., & Song, W.-G. (2011). Superb fluoride and arsenic removal performance of highly ordered mesoporous aluminas. Journal of Hazardous Materials, 198, 143–150.

Limón-Pacheco, J. H., Jiménez-Córdova, M. I., Cárdenas-González, M., Retana, I. M. S., Gonsebatt, M. E., & Del Razo, L. M. (2018). Potential co-exposure to arsenic and fluoride and biomonitoring equivalents for Mexican children. Annals of Global Health, 84(2), 257.

Linares-Hernández, I., Barrera-Díaz, C., Roa-Morales, G., Bilyeu, B., & Ureña-Núñez, F. (2009). Influence of the anodic material on electrocoagulation performance. Chemical Engineering Journal, 148(1), 97–105.

Litter, M. I., Ingallinella, A. M., Olmos, V., Savio, M., Difeo, G., Botto, L., … Herkovits, J. (2019). Arsenic in Argentina: Technologies for arsenic removal from groundwater sources, investment costs and waste management practices. Science of the Total Environment, 690, 778–789.

Makoba, E., & Muzuka, A. N. N. (2019). Water quality and hydrogeochemical characteristics of groundwater around Mt. Meru, Northern Tanzania. Applied Water Science, 9(5), 120.

Mameri, N., Yeddou, A. R., Lounici, H., Belhocine, D., Grib, H., & Bariou, B. (1998). Defluoridation of septentrional Sahara water of North Africa by electrocoagulation. 32(5), 1604–1612.

Mandal, B. K., & Suzuki, K. T. (2002). Arsenic round the world: A review. Talanta, Vol. 58, pp. 201–235. https://doi.org/10.1016/S0039-9140(02)00268-0

Mansoorian, H. J., Mahvi, A. H., & Jafari, A. J. (2014). Removal of lead and zinc from battery industry wastewater using electrocoagulation process: influence of direct and alternating current by using iron and stainless steel rod electrodes. Separation and Purification Technology, 135, 165–175.

Mansouri, K., Ibrik, K., Bensalah, N., & Abdel-Wahab, A. (2011). Anodic dissolution of pure Aluminum during electrocoagulation process: Influence of supporting electrolyte, initial pH, and current density. Industrial & Engineering Chemistry Research, 50(23), 13362–13372.

Mittal, M., & Flora, S. J. S. (2006). Effects of individual and combined exposure to sodium arsenite and sodium fluoride on tissue oxidative stress, arsenic and fluoride levels in male mice. Chemico-Biological Interactions, 162(2), 128–139.

Mjengera, H., & Mkongo, G. (2003). Appropriate deflouridation technology for use in flourotic areas in Tanzania. Physics and Chemistry of the Earth, Parts A/B/C, 28(20–27), 1097–1104.

Mohammadi, A. A., Yousefi, M., Yaseri, M., Jalilzadeh, M., & Mahvi, A. H. (2017). Skeletal

fluorosis in relation to drinking water in rural areas of West Azerbaijan, Iran. Scientific Reports, 7(1), 1–7.

Mollah, M. Y. A., Morkovsky, P., Gomes, J. A. G., Kesmez, M., Parga, J., & Cocke, D. L. (2004). Fundamentals, present and future perspectives of electrocoagulation. Journal of Hazardous Materials, 114(1–3), 199–210.

Moussa, D. T., El-naas, M. H., Nasser, M., & Al-marri, M. J. (2017). A comprehensive review of electrocoagulation for water treatment : Potentials and challenges. Journal of Environmental Management, 186, 24–41. https://doi.org/10.1016/j.jenvman.2016.10.032

Moussa, D. T., El-Naas, M. H., Nasser, M., & Al-Marri, M. J. (2017). A comprehensive review of electrocoagulation for water treatment: Potentials and challenges. Journal of Environmental Management, 186, 24–41.

Nair, S. B., Jhala, D. D., & Chinoy, N. J. (2004). Mitigation of genotoxic effects of fluoride and arsenic by ascorbic acid in human lymphocyte cultures. Fluoride, 37(4), 249–256.

Nasrullah, M., Singh, L., Krishnan, S., & Sakinah, M. (2018). Environmental Technology & Innovation Electrode design for electrochemical cell to treat palm oil mill effluent by electrocoagulation process. Environmental Technology & Innovation, 9, 323–341. https://doi.org/10.1016/j.eti.2017.10.001

Nasrullah, M., Singh, L., & Wahid, Z. A. (2012). Treatment of Sewage by Electrocoagulation and the Effect of High Current Density. Energy and Environmental Engineering Journal, 1(1), 27–31.

Nimick, D. A. (1998). Arsenic hydrogeochemistry in an irrigated river valley - A reevaluation. Groundwater, 36(5), 743–753. https://doi.org/10.1111/j.1745-6584.1998.tb02191.x

Nordstrom, D. K., & Jenne, E. A. (1977). Fluorite solubility equilibria in selected geothermal waters. Geochimica et Cosmochimica Acta, 41(2), 175–188.

Osterwalder, L., Johnson, C. A., Yang, H., & Johnston, R. B. (2014). Multi-criteria assessment of community-based fluoride-removal technologies for rural Ethiopia. Science of The Total Environment, 488, 532–538.

Parga, J. R., Cocke, D. L., Valverde, V., Gomes, J. A. G., Kesmez, M., Moreno, H., … Mencer, D. (2005). Characterization of electrocoagulation for removal of chromium and arsenic. Chemical Engineering & Technology: Industrial Chemistry Plant Equipment Process Engineering Biotechnology, 28(5), 605–612.

Piñón-Miramontes, M., Bautista-Margulis, R. G., & Pérez-Hernández, A. (2003). Removal of arsenic and fluoride from drinking water with cake alum and a polymeric anionic flocculent. Fluoride, 36(2), 122–128.

Qasim, M., Badrelzaman, M., Darwish, N. N., Darwish, N. A., & Hilal, N. (2019). Reverse osmosis desalination: A state-of-the-art review. Desalination, 459, 59–104.

Quelch, K. J., Melick, R. A., Bingham, P. J., & Mercuri, S. M. (1983). Chemical composition of human bone. Archives of Oral Biology, 28(8), 665–674.

Rango, T., Bianchini, G., Beccaluva, L., & Tassinari, R. (2010). Geochemistry and water quality assessment of central Main Ethiopian Rift natural waters with emphasis on source and occurrence of fluoride and arsenic. Journal of African Earth Sciences, 57(5), 479–491.

Rango, T., Vengosh, A., Dwyer, G., & Bianchini, G. (2013). Mobilization of arsenic and other naturally occurring contaminants in groundwater of the main ethiopian rift aquifers. Water Research, 47(15), 5801–5818. https://doi.org/10.1016/j.watres.2013.07.002

Rao, M. V, & Tiwari, H. (2006). Amelioration by melatonin of chromosomal anomalies induced by arsenic and/or fluoride in human blood lymphocyte cultures. Fluoride, 39(4), 255.

Rasool, A., Xiao, T., Baig, Z. T., Masood, S., Mostofa, K. M. G., & Iqbal, M. (2015). Co-occurrence of arsenic and fluoride in the groundwater of Punjab, Pakistan: source discrimination and health risk assessment. Environmental Science and Pollution Research, 22(24), 19729–19746.

Richards, L. A., Richards, B. S., Rossiter, H. M. A., & Schäfer, A. I. (2009). Impact of speciation on fluoride, arsenic and magnesium retention by nanofiltration/reverse osmosis in remote Australian communities. Desalination, 248(1–3), 177–183.

Saeed, M., Rehman, M. Y. A., Farooqi, A., & Malik, R. N. (2020). Co-exposure effects of arsenic and fluoride on intelligence and oxidative stress in school-aged children: a cohort

study. Environmental Research, 110168.

Sandoval, M. A., Fuentes, R., Thiam, A., & Salazar, R. (2020). Arsenic and fluoride removal by electrocoagulation process: A general review. Science of The Total Environment, 142108.

Sandoval, M. A., Fuentes, R., Thiam, A., & Salazar, R. (2021). Science of the Total Environment Arsenic and fl uoride removal by electrocoagulation process : A general review. Science of the Total Environment, 753, 142108. https://doi.org/10.1016/j.scitotenv.2020.142108

Sengupta, S. R., Das, N. K., & Datta, P. K. (2008). Pathogenesis, clinical features and pathology of chronic arsenicosis. Indian Journal of Dermatology, Venereology, and Leprology, 74(6), 559.

Shon, H. K., Kim, S. H., Vigneswaran, S., Aim, R. Ben, Lee, S., & Cho, J. (2009). Physicochemical pretreatment of seawater: fouling reduction and membrane characterization. Desalination, 238(1–3), 10–21.

Shrivastava, B. K., & Vani, A. (2009). Comparative study of defluoridation technologies in India. Asian J. Exp. Sci, 23(1), 269–274.

Smedley, P. L., Zhang, M., Zhang, G., & Luo, Z. (2003). Mobilisation of arsenic and other trace elements in fluviolacustrine aquifers of the Huhhot Basin, Inner Mongolia. Applied Geochemistry, 18(9), 1453–1477. https://doi.org/10.1016/S0883-2927(03)00062-3

Smedley, Pauline L., & Mike Edmunds, W. (2002). Redox patterns and trace-element behavior in the East Midlands Triassic Sandstone Aquifer, U.K. Groundwater, 40(1), 44–58. https://doi.org/10.1111/j.1745-6584.2002.tb02490.x

Song, P., Yang, Z., Xu, H., Huang, J., Yang, X., & Wang, L. (2014). Investigation of influencing factors and mechanism of antimony and arsenic removal by electrocoagulation using Fe–Al electrodes. Industrial & Engineering Chemistry Research, 53(33), 12911–12919.

Srivastava, S., & Flora, S. J. S. (2020). Fluoride in Drinking Water and Skeletal Fluorosis: A Review of the Global Impact. Current Environmental Health Reports, 1–7.

Streat, M., Hellgardt, K., & Newton, N. L. R. (2008). Hydrous ferric oxide as an adsorbent in water treatment. Part 3: Batch and mini-column adsorption of arsenic, phosphorus, fluorine

and cadmium ions. Process Safety and Environmental Protection, 86(1 B), 21–30. https://doi.org/10.1016/j.psep.2007.10.009

Svarovsky, L. (2000). Solid-liquid separation. Elsevier.

Takdastan, A., Emami Tabar, S., Neisi, A., & Eslami, A. (2014). Fluoride removal from drinking water by electrocoagulation using iron and aluminum electrodes. Jundishapur Journal of Health Sciences, 6(3).

Tekle-Haimanot, R., Melaku, Z., Kloos, H., Reimann, C., Fantaye, W., Zerihun, L., & Bjorvatn, K. (2006). The geographic distribution of fluoride in surface and groundwater in Ethiopia with an emphasis on the Rift Valley. Science of the Total Environment, 367(1), 182–190.

Thakur, L. S., & Mondal, P. (2017). Simultaneous arsenic and fl uoride removal from synthetic and real groundwater by electrocoagulation process : Parametric and cost evaluation. Journal of Environmental Management, 190, 102–112. https://doi.org/10.1016/j.jenvman.2016.12.053

Thole, B. (2013). Groundwater Contamination with Fluoride and Potential Fluoride Removal Technologies for East and Southern Africa. In Perspectives in Water Pollution. https://doi.org/10.5772/54985

Tian, Y., Wu, M., Liu, R., Wang, D., Lin, X., Liu, W., … Huang, Y. (2011). Modified native cellulose fibers—A novel efficient adsorbent for both fluoride and arsenic. Journal of Hazardous Materials, 185(1), 93–100.

Tir, M., & Moulai-Mostefa, N. (2008). Optimization of oil removal from oily wastewater by electrocoagulation using response surface method. Journal of Hazardous Materials. https://doi.org/10.1016/j.jhazmat.2008.01.051

Ucar, C., Baskan, M. B., & Pala, A. (2013). Arsenic removal from drinking water by electrocoagulation using iron electrodes. Korean Journal of Chemical Engineering, 30(10), 1889–1895.

UNESCO, W. (2019). The United Nations world water development report 2019: Leaving no one behind. UNESCO Paris.

Vepsäläinen, M., & Sillanpää, M. (2020). Electrocoagulation in the treatment of industrial waters and wastewaters. In Advanced Water Treatment (pp. 1–78). Elsevier.

Verma, K. K., Singh, M., & Verma, C. L. (2018). Fluoride in water: a risk assessment perspective. Asian J. Bot, 1, 1–8.

Vithanage, M., & Bhattacharya, P. (2015). Fluoride in the environment: sources, distribution and defluoridation. Environmental Chemistry Letters, 13(2), 131–147.

Walker, F. P., Schreiber, M. E., & Rimstidt, J. D. (2006). Kinetics of arsenopyrite oxidative dissolution by oxygen. Geochimica et Cosmochimica Acta, 70(7), 1668–1676.

Warren, C., Burgess, W. G., & Garcia, M. G. (2005). Hydrochemical associations and depth profiles of arsenic and fluoride in Quaternary loess aquifers of northern Argentina. Mineralogical Magazine, 69(5), 877–886.

Witek-Krowiak, A., Chojnacka, K., Podstawczyk, D., Dawiec, A., & Pokomeda, K. (2014). Application of response surface methodology and artificial neural network methods in modelling and optimization of biosorption process. Bioresource Technology, 160, 150–160.

Yami, T. L., Chamberlain, J. F., Beshah, F. Z., & Sabatini, D. A. (2018). Performance enhancement of Nalgonda technique and pilot testing electrolytic defluoridation system for removing fluoride from drinking water in East Africa. 12(October), 357–369. https://doi.org/10.5897/AJEST2018.2545

Yao, H., & Wang, G. (1988). Acute and chronic experimental studies on joint effect of fluoride and arsenic. Chin J Prevent Med, 22, 284.

You, H. J., & Han, I. S. (2015). Effects of Dissolved Ions and Natural Organic Matter on Electrocoagulation of As (III) in Groundwater. Biochemical Pharmacology, (Iii). https://doi.org/10.1016/j.jece.2015.12.034

Zewge, F. (2016). Combined Aluminum sulfate/hydroxide process for fluoride removal from drinking water. Bulletin of the Chemical Society of Ethiopia, 30(3), 391–401.

Zhang, J. S., Stanforth, R. S., & Pehkonen, S. O. (2007). Effect of replacing a hydroxyl group with a methyl group on arsenic (V) species adsorption on goethite (α-FeOOH). Journal of

Colloid and Interface Science, 306(1), 16–21.

Zhao, F.-J., McGrath, S. P., & Meharg, A. A. (2010). Arsenic as a food chain contaminant: mechanisms of plant uptake and metabolism and mitigation strategies. Annual Review of Plant Biology, 61, 535–559.

Zhao, X., Zhang, B., Liu, H., & Qu, J. (2011). Simultaneous removal of arsenite and fluoride via an integrated electro-oxidation and electrocoagulation process. Chemosphere, 83(5), 726–729. https://doi.org/10.1016/j.chemosphere.2011.01.055

CHAPTER TWO

The Optimal Operating Current Densities for Individual Al-EC and Fe-EC through Defluoridation Efficiencies

This chapter is based on the two published papers.

Nyangi, M. J., Chebude, Y., & Kilulya, K. F. (2020). Fluoride removal efficiencies of Al-EC and Fe-EC reactors: process optimization using Box–Behnken design of the surface response methodology. Applied Water Science, *10*(9), 1-11. https://doi.org/10.1007/s13201-020-01297-x

Nyangi, M. J., Chebude, Y., Kilulya, K. F., & Salim, C. J. (2021). Comparative Study on Adsorption Isotherm and Kinetics of Defluoridation Using Aluminum and Iron Electrodes in Electrocoagulation. Chemistry Africa, 1-8. https://doi.org/10.1007/s42250-021-00228-w

Fluoride Removal Efficiencies of Al-EC and Fe-EC Reactors: Process Optimization using Box-Behnken Design of the Surface Response Methodology

Abstract

In this study, surface response methodology was employed to investigate the effect of different interacting factors on the removal of fluoride from synthetic water using aluminum electrocoagulation (Al-EC) and iron electrocoagulation (Fe-EC) in different reactors. Box-Behnken Design of a Design Expert version 11 was used for the optimization and evaluation of the process independent variables: applied electric density, initial pH, initial fluoride concentration and treatment time on the efficiency of fluoride removal as a response. Results showed that the effect of current density and initial fluoride concentration were significant model terms for fluoride reduction in Fe-EC and Al-EC reactors, respectively. The Al-EC reactor model presented the R^2 value of 79.2%, while Fe-EC presented R^2 value of 75.8%, showing that both models can predict the response well. The reduction by 94% (initial concentration of 16 mg/L) was established at optimal operating parameters of 18.5 $mAcm^{-2}$, pH 6.80 in 50 minutes using Al-EC. On the other hand, 16 mg/L was reduced by 92% to 1.28 mg/L in Fe-EC reactor at optimal condition of 6.5 $mAcm^{-2}$, pH 6.50 in 50 minutes. Experimental results correlated well to the model predicted results that were 95% and 94% for Al-EC and Fe-EC, respectively. Both reactors manage to reduce fluoride to a level recommended by WHO (≤ 1.5 mg/L) for drinking purpose.

Keywords: Electrocoagulation, defluoridation, Box-Behnken design, surface response

2.0 Introduction

It is estimated that 90% of the population living in African Rift valley is affected with dental and skeletal fluorosis, due to consumption of groundwater water containing elevated levels of fluoride (Fawell et al., 2006). Despite the availability of various methods such as adsorption, ion exchange, filtration, coagulation and membrane processes for defluoridation (Mohapatra et al., 2009), in the African Rift Valley zone, people are mainly using bone char and Nalgonda methods (Osterwalder et al., 2014). This is due to their low cost, effectiveness and availability of materials (García-Lara & Montero-Ocampo, 2010). However, the methods face rejection by some users because of odour and offensive taste especially when there is poor production of bone char (Fawell et al., 2006). On the other hand, Nalgonda method requires high chemical coagulants for effective fluoride removal, resulting in high sludge production that becomes a challenge in their disposal. Thus, electrocoagulation has demonstrated to be an alternative treatment method to avoid high production of sludge, odour and smell as on chemical coagulation.

Electrocoagulation (EC) method involves electricity for in-situ generation of coagulant that destabilizes chemical pollutants in water (Moussa, et al., 2017). The common electrodes include aluminum, titanium, zinc, copper and iron; aluminum and iron being superior than the others, due to their efficiency and availability (Moussa et al., 2017). In EC, the metal ion dissociates from the anode (equation 2.1 and 2.3) while water at the surface of the cathode dissociates into H^+ and OH^- ions, the two react to form metal hydroxide (coagulant) as shown in equations 2.2 and 2.4 for aluminum and iron respectively, with respective standard electrode potential shown. The coagulant then provides surface site for charge neutralization, adsorption, coagulation and co-precipitation which remove fluoride by flocs formation (Kobya et al., 2006).

(2.3)

(2.4)

The efficiency of EC experiments depends on interaction among several independent factors, namely, the current applied, initial pH, treatment time, conductivity of the sample and initial pollutant concentration (Moussa et al., 2017). Recently optimization of EC operation factors has been performed by varying a single factor while keeping other factors fixed at a specific set of conditions. This process is time consuming and requires high number of runs leading to poor optimization due to ignoring of some interaction (Tir & Moulai-Mostefa, 2008). The mentioned

shortfalls can be easily solved by a response surface methodology (RSM). The method uses various designs such as factorial design (FD) (Daghrir et al., 2013), central composite design (CCD) (Amani-Ghadim et al., 2013), D-optimal design (DOP) (Tir & Moulai-Mostefa, 2008), and Box-Behnken design (BBD) (Behbahani, Moghaddam, & Arami, 2011). The first three designs face a challenge of higher number of experiments required and thus become costly. On the other hand, the BBD provides the same information as the others, but with the advantage of less number of experiments (Box & Behnken, 1960). Furthermore, BBD doesn't contain combinations in which all factors are simultaneously at their highest or lowest levels, which is important in avoiding experiments performed under extreme conditions that may cause unsatisfactory results (Box & Behnken, 1960), hence selected for this work.

The aim of this study was to optimize and model fluoride removal from aqueous solutions in two separate electrocoagulation reactors, Al-EC and Fe-EC, establish and compare their efficiencies on fluoride removal and to determine relationship between responses and four quantitative variables (initial pH, initial fluoride concentration, current density and treatment time) using Box-Behnken design (BBD).

2.1 Materials and methods

2.1.1 Material preparation

The fluoride solution was prepared using sodium fluoride (NaF), where 2.21 g of sodium fluoride was dissolved in 1000 mL of distilled water to make 1000 ppm of fluoride in the stock solution. Then serial dilution was used for a specific concentration preparation. Meanwhile the electrodes, aluminum and iron electrode plates of 15 cm × 2 cm, each were pre-cleaned by rubbing with sand paper, rinsed in NaOH (2 M) and HCl (2 M) to remove any particles attached on the surface before washing with distilled water. The electrodes were then dried at 105ºC before the start of experiments. After each experiment, electrodes were dissolved in 1M hydrochloric acid for 10 minutes to remove any remaining particles on the surface that may reduce EC performance.

2.1.2 Design of experiment

In this study, the Box-Behnken design (BBD) was selected for the optimization of EC process used for the fluoride reduction. The four-factorial and a three-level BBD, with five replicas at the center point leading to twenty-nine (29) experiments was employed for response surface modeling in this study. The variables (independent factors) chosen were: the applied electric

current density (A), initial pH of the water sample (B), treatment time (C) and initial concentration of fluoride (D). Meanwhile the percentage fluoride reduction was considered as dependent factor (response).

2.1.3 The electrocoagulation set up and sample analysis

The EC experiments were carried-out in a batch mode reactor (Figure 2.0). The reactions were conducted in 800 cm^3 beaker, with a working volume of 600 cm^3. The two aluminum electrode plates with a total surface area of 80 cm^2 each, were connected to other two aluminum as cathode in a monopolar parallel connection MP-P. This makes the effective surface area to volume ratio the reactors (S) to be 0.13 cm^{-1}. Similar reactor set up for the iron electrode Fe-EC was employed. The anodes and cathodes were placed alternatively and parallel to each other at a specific distance of 1.5 cm. Thereafter, the end poles of sacrificial electrodes were connected to the anode in a direct current (DC) power source, (BK Precision 1796)

The experiments were then performed in series of combination of different operation parameters as shown in Table 2.1. On the other hand, the conductivity of water sample was improved by addition of small amount of sodium chloride (200-300 mg) as it has ability to eliminate the passive films on aluminum electrodes according to corrosion pitting phenomenon (Mansouri et al., 2011). After each set of experiment, samples were taken then filtered (Whatman filter paper 0.6 micron) and analysed using ion selective electrode (ISE) for final fluoride concentration. Percentage of fluoride removal was then calculated (Equation 2.5).

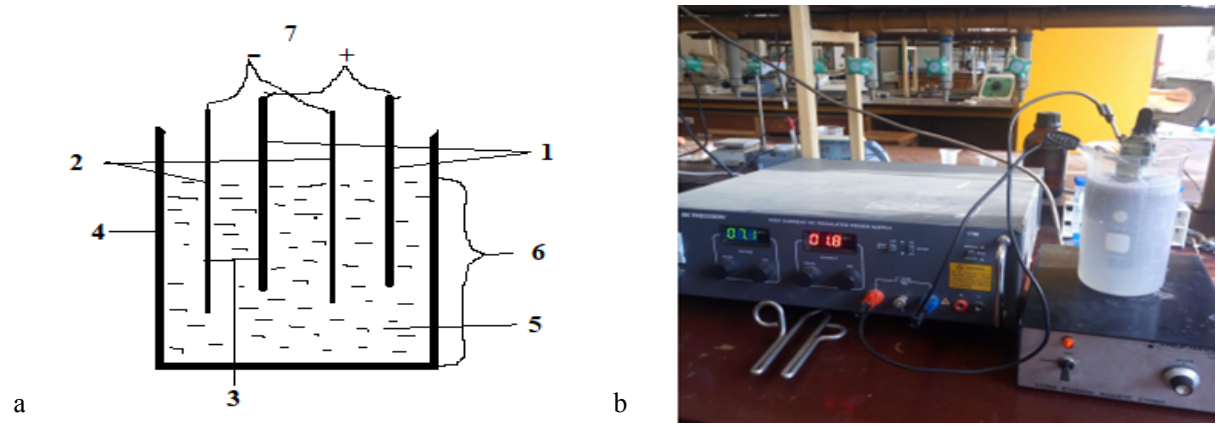

Figure 2.0: Experimental setup for electrocoagulation reactions; a). Schematic diagram; 1. Anode Fe or Al 2. Cathode, 3. Inter-electrode distance 1.5 cm, 4. Reactor (800cm^3), 5. Water sample (600 cm^3), 6. Working volume (600 cm^3), b. Photograph of the reactor setup and experimentation

Where: Fo and Ft are Initial and final fluoride concentration (mg/L).

2.2 Results and Discussion

The actual values of process variables and their variation limits shown in Table 2.1 were selected based on the values obtained from various literatures as well as in preliminary experiments. Results of the experiments performed is presented in Table 2.2 showing the actual and predicted reduction of fluoride at different combinations of operating parameters using aluminum and iron electrodes, respectively.

Table 2.1: Experimental range and levels of independent variables for Al-EC and Fe-EC experiments.

				Range of actual coded variables		
Factor	Variables	Unit	Reactor	Low (-1)	Medium (0)	High (+1)
A	Current density	$mAcm^{-2}$	Al-EC	18.5	28.0	37.5
			Fe-EC	6.25	12.4	18.5
B	pH.		Both	4.0	6.5	9.0
C	Time	min	Both	10	35	60
D	Concentration	mg/L	Both	2	21	40

Table 2.2: The Box Behnken Design (BBD) showing actual and predicted fluoride reduction for Al-EC and Fe-EC reactor at different operation parameters

	Al-EC					Fe-EC					Actual%	
Run						**J**	**pH**	**Time**	**Fo**	**Ft**	**Al-EC**	**Fe-EC**
n	**J**	**pH**	**Time**	**Fo**	**Ft**							
1	28.00	6.50	10.00	02.00	0.32	12.38	6.50	10.00	02.00	0.16	**84.00**	**92.00**
2	28.00	6.50	60.00	40.00	2.73	12.38	6.50	35.00	21.00	1.20	**93.18**	**94.29**
3	28.00	6.50	35.00	21.00	1.45	12.38	4.00	35.00	40.00	2.83	**93.10**	**92.93**
4	18.50	6.50	10.00	21.00	3.12	18.50	4.00	35.00	21.00	1.20	**85.14**	**94.29**
5	28.00	4.00	35.00	02.00	0.75	12.38	6.50	60.00	40.00	2.60	**62.50**	**93.50**
6	28.00	9.00	60.00	21.00	2.07	12.38	6.50	35.00	21.00	1.20	**90.14**	**94.29**
7	18.50	4.00	35.00	21.00	3.14	18.50	6.50	10.00	21.00	1.18	**85.05**	**94.38**
8	28.00	6.50	35.00	21.00	1.40	12.38	6.50	35.00	21.00	1.22	**93.33**	**94.19**
9	37.50	6.50	60.00	21.00	1.20	6.25	6.50	10.00	21.00	1.41	**94.29**	**93.29**
10	37.50	6.50	35.00	02.00	0.13	18.50	6.50	60.00	21.00	1.08	**93.50**	**94.86**
11	37.50	6.50	35.00	40.00	1.36	6.25	4.00	35.00	21.00	1.44	**96.60**	**93.14**
12	37.50	4.00	35.00	21.00	3.00	6.25	6.50	35.00	02.00	0.15	**85.71**	**92.50**
13	28.00	9.00	35.00	40.00	1.78	12.38	6.50	35.00	21.00	1.23	**95.55**	**94.14**
14	28.00	4.00	35.00	40.00	4.85	12.38	6.50	35.00	21.00	0.84	**87.88**	**96.00**
15	28.00	9.00	10.00	21.00	1.85	18.50	6.50	35.00	40.00	2.46	**91.19**	**93.85**
16	37.50	6.50	10.00	21.00	2.57	12.38	9.00	60.00	21.00	1.14	**87.76**	**94.57**
17	37.50	9.00	35.00	21.00	1.09	12.38	9.00	35.00	40.00	2.61	**94.81**	**93.48**
18	28.00	6.50	35.00	21.00	1.40	6.25	9.00	35.00	21.00	1.44	**93.33**	**93.14**
19	28.00	4.00	60.00	21.00	1.60	12.38	9.00	35.00	02.00	0.17	**92.38**	**91.50**
20	28.00	6.50	35.00	21.00	1.41	6.25	6.50	60.00	21.00	1.20	**93.30**	**94.29**
21	28.00	9.00	35.00	02.00	0.17	12.38	4.00	35.00	02.00	0.08	**91.50**	**96.00**

			60.0	21.0		12.3	6.50	10.0	40.0		**93.1**	**93.18**
22	18.50	6.50	0	0	1.43	8		0	0	2.73	**9**	
			35.0	40.0		18.5	9.00	35.0	21.0		**92.3**	**94.24**
23	18.50	6.50	0	0	3.06	0		0	0	1.21	**5**	
			35.0	21.0		12.3	9.00	10.0	21.0		**93.7**	**93.76**
24	28.00	6.50	0	0	1.32	8		0	0	1.31	**1**	
			35.0	21.0		12.3	6.50	60.0	02.0		**93.3**	**94.00**
25	18.50	9.00	0	0	1.40	8		0	0	0.12	**3**	
			35.0	02.0		12.3	4.00	10.0	21.0		**52.0**	**94.10**
26	18.50	6.50	0	0	0.96	8		0	0	1.24	**0**	
			10.0	21.0		6.25	6.50	35.0	40.0		**90.3**	**93.10**
27	28.00	4.00	0	0	2.03			0	0	2.76	**3**	
			10.0	40.0		18.5	6.50	35.0	02.0		**85.3**	**94.50**
28	28.00	6.50	0	0	5.85	0		0	0	0.11	**8**	
			60.0			12.3	4.00	60.0	21.0		**73.5**	**94.33**
29	28.00	6.50	0	2.00	0.53	8		0	0	1.19	**0**	

[1]

2.2.1 Evaluation of the data

For the evaluation of experimental data on their validity in optimization of operation parameters, the response variable was fitted by a second-order model in the form of quadratic polynomial equation given by Equation 2.6 as proposed by (Khedmati et al., 2017).

In this equation Y is the response variables (fluoride reduction) and b_0, b_i, b_{ii}, and b_{ij} are constant coefficients of intercept, linear, quadratic and interactive terms, respectively and Xi and Xj represent the four independent variables (current density, initial pH, treatment time, and initial concentration). Experimental data shown in Table 2.1 were analyzed using Design-Expert version 11 program including ANOVA and regression to obtain the interaction between the process variables to the response. Two-dimensional, contour plots and three-dimensional curves of the response surfaces were developed using the same program to explain the interactions among variables and their effect to the fluoride reduction.

2.2.2 Optimization procedure

Table 2.1 shows the key findings after analysis of variance and regression of the data set presented in Table 2.2 to assess the validity of the model prediction for Al-EC and Fe-EC, respectively. In this study the coefficients of the model for constant terms, cubic effects,

[1] The unit for operation parameters; J ($mAcm^{-2}$); Time (min); F (mg/L)

quadratic effects and interaction effects were evaluated. The model low p-values of 0.0087 and 0.022, and large F-values 3.81 and 3.07 implies that at least one of the terms in each model has a significant effect on the response in Al-EC and Fe-EC setups, respectively (Karimifard & Moghaddam, 2018). The lack of fit p-value of 0.1125 for Al-EC and 0.7344 for Fe-EC both being ≥ 0.05 made lack of fit not significant to both setups (Karimifard & Moghaddam, 2018). As seen from Table 2.3, the initial pH (B), and initial fluoride concentration (D) are both significant to the model ($p < 0.05$), where initial fluoride concentration being the most significant $p < 0.0001$ to Al-EC. For the Fe-EC the current density appears to be the only significant factor $p = 0.01$. The interaction between initial pH and initial concentration (BD), and between initial concentration themselves (D^2) are highly significant factors ($p < 0.05$) as compared to other interaction terms in both reactors.

Table 2.3: ANOVA and regression results for the response surface quadratic model for fluoride reduction by Fe-EC and Al-EC reactors.

Source	Fe-EC		Al-EC		
	F-Value	p-value	F-Value	p-value	
Model	3.07	0.022	3.81	0.0087	significant
A-J	7.75	0.0146	4.48	0.0528	
B-pH	2.93	0.1088	8.13	0.0128	
C-time	4.12	0.0619	0.3444	0.5666	
D-Conc	0.0395	0.8453	17.56	0.0009	
AB	0.0012	0.973	0.0073	0.9331	
AC	0.1441	0.7099	0.0194	0.8911	
AD	0.8207	0.3803	4.08	0.063	
BC	0.1715	0.6851	0.0995	0.7571	
BD	13.39	0.0026	4.71	0.0477	
CD	1.47	0.2449	3.47	0.0837	
A^2	1.22	0.2887	0.0822	0.7786	
B^2	1.32	0.2702	0.6344	0.439	
C^2	0.6246	0.4425	1.18	0.2966	
D^2	11.77	0.0041	10.07	0.0068	

Residual					
Lack of Fit	0.6525	0.7344	3.64	0.1125	not significant

Al-EC: R^2 = 0.79; AdjR^2 = 0.58; Adeq precision = 7.8; Fe-EC: R^2 = 0.75; AdjR^2 = 0.50; Adeq precision = 6.4

The regression coefficient R^2 of 0.79 and 0.75 for Al-EC and Fe-EC, respectively show that the interaction among the factors in experimental data to both models can fairly predict the response (Karimifard & Moghaddam, 2018). The adequate precision which is 7.8 for Al-EC and 6.4 for Fe-EC also signify that the signal to noise ratio is appropriate and adequate. The adjusted R^2 of 0.58 and 0.50 both being lower than the R^2 values suggest that the new number of factors included in the model in trying to modify it, could not improve the model (Karimifard & Moghaddam, 2018). The R^2 values observed indicate that the regression models explained electro-defluoridation fairly. Hence, the response surface model developed in this study for predicting fluoride removal efficiency was considered to be satisfactory.

From the normal probability plot of residuals as shown in Figure 2.1a and b it can be ascertained with assumption that both models were relatively satisfactory as the points in the plot form fairly straight-line. In the case of actual residual against fit plot, for a model to be reliable, no series of increasing or decreasing points, patterns such as increasing residuals with increasing fits and a predominance of positive or negative residuals should be found. Furthermore, the data shown in Tables 2.1 can also be observed and confirmed in Figure 2.2a and b showing alignment between the residuals and predicted fluoride reduction. The predicted and actual plots, Figure 2.4a and b further indicate the close agreement between the actual and predicted results, suggesting that the model could well predict within the range of operation parameter. Therefore, it can be concluded that the quadratic model of the response surface developed in this study correlating fluoride reduction with process variables are best suited to explain the experimental data of electrocoagulation process.

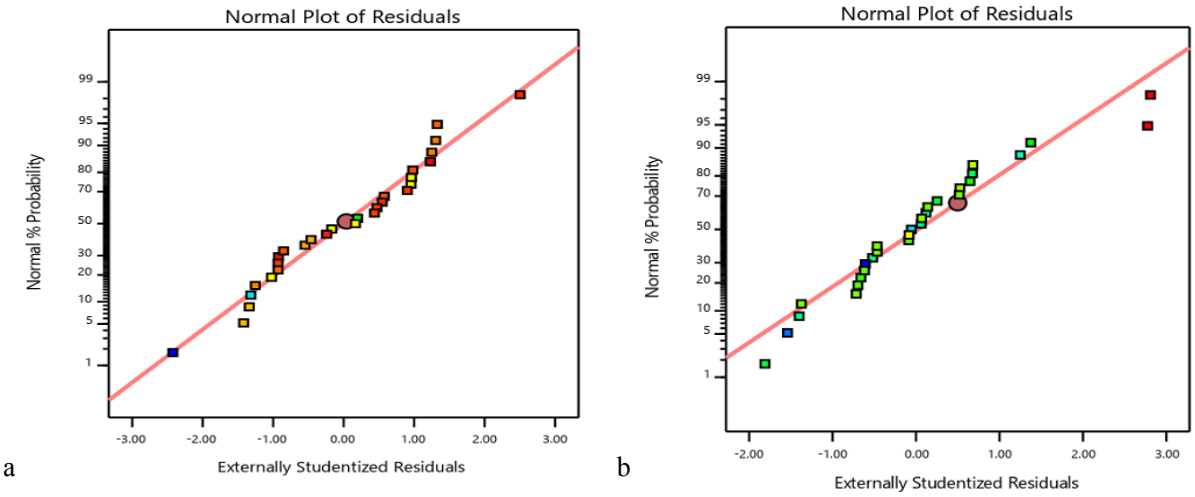

a b

Figure 2.1: Normal probability plots (a). Al-EC (b) Fe-EC reactors

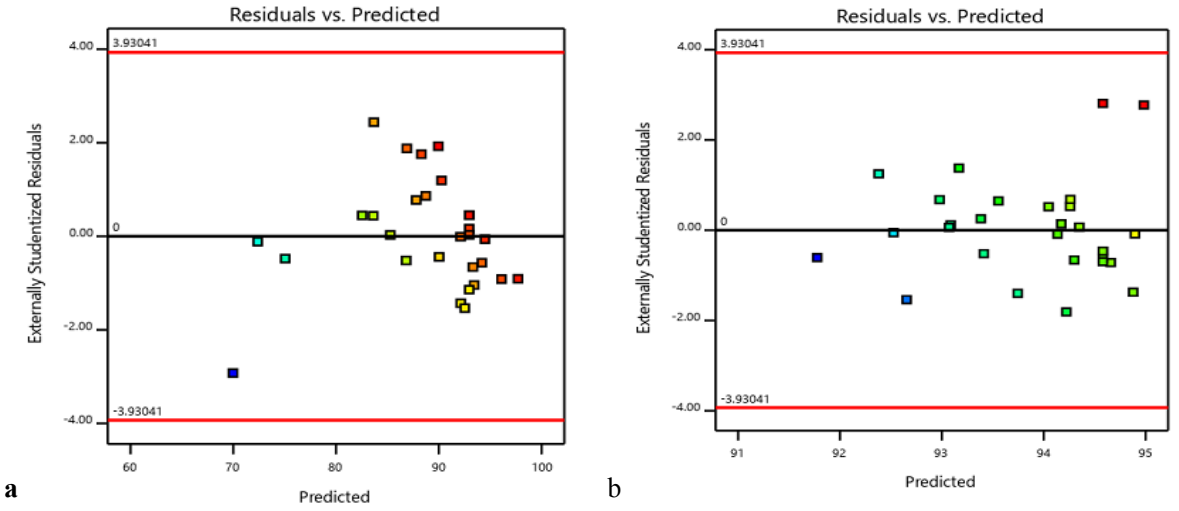

a b

Figure 2.2: Residual vs predicted plots for fluoride removal (a) Al-EC reactor (b) Fe-EC reactor

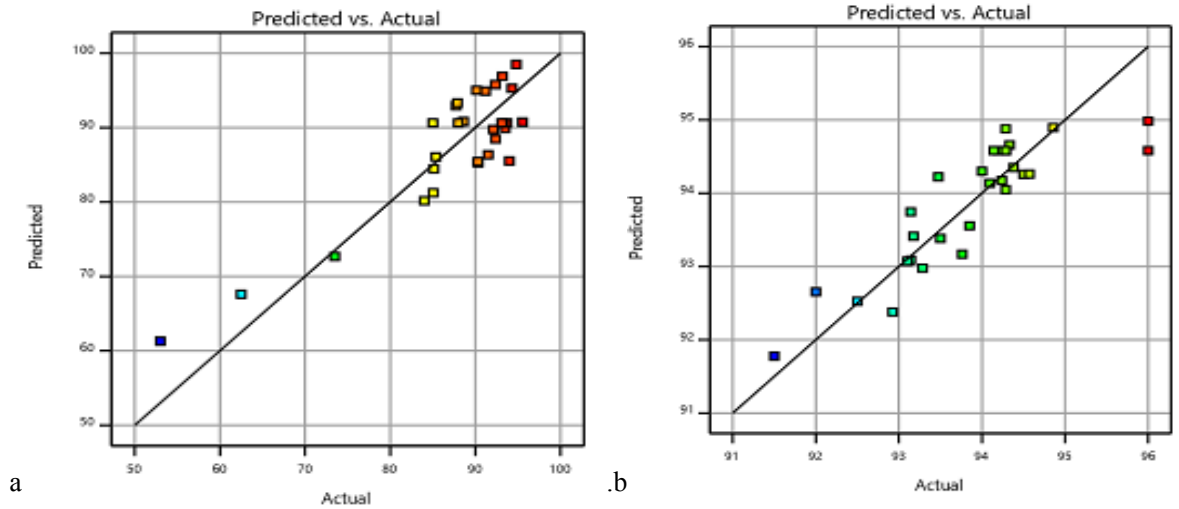

a .b

Figure 2.3: Plots for predicted against actual results for fluoride removal (a) Al-EC (b) Fe-EC

2.2.3 Effect of individual operating parameters

The effect of individual operating parameters, current density, initial pH, treatment time and initial fluoride concentration considered in this study is shown in the plots presented in Figures 2.4 and 2.5 for Al-E and Fe-EC, respectively. The parameters were measured as the function of fluoride reduction. These parameters are known to be key factors for operation of electrocoagulation system (Moussa et al., 2017).

2.2.3.1 The effect of current density

From the plots, it can be observed that, from the lower current density there is a linear increase on fluoride reduction to a maximum current of 38.5 mA/cm^2 and 16 mA/cm^2 for Al-EC and Fe-EC, respectively. At these points there is maximum removal of fluoride by 97% for Al-EC and 95% for Fe-EC. According to Faraday's law (Equation 2.6), as the applied current increases, dissolution of aluminum and iron ions also tend to increase, leading to high formation of coagulant $Al(OH)_3$ and $Fe(OH)_3$, bubble and flocs size (Kobya et al., 2011).

Where W is the theoretical amount of aluminum or iron produced by current I (A) passed for a period of time t (s), M is molecular mass (Al; 26.98 g/mol: Fe; 55.84 g/mol), N is number of electrons transferred (N - 3 for Al; 2 for Fe), F is Faradays constant (96,485 C/mol).

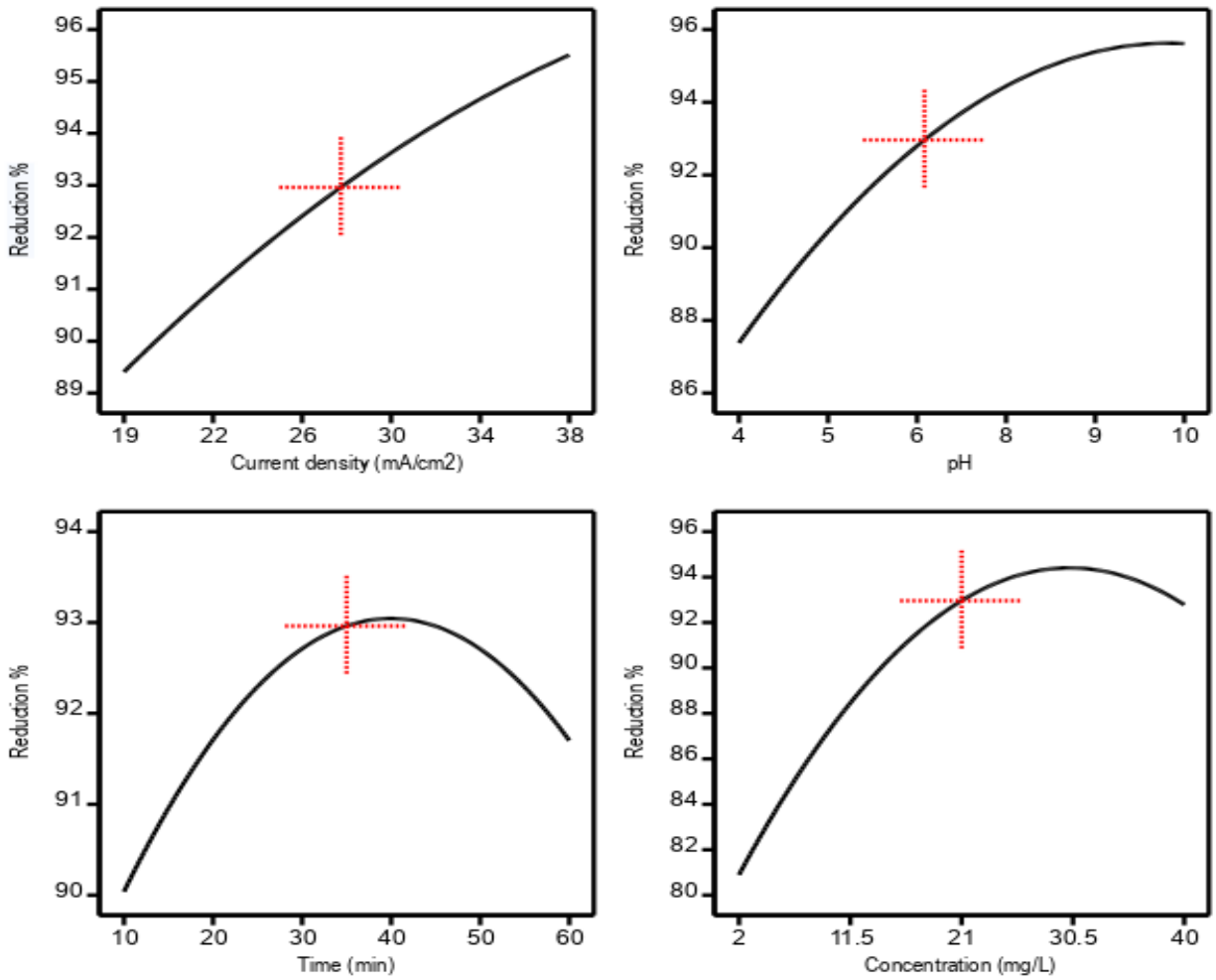

Figure 2.4: Main effect plots of parameters for fluoride removal efficiency on Al-EC reactor

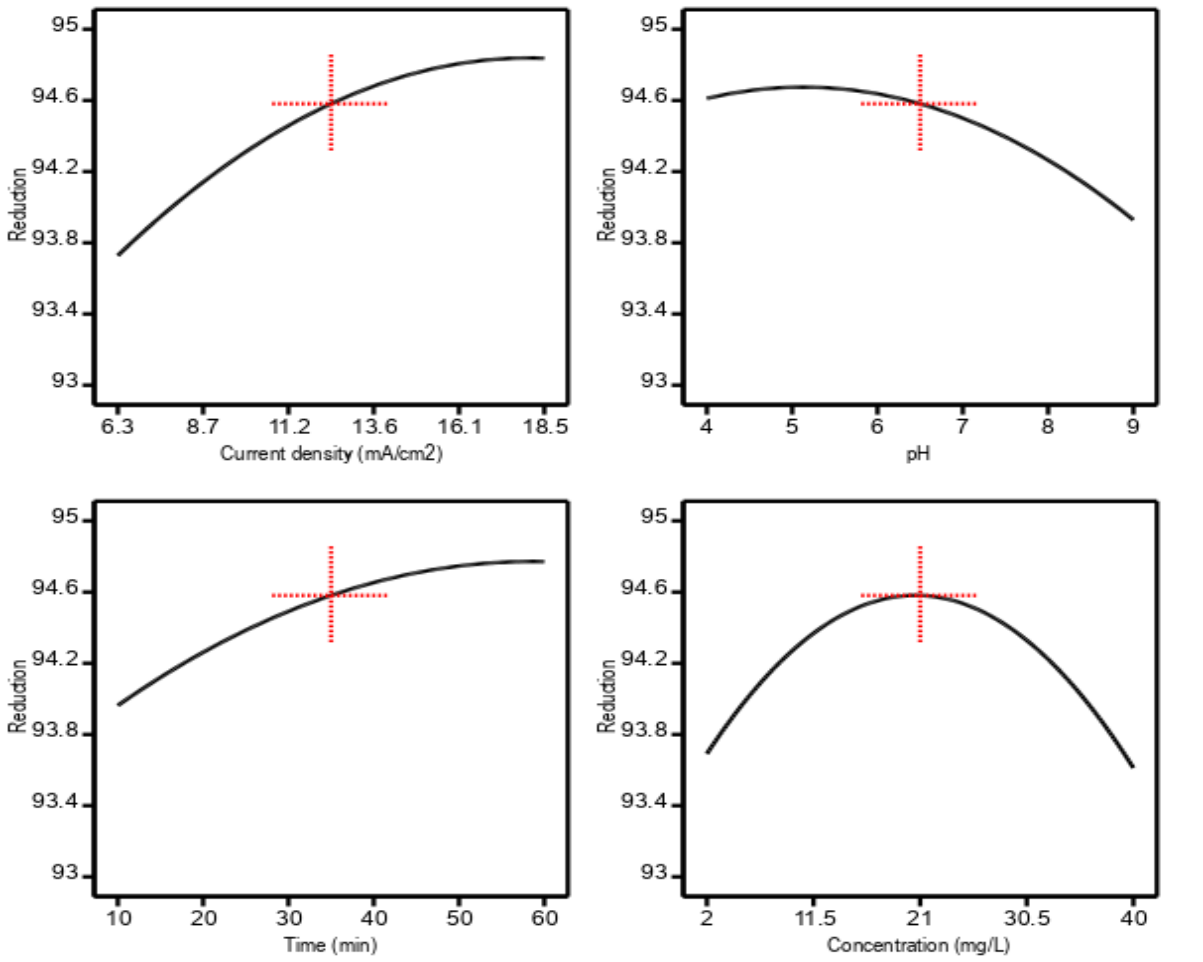

Figure 2.5: Main effect plots of parameters for fluoride removal efficiency on Fe-EC reactor

However, removal efficiencies started to decline when the J ≥ 16.1 $mAcm^{-2}$ for Fe-EC and J ≥ 50 mA/cm^2 for Al-EC. Higher current density means high generation of coagulant near the electrode that restrict the free movement of particles causing over potential to build up in the reactor due to ohmic drop (Nasrullah et al., 2012). This prevents further adsorption of the fluoride ion as observed at J ≥ 16.1$mAcm^{-2}$ and J ≥ 50 $mAcm^{-2}$. The ohmic drop was also confirmed that at the same treatment time both reactors attained the same amount of coagulant dosage of 0.000063 g/L. It can be ascertained that at the coagulant dose ≥ 0.000063 g/L no further fluoride reduction can be achieved as the kinetic of particles become restricted. The lower ohmic drop in Fe-EC than Al-EC is attributed to the higher molar mass of iron that achieved the same amount of coagulant as aluminum at lower electric current by a factor of ~0.3.

2.2.3.2 Initial fluoride concentration

The influence of initial fluoride concentration appears to be similar to both Al-EC and Fe-EC systems. For Al-EC, at a lower fluoride concentration starting from 2 mg/L to 26 mg/L there is increase in fluoride reduction rate from 78% to 95%. At this point the ratio between adsorbate (F-) and adsorbent $Al(OH)_3$ and $Fe(OH)_3$ is very low and permits rapid uptake of fluoride. But as the initial fluoride level reaches ~27 mg/L the removal rate slows down and remains constant as its limited by availability of free surfaces on the coagulant for further uptake (Vasudevan, Lakshmi, & Sozhan, 2009). However, above 30 mg/L, the reduction appears to decrease to 92%. Likewise, for Fe-EC the removal increases with initial fluoride concentration from 2 mg/L and reaches maximum at 21 mg/L. Above this level there is decrease in removal efficiency to 91% from 95% at highest initial concentration of 40 mg/L. The decrease in removal is due to competition for complexation sites which limit fluoride removal and subsequence further stirring tend to lead to desorption (Vasudevan et al., 2009). This study also found that $Fe(OH)_3$ reaches saturation point at a lower fluoride concentration of 21 mg/L compared to 27 mg/L of $Al(OH)_3$.

2.2.3.3 Initial pH of the water sample

From the plot, it is interesting to see that the fluoride removal by Al-EC increases 78%-96% as the initial pH of the sample increase. The maximum fluoride removal being attained at pH 7.5 - 8.5. This is because at a lower pH ~ 4 there is a higher hydrogen ion concentration leading to formation of soluble HF. At a pH $\geq$ 4 amorphous hydroxide $Al(OH)_3$ starts to form due to hydrolysis of water at the cathode, the amount of this amorphous further increases with pH as more hydroxide is added that lead to more uptake of fluoride. The amorphous $Al(OH)_3$ has minimum solubility and is finally polymerized into $Aln(OH)_{3n}$, which results into dense flocs formation with large surface area (Holt et al., 1999) for high fluoride uptake. However, at pH $\geq$ 9 the removal remains constant signifying formation of negatively charged aluminum hydroxide $Al(OH)_4^-$ that repels with the fluoride ion in the solution (Mechelhoff et al., 2013). Meanwhile, Fe-EC behaves differently, the highest reduction is attained at pH 4.5 - 5.5 beyond which there is insignificantly slow down from 95% to 92% at pH 9. In acidic medium there is higher dissolution of iron (Cañizares et al., 2007) leading to the formation of high amount coagulant $Fe(OH)_2$. Study by (Sasson et al., 2009) also revealed significant high Fe^{2+} dissolution rate at pH values of 5 - 6 than that at pH 8 - 9. In this context, it is important to note that the chemical dissolution of the electrode surfaces is promoted at alkaline pHs (for the case of aluminum) and at acidic pHs (for the case of iron).

2.2.3.4 Treatment time

In this investigation, the reduction efficiencies in both aluminum and iron electrodes appeared to exhibit exponential relation to time. For Al-EC there is an increase in fluoride reduction from 90% at 10 min to 93% with the maximum removal at 40 min. After 40 min, there is significant decrease on removal efficiency to 91.7% in 60 min. For the Fe-EC, a similar trend is observed, however the removal efficiency remained constant at a longer time of 50 to 60 min. This indicates that further treatment time beyond 40 min and 50 min for Al-EC and Fe-EC, respectively have negative influence on the fluoride removal. In both cases during the first 10 minutes there is appreciable enough in situ generated hydroxides of aluminum and iron to reduce fluoride by 90%. The longer time needed for iron to reach maximum fluoride reduction may be due to small current density applied during this investigation as compared to aluminum electrode. This is attributed to high adsorption capacity of in situ generated aluminum coagulant for fluoride ion (Smedley et al., 2003).

2.2.4 Combined effect of operational parameters on fluoride removal efficiency

The current density is considered as the key factor controlling efficiency of any electrocoagulation reaction (Moussa, El-Naas, et al., 2017). However, in this study other factors when correlated to current density are observed to limit fluoride removal in both reactors (Figure 2.6 and 2.7 (a), (b) (c) Generally, the maximum fluoride removal observed is ~96% and ~94% for Al-EC and Fe-EC, respectively. At a lower treatment time $\leq$ 39 min and $\leq$ 45 min and initial fluoride concentration $\leq$ 27 mg/L and $\leq$ 21 mg/L for Al-EC and Fe-EC, respectively; the removal increased at all current density applied. However, above these levels there is significant reduction in fluoride removal, despite the increase in current density. This indicates that the treatment time and initial fluoride concentration are limiting factors in their higher levels. Despite further dissolution of Al^{3+} and Fe^{2+} as the function of current and time, when the $F^-/Al(OH)_3$ and $F^-/Fe(OH)_2$ is $\geq$ 1 adsorption can't take place (Vasudevan et al., 2009). Figures 2.6 and 2.7 (d) also verify similar finding that an increase in treatment time at initial concentration $\geq$ 27 mg/L and $\geq$ 21 mg/L has no significant impact on the fluoride removal. At any suggested operation condition of current density, initial pH and treatment time, the maximum initial fluoride that can be removed effectively (i.e. $\leq$ 1.5 mg/L) is 27 mg/L and 21 mg/L for Al-EC and Fe-EC, respectively.

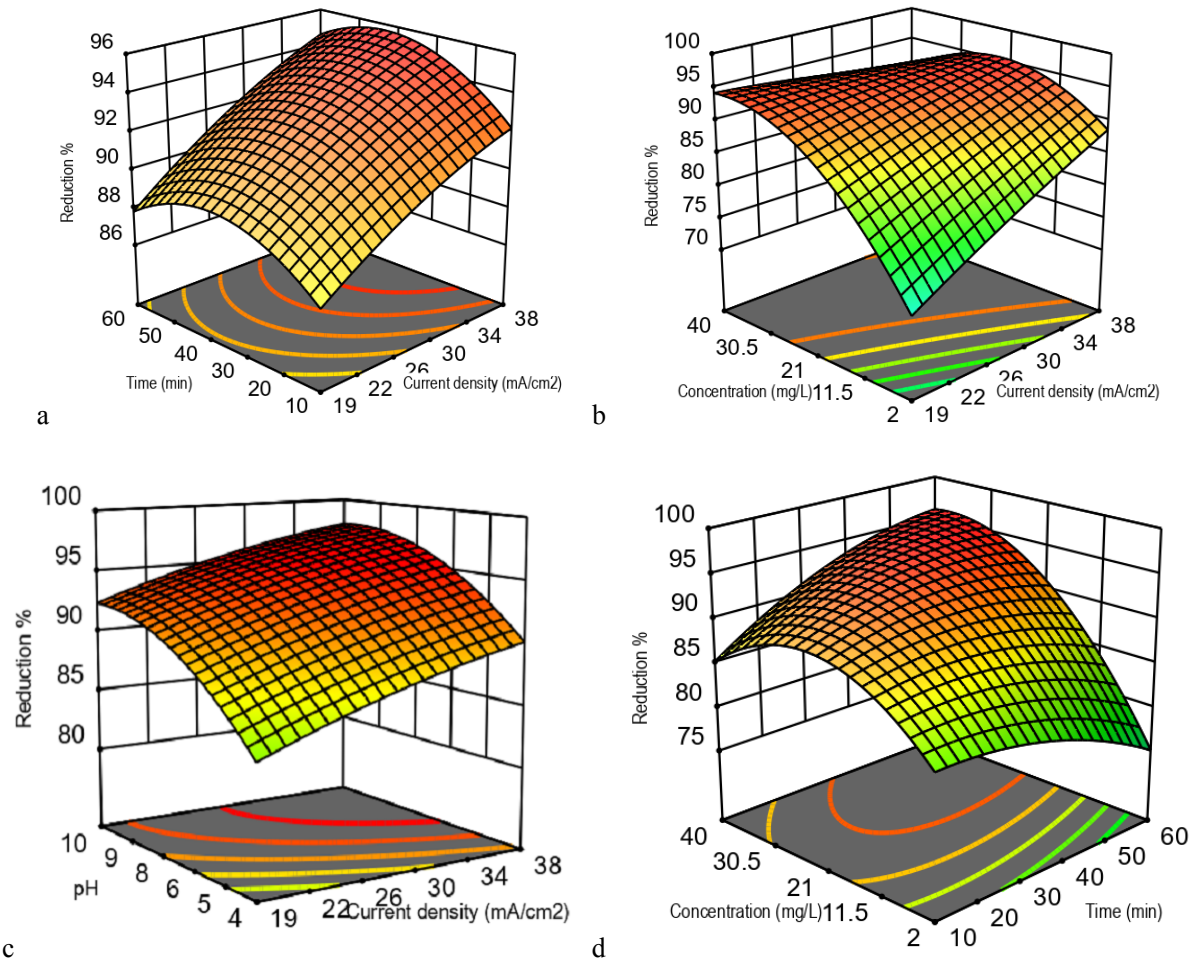

Figure 2.6: Surface plots with contour as a function of (a) treatment time and current density at pH 6.5 and initial concentration 21 mg/L (b) initial concentration and current density at pH 6.5 and treatment time 35 min (c) pH and current density at initial concentration of 21 mg/L and time 35 min (d) concentration and time at current density 28 $mAcm^{-2}$ and pH 6.5.

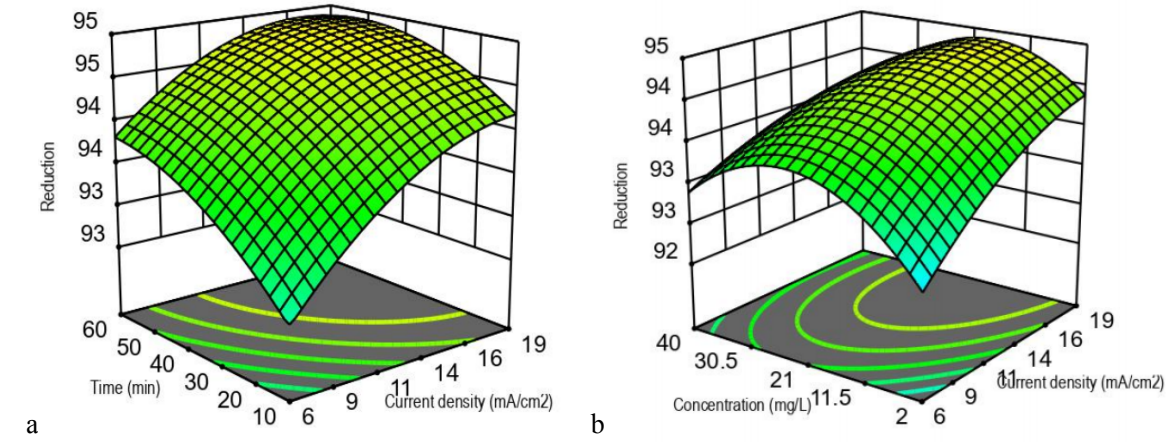

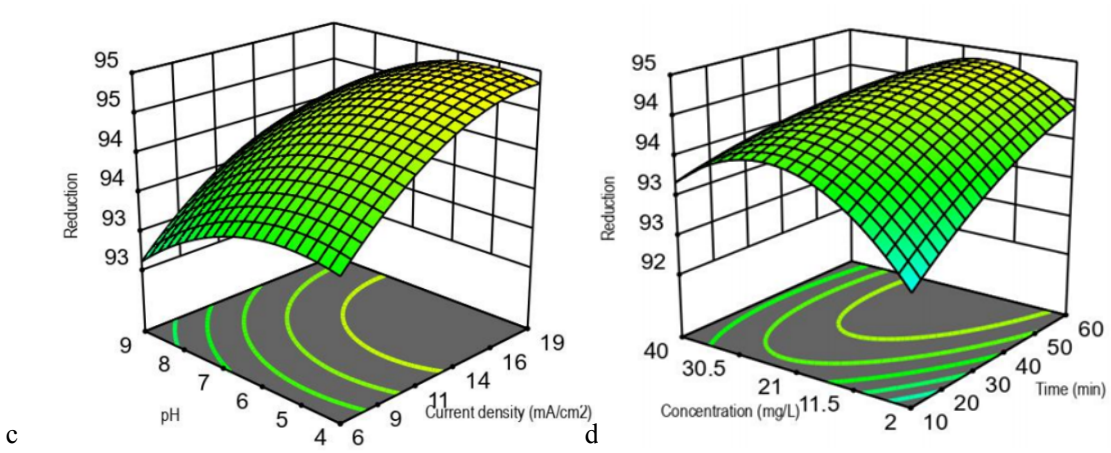

c d

Figure 2.7: Surface plots with contour as a function of (a) treatment time and current density at pH 6.5 and initial concentration 21 mg/L (b) initial concentration and current density at pH 6.5 and treatment time 35min (c) pH and current density at initial concentration of 21 mg/L and time 35min (d) concentration and time at current density 12.4 $mAcm^{-2}$ and pH 6.5.

2.2.5 Model equations

2.2.5.1 Final equation in terms of coded factors

The final regression model in terms of coded factors has been expressed by the following second-order polynomial equations:

2.2.5.2 Final equation in terms of actual factors

In terms of actual factors, an empirical relationship between F- removal efficiency and the variables has been expressed by the following second-order polynomial equations:

2.2.6 Fluoride removal by Al-EC and Fe-EC optimization

The main objective of optimization was to determine the optimum values of variables for fluoride removal with EC from the model obtained using experimental data. In both reactors Al-EC and Fe-EC, the operating parameters were chosen so as to maximize fluoride reduction at the

minimal current density, pH, initial fluoride concentration and treatment time were left at a range. Several sets of experiments were suggested by the model and two of them were performed.

Table 2.4: Experimental and predicted results on a few selected solutions suggested for optimization tests for AL-EC and Fe-EC

Reactor	S/N	J	pH	Time	Fo	Ft	Actual	Pred
Al-EC	1	18.50	6.80	50.00	16.00	0.92	94.25	95.00
	2	19.56	6.50	50.00	29.00	1.97	93.00	95.31
Fe-EC	1	06.25	6.50	50.00	16.00	1,28	92.00	94.10
	2	06.25	6.80	55.00	20.00	1.67	91.65	93.92

From the experimental results shown in Table 2.4, Al-EC achieved the reduction of initial 16 mg/L to 0.92 mg/L that satisfies WHO minimum fluoride level for drinking water. This 94.25% reduction was achieved at optimal conditions of initial fluoride concentration of 16 mg/L, current density 18.5 $mAcm^{-2}$ initial pH 6.8 and treatment time 50 min. For the Fe-EC, the best removal was predicted to be 94% at initial fluoride concentration of 16 mg/L, current density 6.25 $mAcm^{-2}$ in 50 minutes. The observed result at this optimum condition was 92.00% that confirmed to be close to the predicted removal.

2.3 Conclusion

In this research work, the effects of four main parameters in the electrocoagulation process, i.e., initial pH, initial fluoride concentration, current density and reaction time were evaluated and compared on the reduction of fluoride in Al-EC and Fe-EC reactors. The results showed that the initial fluoride concentration was a significant factor on Al-EC reactor and current density was the only main factor in Fe-EC reactor. The ANOVA results presented fairly R^2 values of 79.23% and 75.45% for Al-EC and Fe-EC fluoride removal, respectively, indicating the good accuracy of the polynomial models for both models. From the optimization, the Al-EC attained 94% fluoride removal at initial pH of 6.8, initial fluoride concentration of 16 mg/L, current density of 18.5 $mAcm^{-2}$ and reaction time of 50 min. The Fe-EC attained 92% removal at pH of 6.5, initial fluoride concentration of 16 mg/L, current density of 6.25 $mAcm^{-2}$ and reaction time of 50 min. It

can be ascertained that both electrodes Al and Fe attained reduction of fluoride to a permissible WHO standard for drinking water (≤ 1.5 mg/L) at optimized operational parameters.

2.4 References

Amani-Ghadim, A. R., Aber, S., Olad, A., & Ashassi-Sorkhabi, H. (2013). Optimization of electrocoagulation process for removal of an azo dye using response surface methodology and investigation on the occurrence of destructive side reactions. Chemical Engineering and Processing: Process Intensification. https://doi.org/10.1016/j.cep.2012.10.012

Behbahani, M., Moghaddam, M. R. A., & Arami, M. (2011). Techno-economical evaluation of fluoride removal by electrocoagulation process: Optimization through response surface methodology. Desalination, 271(1–3), 209–218. https://doi.org/10.1016/j.desal.2010.12.033

Box, G. E. P., & Behnken, D. W. (1960). Some New Three Level Designs for the Study of Quantitative Variables. Technometrics. https://doi.org/10.1080/00401706.1960.10489912

Cañizares, P., Jiménez, C., Martínez, F., Sáez, C., & Rodrigo, M. A. (2007). Study of the electrocoagulation process using aluminum and iron electrodes. Industrial and Engineering Chemistry Research, 46(19), 6189–6195. https://doi.org/10.1021/ie070059f

Daghrir, R., Drogui, P., & Zaviska, F. (2013). Effectiveness of a hybrid process combining electro-coagulation and electro-oxidation for the treatment of domestic wastewaters using response surface methodology. Journal of Environmental Science and Health - Part A Toxic/Hazardous Substances and Environmental Engineering. https://doi.org/10.1080/10934529.2013.726840

Fawell, J., Bailey, K., Chilton, J., Dahi, E., & Magara, Y. (2006). Fluoride in drinking-water. IWA publishing.

García-Lara, A. M., & Montero-Ocampo, C. (2010). Improvement of arsenic electro-removal from undergroundwater by lowering the interference of other ions. Water, Air, and Soil Pollution, 205(1–4), 237.

Holt, P., Barton, G., & Mitchell, C. (1999). Electrocoagulation as a wastewater treatment. The Third Annual Australian Environmental Engineering Research Event, 1000, 41–46.

Karimifard, S., & Moghaddam, M. R. A. (2018). Application of response surface methodology

in physicochemical removal of dyes from wastewater: A critical review. Science of The Total Environment, 640, 772–797.

Khedmati, M., Khodaii, A., & Haghshenas, H. F. (2017). A study on moisture susceptibility of stone matrix warm mix asphalt. Construction and Building Materials, 144, 42–49. https://doi.org/10.1016/j.conbuildmat.2017.03.121

Kobya, M, Hiz, H., Senturk, E., Aydiner, C., & Demirbas, E. (2006). Treatment of potato chips manufacturing wastewater by electrocoagulation. Desalination, 190(1–3), 201–211.

Kobya, Mehmet, Ulu, F., Gebologlu, U., Demirbas, E., & Oncel, M. S. (2011). Treatment of potable water containing low concentration of arsenic with electrocoagulation: Different connection modes and Fe–Al electrodes. Separation and Purification Technology, 77(3), 283–293.

Mansouri, K., Ibrik, K., Bensalah, N., & Abdel-Wahab, A. (2011). Anodic dissolution of pure Aluminum during electrocoagulation process: Influence of supporting electrolyte, initial pH, and current density. Industrial & Engineering Chemistry Research, 50(23), 13362–13372.

Mechelhoff, M., Kelsall, G. H., & Graham, N. J. D. (2013). Super-faradaic charge yields for Aluminum dissolution in neutral aqueous solutions. Chemical Engineering Science, 95, 353–359.

Mohapatra, M., Anand, S., Mishra, B. K., Giles, D. E., & Singh, P. (2009). Review of fluoride removal from drinking water. Journal of Environmental Management, 91(1), 67–77.

Moussa, D. T., El-naas, M. H., Nasser, M., & Al-marri, M. J. (2017). A comprehensive review of electrocoagulation for water treatment : Potentials and challenges. Journal of Environmental Management, 186, 24–41. https://doi.org/10.1016/j.jenvman.2016.10.032

Moussa, D. T., El-Naas, M. H., Nasser, M., & Al-Marri, M. J. (2017). A comprehensive review of electrocoagulation for water treatment: Potentials and challenges. Journal of Environmental Management, 186, 24–41.

Nasrullah, M., Singh, L., & Wahid, Z. A. (2012). Treatment of Sewage by Electrocoagulation and the Effect of High Current Density. Energy and Environmental Engineering Journal,

1(1), 27–31.

Osterwalder, L., Johnson, C. A., Yang, H., & Johnston, R. B. (2014). Multi-criteria assessment of community-based fluoride-removal technologies for rural Ethiopia. Science of The Total Environment, 488, 532–538.

Sasson, M. Ben, Calmano, W., & Adin, A. (2009). Iron-oxidation processes in an electroflocculation (electrocoagulation) cell. Journal of Hazardous Materials, 171(1–3), 704–709. https://doi.org/10.1016/j.jhazmat.2009.06.057

Smedley, P. L., Zhang, M., Zhang, G., & Luo, Z. (2003). Mobilisation of arsenic and other trace elements in fluviolacustrine aquifers of the Huhhot Basin, Inner Mongolia. Applied Geochemistry, 18(9), 1453–1477. https://doi.org/10.1016/S0883-2927(03)00062-3

Tir, M., & Moulai-Mostefa, N. (2008). Optimization of oil removal from oily wastewater by electrocoagulation using response surface method. Journal of Hazardous Materials. https://doi.org/10.1016/j.jhazmat.2008.01.051

Vasudevan, S., Lakshmi, J., & Sozhan, G. (2009). Studies on a Mg-Al-Zn alloy as an anode for the removal of fluoride from drinking water in an electrocoagulation process. Clean - Soil, Air, Water. https://doi.org/10.1002/clen.200900031

Comparative Study on Adsorption Isotherm and Kinetics of Defluoridation using Aluminum and Iron Electrodes in Electrocoagulation

Abstract

Adsorption equilibrium and kinetics of fluoride removal by aluminum and iron electrodes in electrocoagulation technology were investigated and compared in a batch reactor. Adsorption equilibrium for Al-EC and Fe-EC were conducted at a range of current density (*J*) 19-38 $mAcm^{-2}$ and 10-18.50 $mAcm^{-2}$, respectively, while the treatment time was at a range of 15-60 min to study the adsorption kinetics. The surfaces of flocs produced were characterized using Fourier Transform Infrared Spectroscopy (FTIR). The adsorption equilibrium and kinetics of fluoride in both Al-EC and Fe-EC fitted well with the Freundlich model and pseudo second order. The removal mechanisms of fluoride were through ion exchange and electrostatic attraction in Al-EC and Fe-EC, respectively both occurred spontaneously and were physical in nature. The $Al(OH)_3$ and $Fe(OH)_2$ exhibited monolayer adsorption capacities of 131 and 0.08 mg/g, respectively. Thus, the $Al(OH)_3$ in Al-EC is a better candidate for defluoridation compared to $Fe(OH)_2$ of Fe-EC during electrocoagulation technology.

Keywords: Electrocoagulation, remediation, adsorption, defluoridation

2.5 Introduction

Dental and skeletal fluorosis due to consumption of groundwater containing elevated levels of fluoride ≥ 1.5 mg/L has been a major health concern in the East African rift-valley zone (Demelash et al., 2019; Malago et al., 2017). The fluorosis is reported to affect 70-90% of population of people living in the Eas Africa Rift valley (Mohammadi et al., 2017). Despite the efforts to remediate fluoride from water sources, the available methods are still facing challenges mainly to users. For example, the Nalgonda method requires high chemical coagulants for effective fluoride removal, resulting into a high sludge production that becomes a challenge in their disposal (Marwa et al., 2018). On the other hand, the use of bone char faces rejection by some users because of its smell and offensive taste mainly when bone char is poorly produced (Mohammadi et al., 2017). Therefore, efforts to investigate for an efficient, cost effective and green-technology option for remediation of fluoride are required.

The electrocoagulation (EC) has demonstrated to be the best alternative treatment method to avoid high production of sludge and smell as on chemical coagulation (Moussa et al., 2017). The EC method relies upon the generation of metal species from sacrificial Al or Fe electrodes accompanied with water electrolysis at the cathode to produce hydrogen and hydroxide ions, and electro-migration of the various charged species (Moussa et al., 2017). During EC, the metal ion dissolute from the anode while water at the surface of the cathode dissociates into H^+ and OH^- ions, the two react to form a mixture of metal oxy-(hydroxides) as adsorbent. There are various complexes that are formed in the reactor however, the dominant adsorbent being hydroxide of iron and aluminum. The adsorbent will then react with pollutant in various ways to form flocs during separation process. Though the mechanism of defluoridation is not well understood, the three suggested possible mechanisms for defluoridation using electrocoagulation, include adsorption on metal oxy-(hydroxide) particles, co-precipitation and attachment on the electrode surface (Nepo et al., 2017).

The removal mechanism by electrocoagulation depends on the kind of electrode, current density and pH of the solution (Nepo et al., 2017; Al-ghouti & Da, 2020). Currently, there is no single study conducted to compare the adsorption isotherm and kinetics of the defluoridation by aluminum and iron-based adsorbents generated in electrocoagulation. Therefore, this study

attempts to investigate and compare the adsorption isotherm and kinetic of the fluoride removal by the two systems, Al-EC and Fe-EC in a batch reactor.

2.6 Materials and methods

2.6.1 Adsorption isotherm

Equilibrium isotherm expresses the amount of adsorbate at equilibrium by a unit amount of adsorbent at constant temperature (Singh & Balomajumder, 2017). There are various isotherm models that can study behavior of the relationship between adsorbate and adsorbent at equilibrium, however in this study, experimental equilibrium data were fitted by two isotherm models: Freundlich and Langmuir models. The linear forms of each model equation and plot parameters are provided in Table 2.5. The Freundlich isotherm assumes that adsorbent has heterogeneous surface where each site possesses different affinity and they are non-uniformly distributed on the surface (Al-ghouti & Da, 2020). The Langmuir theory on the other hand, takes assumption that the adsorbent sites are uniform and homogenous and each site has equal chance of adsorbing pollutant. It assumes presence of equal energy on the adsorption sites (Al-ghouti & Da, 2020).

2.6.2 Adsorption kinetics

The mechanism involved in the removal of pollutant by electrocoagulation is similar to the chemical coagulation, differs only on production of coagulant. In electrocoagulation system, the amount of adsorbent that removes pollutant from solution can be estimated using Faraday's law (Equation 2.7). The kinetic modeling gives information about adsorption mechanisms and possible rate-controlling steps. The adsorption rate is an important factor for a better choice of material to be used as an adsorbent, where the adsorbent should have a large adsorption capacity higher affinity and a fast adsorption rate. In this study, the rate of fluoride adsorption on the surface of aluminum and iron oxy-hydroxides were evaluated by adsorption kinetic models: pseudo-first-order PFO and pseudo-second-order PSO while intra-particle diffusion IPD model was used to evaluate the rate of fluoride diffusion into the pores of the adsorbents (Wang & Guo, 2020). The linear equations and their associated plots are presented in Table 2.5.

Table 2.5: List of adsorption equilibrium models and adsorption kinetic models with their linear forms

Model	Linear form	Plot
Isothermal equilibrium model		
Langmuir		Ce (2.8)
Freundlich		vs (2.9)
Isothemal kinetic model		
Pseudo first order	(2.10)	
Pseudo second order	(2.11)	
Intraparticle diffusion	(2.12)	

Where; Ce is equilibrium concentration in solution (mg/L); qt and qe concentration at time t and at equilibrium in solid phase (mg/g);1/n is Freundlich adsorption intensity; qm monolayer maximum adsorption capacity (mg/g); K_F, K_L, equilibrium constant for Freundlich, Langmuir (L/mg); K_1, K_2 and Kin pseudo first order kinetic rate constant (h^{-1}), pseudo second order rate constant ($gmg^{-1}min^{-1}$), intra-particle diffusion kinetic rate constant ($gmg^{-1}\ h^{-0.5}$); t treatment time (min)

2.6.3 Material preparation

The sodium fluoride NaF (99.9 % purity) (Lions International Trading PLC, Ethiopia) was used to prepare solution of fluoride. To prepare the solution, 2.21 g of sodium fluoride was dissolved in 1000 mL of distilled water to make 1000 mg/L of fluoride in the stock solution. Then serial dilution (following dilution law) was used for a specific concentration preparation. On the other hand, electrodes of aluminum and iron electrodes plates (15 cm x 2 cm, each) were pre-cleaned by rubbing with sandpaper, rinsed in NaOH (2 M) and HCl (2 M) to remove particles on the surface. The electrodes were then dried at 105ºC before the start of experiments. Electrodes cleaning procedure followed ref (Khaled et al., 2019). After each experiment, electrodes were dissolved in 1 M hydrochloric acid for 10 minutes to remove any remaining particles on the surface that may reduce EC performance.

2.6.4 Experimental set up

The 800 cm^3 beaker was used as the lab-scale reactor to perform adsorption and kinetic studies at a working volume of 600 cm^3. The two aluminum or iron electrodes, each used as anode, were connected to other two as cathode in a monopolar parallel connection MP-P, making surface area of 80 cm^2 (4 surfaces x 10 x 2 cm) (Figure 2.8). Thus, the effective surface area to volume ratio of the reactors (S) becomes 0.13 cm^{-1}. The anodes and cathodes were placed alternatively and parallel to each other at a specific distance of 1.5 cm to ensure optimum hydrodynamic of particles in a reactor during reaction (Mameri et al., 1998). Thereafter, the end poles of sacrificial electrodes were connected to the direct current power source (BK Precision 1796), similar reactor set up was made for the iron electrode Fe-EC. The electric driving force to the electric current was maintained at 7V.

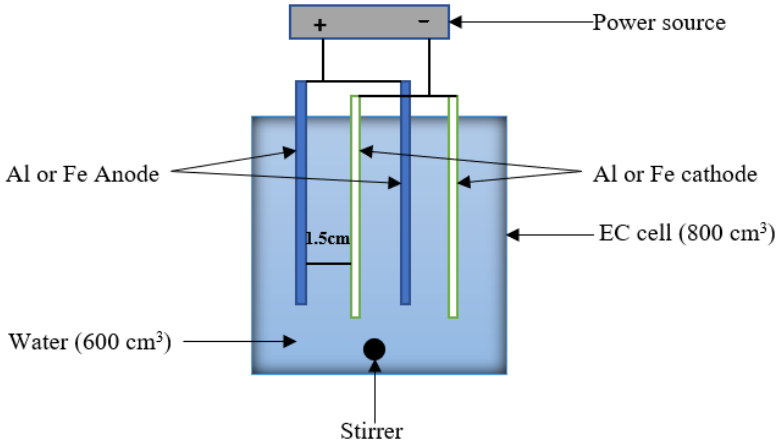

Figure 2.8: The monopolar parallel connection MP-P electrocoagulation setup

2.6.5 Adsorption equilibrium experiments

The experiments for adsorption equilibrium study were performed by varying the amount of adsorbents at a fixed concentration of fluoride. The adsorption isotherm study in Al-EC was conducted at different current density (*J*) of 19, 25, 32 and 38 $mAcm^{-2}$ corresponding to 0.29, 0.39, 0.48 and 0.58 g of $Al(OH)_3$. On the other hand, in Fe-EC experiments were performed at (*J*) 6.30, 10.30, 14.40 and 18.50 $mAcm^{-2}$ equivalent to 0.30, 0.49, 0.69, and 0.89 g of $Fe(OH)_2$. The range of the current density used for Al-EC and Fe-EC adsorption isotherm reactions were selected basing on our previous study (Nyangi et al., 2020). The reactions were conducted for 35 minutes while the initial pH was maintained at 6.5. The theoretical mass of adsorbent (m) was then calculated using Equation 2.13 (M is molar mass of Al (26.98 g/mol) and Fe (55.84 g/mol); F is Faraday constant (96485 C/mol); N is the number of electrons transferred, Al = 3 and Fe = 2. The initial concentration of fluoride (Co) used in both cases was fixed at 21 mg/L. Meanwhile, 1

M NaOH and 1 M HCl solutions were added for the pH adjustment during experiments. The amount of fluoride adsorbed at equilibrium was then calculated using Equation 2.14 (V is the volume of water sample, 0.6 L)**.**

(2.13)

(2.14)

2.6.6 Adsorption kinetic experiments

The kinetic study was performed using initial concentration of fluoride 21 mg/L at operation conditions of Al: J = 28 mAcm^{-2}; and Fe-EC: J = 12.45 mAcm^{-2} both at initial pH 6.5. The treatment time was varied at 10, 22, 34, and 48 minutes, where after each specific treatment time, 15 mL of the sample was quickly taken from the reactor for analysis. Then the amount of the fluoride adsorbed after treatment time (t) was calculated using Equation 2.15, while the percentage fluoride removal was calculated using Equation 2.16

(2.15)

(2.16)

2.6.7 Sample analyses

The analyses of water samples for fluoride were carried using Ionic Selective Electrode (ISE). Meanwhile, the residues of the floc samples were filtered, dried at 105 ˚C for 24 hours, and then analyzed using Fourier Transform Infrared (FT-IR) in a range 4000-450 cm^{-1}. Analysis of floc samples were performed in Department of Chemistry, Addis Ababa University. The MS Excel was used for nonlinear regression analysis method to obtain the least square fit for all the models.

2.7 Results and Discussion

2.7.1 Flocs characterization

FTIR analyses were performed in a range 4000–450 cm^{-1} using Spectrum 65 FT-IR (PerkinElmer) to analyze the chemical bonds of the elements present in a dried floc and the results is shown in Figure 2.9a and 2.9b. For the floc generated by Al-electrode Figure 2a, the peak with broad band observed at 3490-3550 cm^{-1} corresponds likely to the O-H stretch (Gross et al., 2007). Another stretching at 1100 cm^{-1} signifies the presence of the Al-O while a short wide band at 610 cm^{-1} is a characteristic stretch for Al-F and the bend at 1690 cm^{-1} indicates presence of Na-F bond (Drouiche et al., 2009). This suggests that the removal of fluoride to be through

ionic exchange by replacing hydroxyl ion of the $Al(OH)_3$. The aluminum flocs FTIR spectrogram matches with the study reported in literatures (Drouiche et al., 2009; Sundaram, et al., 2008)

The FTIR spectra for the sludge generated by Fe electrode Figure 2b, demonstrated main absorption bands at 590 cm^{-1} which is associated with Fe-O group, another band at 1030 cm^{-1} was due to vibration of crystalline Fe-O (Rout et al., 2015). The reduced band at 3450 cm^{-1} reflected the exchange of O-H vibration with the fluoride. Meanwhile, the presence of low intensity bands at 800 cm^{-1} may suggest the formation of O–H···F bond (Sundaram et al., 2008). The appearance of band at 460 cm^{-1} indicated bending vibration of strong and lower frequency O–F bond. Thus, the FTIR analysis indicates that the removal of fluoride by Al-EC could be through ionic exchange between hydroxyl of the aluminum hydroxide and the fluoride while the Fe-EC could remove fluoride by adsorption on the surface of iron oxyhydroxide.

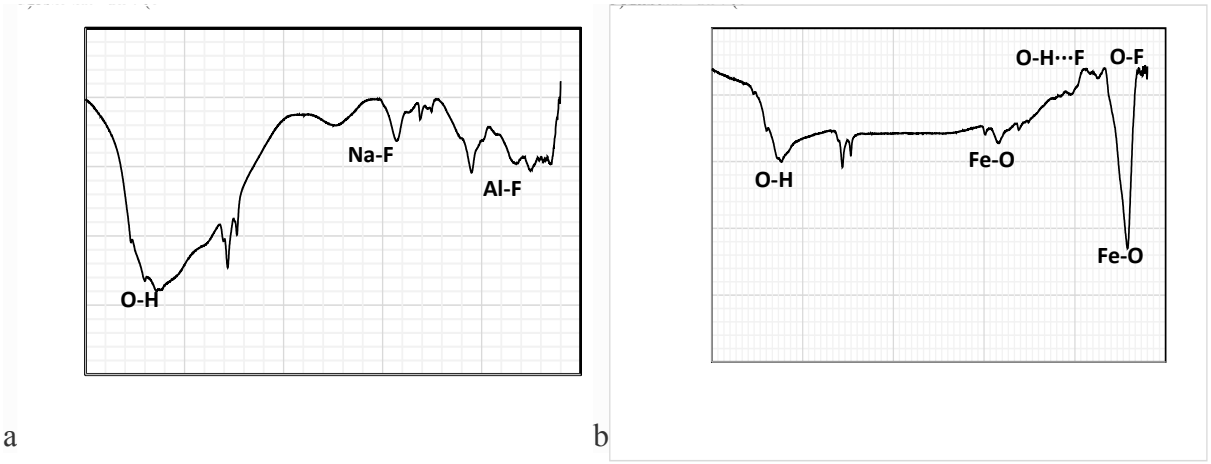

Figure 2.9: FTIR spectrum for (a) Al-EC floc and (b) Fe-EC generated floc

2.7.2 Effect of adsorbent dosage and treatment time

As revealed in Table 2.6 and Figure 2.10a there is higher percentage fluoride adsorbed in Al-EC than in Fe-EC reactor. However, in both cases the removal efficiency increased with the increase in the mass of adsorbent. At lowest adsorbent dosage of 0.29 and 0.30 g of $Al(OH)_3$ and $Fe(OH)_2$, respectively the fluoride removal were 89 and 87 %, respectively. This is attributed to the fact that at a low adsorbent dosage there is few surface sites for fluoride uptake leading to a low fluoride uptake. Moreover, when the mass of adsorbent increases to 0.58 and 0.86 g the percentage removal reaches 95 and 96 % for Al-EC and Fe-EC, respectively. As the adsorbent dosage tend to increase it provides more surface sites as well as increase on the driving force for the fluoride uptake (Rout et al., 2015). As it can be seen in the Figure 2.10a the curves appears to

flaterning as the adsorbent dosage increases suggesting the adsrption to be approaching equilibrium. Meanwhile, there was a sharp increase on the fluoride removal with time up to 22 min in both Al-EC and Fe-EC (Figure 2.10b). This is due to the fact that the metal dissolution Al^{3+} and Fe^{2+} and subsequence adsorbents formation is dependent on treatment time according to the Faraday's law. Treatment time determines flocs growth, and charge loading to the reactor (Kobya et al., 2016), however, at 22 min and above, corresponding to the charge load Q = (It/V) ≥ 82.13 C/L and 36.22 C/L for Al-EC and Fe-EC, respectively there were decrease on the fluoride adsorption (Al-EC; J = 28 mAcm^{-2} & Fe-EC: J = 12.45 mAcm^{-2}; V = 0.6 L). This may be caused by excessive mass accumulated in a reactor that leads to the IR drop and subsequent decline in the fluoride uptake (Kobya et al., 2011).

Table 2.6: The effect of $Al(OH)_3$ and $Fe(OH)_2$ adsorbent dosage on the removal of fluoride from water

$Al(OH)_3$ g	CoF	Ce	Removal %	$Fe(OH)_2$ g	Ce	Removal %
0.29	21.00	2.31	89.00	0.30	2.73	87.00
0.39	21.00	1.68	92.00	0.49	1.68	92.00
0.49	21.00	1.26	94.00	0.69	1.09	94.80
0.58	21.00	1.05	95.00	0.89	0.84	96.00

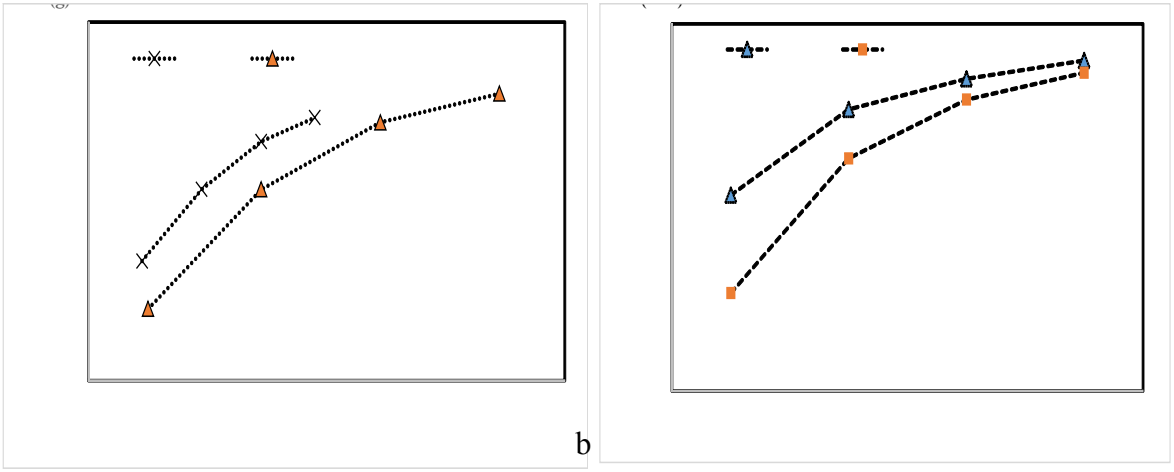

a b

Figure 2.10: Effect of (a) adsorbent dosage in 35 minutes (b) treatment time by 0.4 g of adsorbent on the adsorption of fluoride by Al-EC and Fe-EC

2.7.3 Adsorption isotherm parameters

As shown in Table 2.7 and Figure 2.11a-c adsorption of fluoride in both Al-EC and Fe-EC presented higher correlation values (R^2) to the Freundlich model than Langmuir. The Freundlich model has R^2 of 0.998 and 0.999 to the to Al-EC and Fe-EC, respectively, implying that the adsorption of fluoride in Al-EC and Fe-EC is well described by the Freundlich model. This means that the adsorption of fluoride on the surfaces of both $Al(OH)_3$ and $Fe(OH)_2$ were not equaly distributed in term of heat and affinity of adsorption, and both surfaces sites are heterogenous (Al-ghouti & Da, 2020). The fluoride molecules were adsorbed sequantially basing on the affinity of the adsorbent surface, starting with stronger binding sites. This led to the removal through the formation of multilayer surfaces (Al-ghouti & Da, 2020). On the other hand, the Freundlich constants (1/n) values were found to be 0.78 and 0.83 to Al-EC and Fe-EC, respectively, confirming favorable fluoride adsorption to both $Al(OH)_3$ and $Fe(OH)_2$ (Al-ghouti & Da, 2020). However, as shown by Freundlich model, F-$Al(OH)_3$ have the K_F = 981 L/mg and F-$Fe(OH)_2$ the K_F = 571 L/mg which means that $Al(OH)_3$ exhibits higher affinity to fluoride than the $Fe(OH)_2$.

Moreover, the separation factor (calculated from); lies $0 < R_L < 1$ as found in the Langmuir model suggests favorable adsorption of fluoride to both Al-OH and $Fe(OH)_2$ (Al-ghouti & Da, 2020). Meanwhile, the monolayer adsorption capacity for $Al(OH)_3$ and $Fe(OH)_2$ are found to be 131 mg/g, and 0.08 mg/g. The higher adsorption capacity by $Al(OH)_3$ could be due to the higher electropositivity value of Al than Fe that permits higher affinity to fluoride. To find the free energy released during adsorption of fluoride on the $Al(OH)_3$ and $Fe(OH)_2$, the Langmuir equilibrium constant (K_L) was utilized in the equation $\Delta G = -RTlnK'$, where $K' = K_L*M*0.055$ (Zhou & Zhou, 2014). Here (R is the gas constant 8.314 kJ/mol; T is the room temperature 298 K and K' equlibrium constant). The values for ΔG are found to be -3.89 kJ/mol and -3.31 kJ/mol for F-$Al(OH)_3$ and F-$Fe(OH)_2$, respectively. This suggests the adsorption of fluoride to both $Al(OH)_3$ and $Fe(OH)_2$ to be spontenous and physical in nature. The higher adsorption energy in F-$Al(OH)_3$ further proof stronger affinity of $Al(OH)_3$ towards fluoride compared to that of F-$Fe(OH)_2$ which could be attributed to the higher electropositivity of Al than the Fe leading to a stronger electrostatic bond between Al-F.

Table 2.7: Parameter values from adsorption models of fluoride removal by Al-EC and Fe-EC

Model	Parameter	Al-EC	Fe-EC
Langmuir	R^2	0.998	0.950
	qm (mg/g)	131	0.08
	R_L	0.21	0.01
	K_L (L/mg)	0.18	3.30
Freundlich	R^2	0.999	0.998
	1/n	0.78	0.83
	K_F (L/mg)	981	573

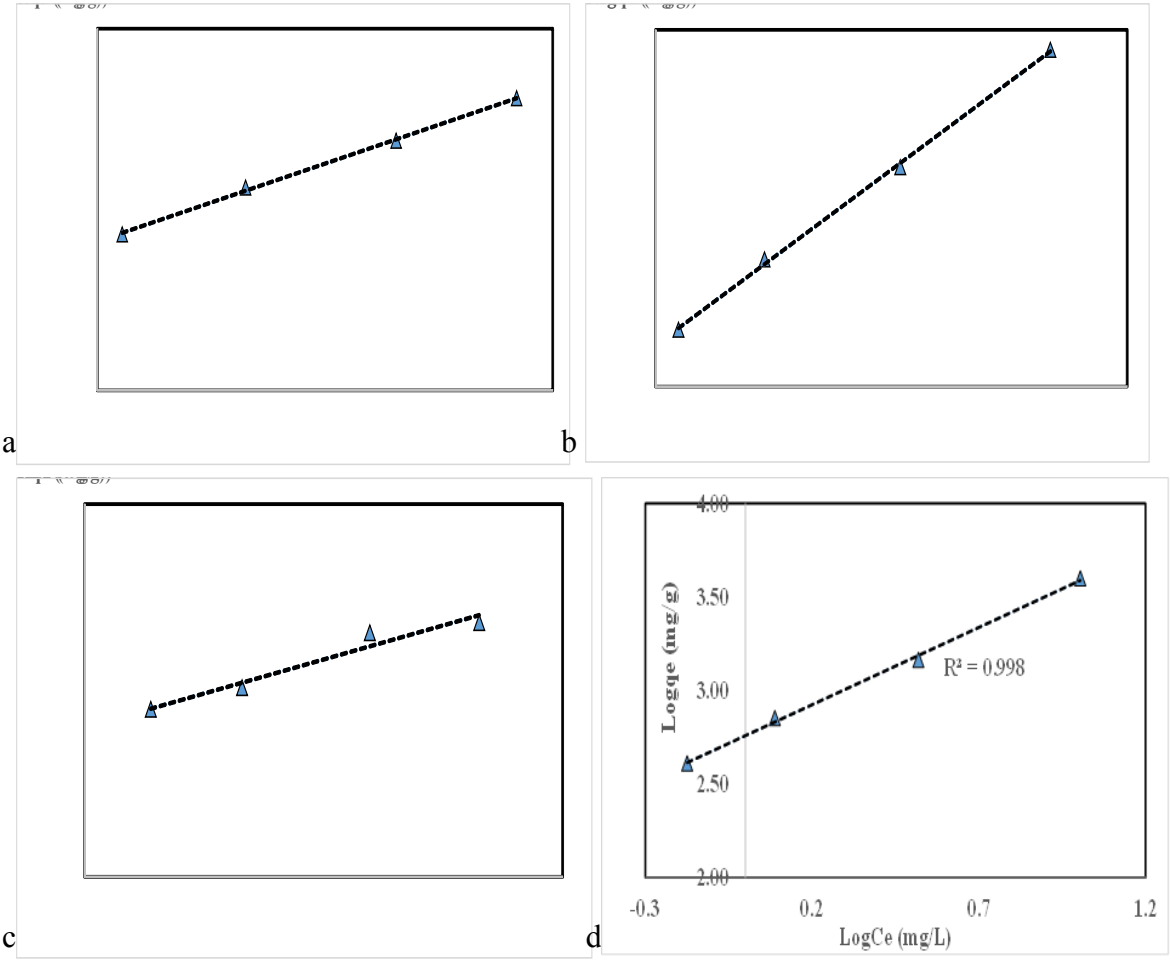

Figure 2.11: Adsorption isotherm plots for (a)(c) Langmuir model (b)(d) Freundlich isotherm model for adsorption of fluoride in Al-EC and Fe-EC, respectively

2.7.4 Adsorption kinetic parameters

Parameters of the pseudo-first order, pseudo-second order and intra-particle diffusion and their validation results have been reported in Table 2.8 and Figure 2.12a-c, respectively. The second order kinetic model exhibited highest correlation values $R^2 = 1$ and 0.999 to Al-EC and Fe-EC, respectively (Figure 2.12b) suggesting that the kinetic of defluoridation by $Al(OH)_3$ and $Fe(OH)_2$ were controlled by pseudo second order. By obeying pseudo second order it signifies that both adsorbent have abundant of active sites (Wang & Guo, 2020) and in this case the rate of fluoride adsorption onto $Al(OH)_3$ and $Fe(OH)_2$ were 0.007 g/mg/min[1]) and 0.003 g/mg/min), respectively. The higher rate of fluoride adsorption towards $Al(OH)_3$ than $Fe(OH)_3$ could be due to the higher adsorption affinity of $Al(OH)_3$ to fluoride as shown in the Freundlich constant K_F value found in this work.

The intra-particle model was evaluated to deduce diffusion mechanism of the fluoride onto the surface of adsorbents. In this study the plot presented one linear line with fairly correlation $R^2 =$ 0.932 and 0.940 for Al-EC and Fe-EC, respectively (Figure 2.12c) suggesting that the diffusion of fluoride onto the surface of adsorbents was also the rate limiting step for fluoride uptake. However, the lines of linearity in both cases did not pass through the origin which reflect that the rate of fluoride uptake during initial stages and final stages differ and that adsorption is limited by other kinetic models that could be operating simultaneously as well (Lattanzi et al., 2020). Moreover, the value of diffusion layer boundary (C) that gives the idea about thickness of the boundary layer between adsorbate-adsorbent interfaces are found to be appear to be 8.87 and 17.23 mg/g in the Fe-EC and Al-EC reactors, respectively. The larger the intercept the greater is the boundary layer effect and the slower the rate (Lattanzi et al., 2020), as a results the rate of fluoride diffusing towards $Fe(OH)_2$ (2.987 g/mg $h^{-0.5}$) was higher than that towards $Al(OH)_3$ (1.81 g/mg $h^{-0.5}$). This implies that the rate of fluoride uptake into the pores on the surface of adsorbent was also controlled by the boundary layer/film formed.

Table 2.8: List of parameters and their values obtained from Pseudo-first-order, Pseudo-second-order and Intra-particle diffusion kinetic model parameters.

Kinetic model	Parameter	Al-EC	Fe-EC
Pseudo first order	R^2	0.947	0.982
	qe (mg/g)	29.52	35.94
	K_1 (min^{-1})	0.116	0.098
Pseudo second order	R^2	1	0.99
	qe. (mg/g)	32.25	34.32
	K_2 (g/mg/min)	0.007	0.003
Intraparticle model	R^2	0.932	0.940
	C	17.234	8.87
	K_{in} (g/mg $h^{-0.5}$)	1.81	2.987

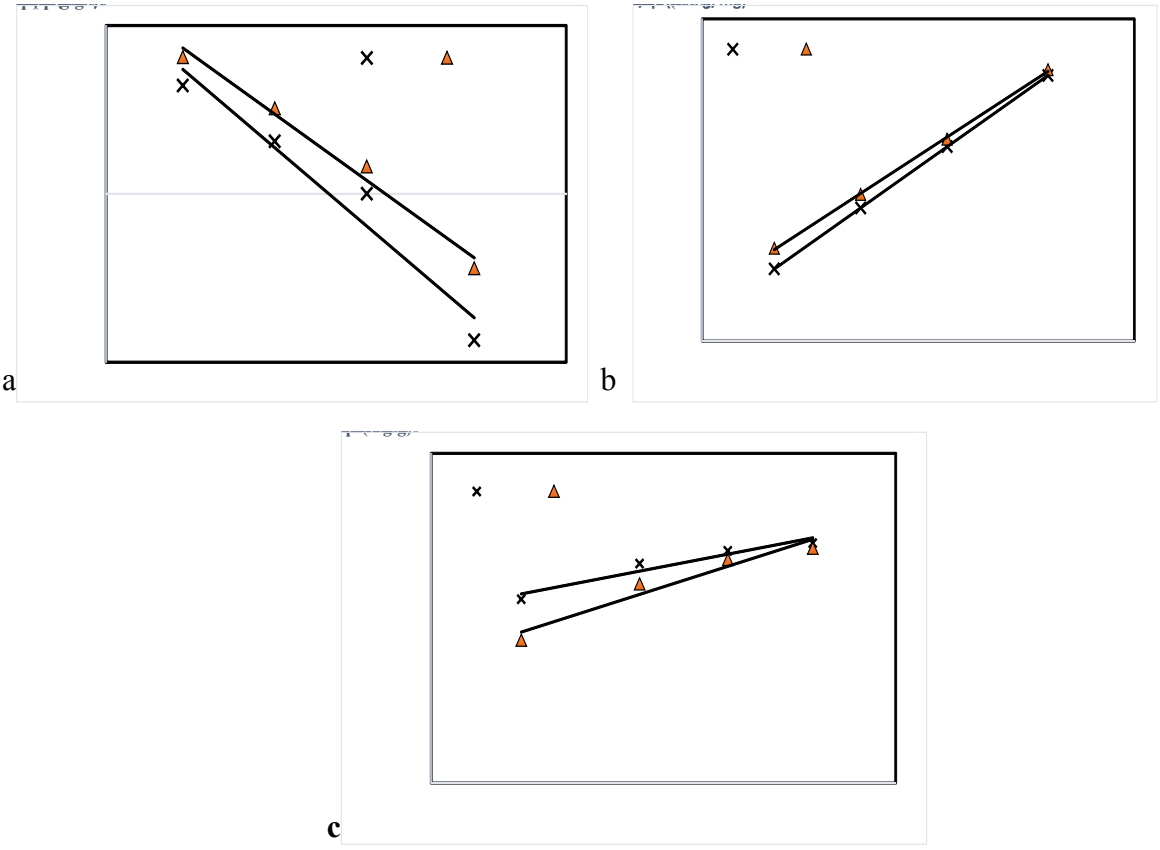

Figure 2.12: Plots for (a) pseudo first order (b) pseudo second order (c) intra-particle diffusion models for adsorption kinetic of fluoride in Al-EC and Fe-EC

2.7.5 Suggested removal mechanisms of fluoride by Al-EC and Fe-EC

From adsorption isotherm models study analysis of flocs its evident that fluoride must have replaced hydroxide of $Al(OH)_3$ in Al-EC in an ionic exchange reaction. On the other hand, fluoride is found to be attached on the surface of $Fe(OH)_3$ and removed through adsorption. Reaction equations 2.17 and 2.18 represent suggested removal mechanisms of fluoride by $Al(OH)_3$ and $Fe(OH)_3$, respectively.

(2.17)

(2.18)

2.8 Conclusion

In this study the adsorption isotherm and kinetic experiments were performed to investigate and compare fluoride removal mechanisms by Al-EC and Fe-EC. As revealed by FTIR data, fluoride was removed by replacing hydroxide of $Al(OH)_3$ in Al-EC, while it was adsorbed or attached on the surface of $Fe(OH)_2$ in the Fe-EC. It can be ascertained that both electrodes Al and Fe followed Freundlich adsorption suggesting that the removal was through formation of multiple layers on the surface of both Al and Fe based adsorbents. The kinetic data fitted well with pseudo second order and that Intraparticle diffusion was not the sole step in the diffusion rate of fluoride through the pores of adsorbents in both cases. Thus, the Al-EC is found to have higher affinity and higher monolayer adsorption capacity to fluoride compared to Fe-EC making it better candidate to defluoridation.

2.9 References

Al-ghouti, M. A., & Da, D. A. (2020). Guidelines for the use and interpretation of adsorption isotherm models : A review. Journal of Hazardous Materials, 393(February), 122383. https://doi.org/10.1016/j.jhazmat.2020.122383

Malago, J., Makoba, E., & Muzuka, A. N. N. (2017). Fluoride Levels in Surface and Groundwater in Africa : A Review 2 . Sources of Fluoride in Surface and Groundwater in Africa. 3(1), 1–17. https://doi.org/10.11648/j.ajwse.20170301.11

Demelash, H., Beyene, A., Abebe, Z., & Melese, A. (2019). Fluoride concentration in groundwater and prevalence of dental fluorosis in Ethiopian Rift Valley: systematic review and meta-analysis. BMC Public Health, 19(1), 1298.

Drouiche, N., Aoudj, S., Hecini, M., Ghaffour, N., Lounici, H., & Mameri, N. (2009). Study on the treatment of photovoltaic wastewater using electrocoagulation: Fluoride removal with

Aluminum electrodes—Characteristics of products. Journal of Hazardous Materials, 169(1–3), 65–69.

Gross, U., Rüdiger, S., Kemnitz, E., Brzezinka, K.-W., Mukhopadhyay, S., Bailey, C., … Harrison, N. (2007). Vibrational analysis study of aluminum trifluoride phases. The Journal of Physical Chemistry A, 111(26), 5813–5819.

Khaled, B., Wided, B., Béchir, H., Elimame, E., Mouna, L., & Zied, T. (2019). Investigation of electrocoagulation reactor design parameters effect on the removal of cadmium from synthetic and phosphate industrial wastewater. Arabian Journal of Chemistry, 12(8), 1848–1859.

Kobya, M., Demirbas, E., & Ulu, F. (2016). Evaluation of operating parameters with respect to charge loading on the removal efficiency of arsenic from potable water by electrocoagulation. Biochemical Pharmacology. https://doi.org/10.1016/j.jece.2016.02.016

Kobya, M., Gebologlu, U., Ulu, F., Oncel, S., & Demirbas, E. (2011). Electrochimica Acta Removal of arsenic from drinking water by the electrocoagulation using Fe and Al electrodes. Electrochimica Acta, 56(14), 5060–5070. https://doi.org/10.1016/j.electacta.2011.03.086

Lattanzi, A. M., Pecha, M. B., Bharadwaj, V. S., & Ciesielski, P. N. (2020). Beyond the effectiveness factor: Multi-step reactions with intraparticle diffusion limitations. Chemical Engineering Journal, 380, 122507.

Mameri, N., Yeddou, A. R., Lounici, H., Belhocine, D., Grib, H., & Bariou, B. (1998). Defluoridation of septentrional sahara water of north Africa by electrocoagulation. 32(5), 1604–1612.

Marwa, J., Lufingo, M., Noubactep, C., & Machunda, R. (2018). Defeating fluorosis in the East African Rift Valley: Transforming the Kilimanjaro into a rainwater harvesting park. Sustainability, 10(11), 4194.

Mohammadi, A. A., Yousefi, M., Yaseri, M., Jalilzadeh, M., & Mahvi, A. H. (2017). Skeletal fluorosis in relation to drinking water in rural areas of West Azerbaijan, Iran. Scientific Reports, 7(1), 1–7.

Moussa, D. T., El-naas, M. H., Nasser, M., & Al-marri, M. J. (2017). A comprehensive review of electrocoagulation for water treatment : Potentials and challenges. Journal of Environmental Management, 186, 24–41. https://doi.org/10.1016/j.jenvman.2016.10.032

Hakizimana, J. N., Gourich, B., Chafi, M., Stiriba, Y., Vial, C., Drogui, P., & Naja, J. (2017). Electrocoagulation process in water treatment: A review of electrocoagulation modeling approaches. Desalination, 404, 1-21. https://doi.org/10.1016/j.desal.2016.10.011

Nyangi, M. J., Chebude, Y., & Kilulya, K. F. (2020). Fluoride removal efficiencies of Al EC and Fe EC reactors : process optimization using Box – Behnken design of the surface response methodology. Applied Water Science, 1–11. https://doi.org/10.1007/s13201-020-01297-x

Rout, T. K., Verma, R., Dennis, R. V, & Banerjee, S. (2015). Study the removal of fluoride from aqueous medium by using nano-composites. Journal of Encapsulation and Adsorption Sciences, 5(01), 38.

Singh, N., & Balomajumder, C. (2017). Equilibrium isotherm and kinetic studies for the simultaneous removal of phenol and cyanide by use of S. odorifera (MTCC 5700) immobilized on coconut shell activated carbon. Applied Water Science, 7(6), 3241–3255.

Sundaram, C. S., Viswanathan, N., & Meenakshi, S. (2008). Defluoridation chemistry of synthetic hydroxyapatite at nano scale: equilibrium and kinetic studies. Journal of Hazardous Materials, 155(1–2), 206–215.

Wang, J., & Guo, X. (2020). Adsorption kinetic models: Physical meanings, applications, and solving methods. Journal of Hazardous Materials, 390, 122156.

Wu, G., Tan, X., Li, G., & Hu, C. (2010). Effect of preparation method on the physical and catalytic property of nanocrystalline Fe_2O_3. Journal of Alloys and Compounds, 504(2), 371–376.

Zhou, X., & Zhou, X. (2014). The unit problem in the thermodynamic calculation of adsorption using the Langmuir equation. Chemical Engineering Communications, 201(11), 1459-1467.

CHAPTER THREE

Simultaneous Removal of Fluoride and Arsenic from Water by Hybrid Al-Fe Electrocoagulation: Process Optimization through Surface Response Method

This chapter is based on the published paper

Magori J. Nyangi, Yonas Chebude, Kessy F. Kilulya & Minu Andrew (2020) Simultaneous removal of fluoride and arsenic from water by hybrid Al-Fe electrocoagulation: process optimization through surface response method, Separation Science and Technology, DOI: 10.1080/01496395.2020.1837877

Abstract

The electrocoagulation process using hybrid aluminum-iron electrode was used for removal of arsenic and fluoride from water. The operation parameters; current density, initial pH, treatment time, initial concentration of arsenic and fluoride were optimized using the Box Behnken Design. The R^2 values for arsenic and fluoride removal were 0.83 and 0.96, respectively ensure a satisfactory of a developed quadratic model. At the optimized operation parameter of 9.90 $mAcm^{-2}$, pH 7.5; the Al-Fe EC reduced fluoride 16 mg/L and arsenic 200 µg/L to 1.12 mg/L and 9.60 µg/L, respectively in 50 minutes with an operation cost estimated to 0.99 $/$m^3$.

Keywords: Electrocoagulation; groundwater; arsenic; fluoride; reduction; response surface methodology

3.0 Introduction

The co-contamination of toxic pollutants, arsenic and fluoride in groundwater is frequently observed in countries like USA (Levy et al., 1999). China (Currell et al., 2011), Argentina (Gomez et al., 2009), Mexico (Mahlknecht et al., 2004) and Pakistan (Saeed et al., 2020). Meanwhile, groundwater of the rift valley zone of East Africa which is dominated by volcanic rock is characterized by elevated levels of fluoride (≥ 1.5 mg/L). Its estimated that 90 % of groundwater along the Rift Valley region especially in Kenya, Tanzania and Ethiopia have high levels of fluoride in drinking water sources (Fawell et al., 2006). Geochemical and occurrence of fluorine in volcanic rocks is anomaly associated with other potentially toxic chemicals including arsenic (Rango et al., 2013). However, despite scarce of enough research on the level of arsenic in the groundwater of East Africa rift-valley zone one research conducted in Ethiopia has reported 54 % of the groundwater to have elevated arsenic level (i.e., > 10 µg/L) (Rango et al., 2013).

The long term exposure to arsenic (i.e., > 10 µg/L) is associated to cancer (Jabir et al., 2015) gastrointestinal problems, arsenicosis (Chatterjee et al., 2010) and non-cancerous diseases (Karim, 2000). Meanwhile above threshold level of 1.5 mg/L fluoride is known to cause fluorosis (Dissanayake, 1991). The individual harmful effects of arsenic and fluoride to human is well documented; however, little is known on their co-exposure. It's believed that upon chemical mix there is synergistic effect on their toxicity even at their lower limit (Rao & Tiwari, 2006; Flora et al., 2009). At higher concentrations co-exposure can damage children intelligence and their growth (Jiang et al., 2014). Thus, necessitates effort to lower their levels from potable water.

In East Africa rift valley zone people are mainly using bone char and Nalgonda methods for fluoride reduction (Osterwalder et al., 2014). A high-quality bone char can reduce up to 23 mg/L to a concentration below 1.5 mg/L (Esayas, Mattle, & Feyisa, 2009). Unfortunately, poor production of bone char is associated with odour and offensive taste of the treated water and in some cases face rejection by the users due to cultural beliefs (Esayas et al., 2009). On the other hand, Nalgonda treatment demands high chemical coagulants (alum and aluminum sulphate) for effective F removal. For example, treatment of 22.1 mg/L may consume up to 800 mg/L alum resulting into high fluoride sludge that become a challenge in their disposal. These necessitates further research for acceptable and cost-effective technology to be used not only for fluoride but

also for arsenic removal to be used for arsenic and or fluoride in the groundwater in East Africa Rift-Valley zone.

One of the effective methods that has recently received considerable attention for remediating inorganic pollutants from water with negligible generation of by-product wastes is electrocoagulation (Chen, 2004). The method also has high removal efficiency, easy to operate, cost effectiveness and possibility of complete automation of process (Emamjomeh & Sivakumar, 2009). The electrocoagulation has been utilizing common electrodes such as aluminum, titanium, zinc copper iron and so on. Among the electrodes, aluminum and iron are mostly used due to their efficiency and easily available (Moussa et al., 2017). During the electrocoagulation process the coagulant is formed in-situ when aluminum and iron electrodes undergo electro-dissolution. The aluminum and iron cations are generated at the anode and the hydrogen gas emerges at the cathode. The EC process form aluminum and iron hydroxide as shown in the overall equations 3.1 and 3.2 taking place at near neutral pH-7.

(3.2)

The iron and aluminum electrodes have been proven effective in removal of individual arsenic and fluoride in a separate set of experiments (Vasudevan et al., 2009). The aluminum is more effective for the removal of fluoride while iron electrode is efficient on the arsenic remediation (Wan et al., 2011). On the other hand, the combination of aluminum and iron in a single sacrificial electrode is reported to improve EC performance than individual electrode (Alarcón-Herrera et al., 2013). However, few researchers have reported on the simultaneous removal of fluoride and arsenic in a single EC set up (Zhao et al., 2011; Guzmán et al., 2016; Rosales et al., 2018; Hernández, 2018). Among them, only Zhao et al. 2011 has reported on the use of hybrid Al-Fe which was integrated with titanium anode for simultaneous removal of arsenic and fluoride. The titanium electrodes are costly (18 $/Kg), this makes their findings unreliable cost-effective method, especially for developing countries. Therefore, investigation for the optimal conditions for simultaneous removal of arsenic and fluoride using a combined Fe-Al as the sacrificial electrode can be an attractive work towards access of arsenic-fluoride free water.

The aim of this work was to design and develop a cost effective method for fluoride and arsenic removal applicable to the East Africa Rift valley zone by investigating for the optimal operational parameters in a hybrid Al-Fe electrocoagulation that will successfully lower both arsenic and fluoride from the contaminated groundwater sources to WHO acceptable levels, to determine relationship between responses and four quantitative variables (initial pH, initial fluoride concentration, initial arsenic concentration, current density and treatment time). The technology will enable application of the technology to a various initial concentration.

3.1 Methodology

3.1.1 Material preparation

Standard 1000 μg/L arsenic and 1000 mg/L fluoride solution were prepared according to the standard procedure (Federation & Association, 2005). Meanwhile, iron and aluminum electrodes plates (Fe; 15 cm × 2 cm × 0.05 cm; and Al; 15 cm × 2 cm × 0.05 cm) were pre-cleaned by rubbing with sandpaper, rinsed in 2 M NaOH and 2 M HCl to remove any particles attached on the surface then washed with distilled water. The electrodes were then dried at 103ºC before the start of experiments. After each experiment, electrodes were dissolved in 1 M hydrochloric acid for 10 minutes to remove any remaining particles on the surface that may reduce EC performance. Thus, the synthetic water samples used in this study was composed up of the ions of Na+ As^{3+}, F^{-} and Cl^{-} with electrical conductivity at a range of 550-680 μS/cm and total dissolved solid of 320-440 mg/L.

3.1.2 Design of experiment

The Box-Behnken design BBD was selected for the optimization of operation parameters in EC process used for the simultaneous arsenic and fluoride removal. The five-factorial and a three-level BBD, with five replicas at the center point leading to a total number of forty-six (46) experiments was employed for response surface modeling in this study. The variables (independent factors) chosen were: the applied electric current density (A), treatment time (B), initial pH of the water sample (C), initial fluoride concentration (D) and initial concentration of arsenic (D). Meanwhile the percentage fluoride and arsenic reduction were considered as dependent factors (response). The actual values of process variables and their variation limits were selected based on the values obtained from various literatures while the limit for current density was obtained in preliminary experiments and are shown in Table 3.0.

Table 3.0: Experimental range and levels of independent variables for the combined Al-Fe electrocoagulation

Operational parameters			Range of actual coded variables		
Factor	Variables	Units	Low	Medium	High
A	Current density (J)	$mAcm^{-2}$	6.25	13.15	20
B	Time (t)	min	10	35	60
C	pH.		4	6.5	9
D	Concentration (F)	mg/L	2	13.5	25
E	Concentration (As)	µg/L	15	158	300

3.1.3 The experiment set up and sample analysis

The batch mode reactor was used to conduct EC experiments in 800 cm^3 beaker having a working volume of 600 cm^3. The two electrodes of aluminum and iron were connected as sacrificial anode in a monopolar parallel mode MP-P to the cathode made of the same electrode at inter electrode distance of 1.5 cm. Two electrodes one of each type were connected as sacrificial electrodes (total area, 80 cm^2 (4 surfaces x 10 x 2 cm, dipped in water)). The total surface area to volume ratio for the reactors (S) thus became 0.13 cm^{-1}. Thereafter, the end poles of electrodes were connected to the positive pole (anode) in a direct current (DC) power source. The voltage was maintained at 7 V while current density was varied at a range of 6.25-20 $mAcm^{-2}$.

The initial pH of the water sample was adjusted by addition of 0.1 M sodium hydroxide for increasing the pH or 0.1 M hydrochloric acid to lower the pH of the water sample. The experiments as shown in Table 3.1 were then performed with constant stirring at 300 rpm. Meanwhile, the conductivity of water sample was improved by addition of small amount (0.2 - 0.3) mg of sodium chloride. The selection of NaCl as supporting electrolyte was not only due to its ability to improve solution conductivity but also the ability of chloride ions to eliminate the passive films on electrodes the surfaces of electrodes (Mansouri et al., 2011). At the end of each experiment sample were taken from the reactor filtered using Whatman paper (2.5 µm) before

being analysed. The analysis of fluoride and arsenic were then carried using ISE and ICP-OES, respectively. The percentage of fluoride and arsenic removal was calculated using equation 3.3 below.

(3.3)

Where: Co and Ct are initial and final concentration (mg/L), respectively for fluoride and arsenic.

3.1.4 Statistical analysis

Experimental data shown in Table 3.1 were analyzed using Design-Expert version 11 program including ANOVA and regression to obtain the interaction between the process variables and the response. Two-dimensional, contour plots and three-dimensional curves of the response surfaces were developed using the same program to explain the interactions among variables and their effect to the fluoride and arsenic reduction. The fit of the model was expressed by R-square (R^2), while the statistical significance of the model obtained and factors involved were examined using F-value and P-value at 95% confidence level.

3.2 Results and discussion

3.2.1 Simultaneous removal of arsenic and fluoride

Table 3.1 shows the results from the simultaneous removal of arsenic and fluoride using a combined Fe-Al electrocoagulation at different combination of operational parameters. The arsenic removal was generally higher than the fluoride in various operational conditions. This is attributed to the fact that at any set of operational conditions there is higher production of iron-based coagulant than aluminum-based because of the higher molecular weight of iron. Theoretically, according to Faraday's law, whenever one Faraday of charge passes through the circuit, 9.0 g of aluminum and 28 g of iron are dissolved at each anode in any EC unit. This makes iron hydr(oxides) dominate the proportion in a reactor. Since iron coagulant have stronger affinity for arsenic due to their higher surface areas and partial surface positive charges, it will favour arsenic removal. In both cases there is decrease in removal of each pollutant at higher concentration of another. This is probably because of competition for adsorption sites in the Fe-Al oxy-hydroxides formed during the reaction (Dhadge et al., 2018).

Table 3.1: The BBD showing actual fluoride and arsenic reduction for Al-Fe electrocoagulation at different operation parameters

S/No	J	pH.	Time	Fo mg/L	As0 ug/L	Red F (%)	Red As (%)
1.0	13.1	4.0	60.0	13.5	157.5	91.4	95.0
2.0	13.1	6.5	37.5	13.5	157.5	86.6	93.0
3.0	20.0	9.0	37.5	13.5	157.5	90.8	94.3
4.0	13.1	6.5	37.5	2.0	300.0	86.0	97.4
5.0	13.1	6.5	37.5	13.5	157.5	89.0	93.6
6.0	13.1	6.5	15.0	13.5	300.0	82.1	94.8
7.0	13.1	6.5	37.5	13.5	157.5	95.2	88.9
8.0	20.0	6.5	37.5	13.5	15.0	83.0	58.0
9.0	13.1	4.0	15.0	13.5	157.5	82.7	88.1
10.0	13.1	6.5	37.5	25.0	15.0	87.6	58.2
11.0	20.0	6.5	37.5	13.5	300.0	93.4	94.2
12.0	20.0	6.5	60.0	13.5	157.5	94.8	95.7
13.0	13.1	6.5	60.0	25.0	157.5	89.6	94.5
14.0	13.1	4.0	37.5	2.0	157.5	88.0	95.1
15.0	6.3	6.5	37.5	13.5	300.0	82.0	92.7
16.0	13.1	6.5	37.5	13.5	157.5	93.7	92.4
17.0	13.1	6.5	37.5	25.0	300.0	91.4	86.0
18.0	20.0	6.5	37.5	25.0	157.5	92.8	96.0
19.0	13.1	9.0	15.0	13.5	157.5	84.9	77.5
20.0	6.3	6.5	37.5	2.0	157.5	78.2	89.0
21.0	20.0	6.5	37.5	2.0	157.5	87.5	89.0
22.0	13.1	4.0	37.5	13.5	15.0	89.1	51.0
23.0	13.1	9.0	37.5	13.5	300.0	90.0	85.3
24.0	13.1	6.5	37.5	13.5	157.5	97.3	99.3
25.0	13.1	9.0	37.5	13.5	15.0	85.8	53.8

26.0	6.3	4.0	37.5	13.5	157.5	85.0	89.9
27.0	6.3	9.0	37.5	13.5	157.5	85.0	88.7
28.0	13.1	4.0	37.5	25.0	157.5	94.0	89.3
29.0	6.3	6.5	37.5	13.5	15.0	84.0	56.6
30.0	20.0	4.0	37.5	13.5	157.5	93.8	95.9
31.0	13.1	6.5	60.0	13.5	15.0	92.5	46.5
32.0	13.1	6.5	37.5	2.0	15.0	80.0	60.6
33.0	13.1	9.0	37.5	2.0	157.5	87.0	90.0
34.0	6.3	6.5	37.5	25.0	157.5	82.5	80.6
35.0	13.1	6.5	15.0	2.0	157.5	77.0	89.4
36.0	6.3	6.5	60.0	13.5	157.5	83.0	90.3
37.0	13.1	6.5	60.0	2.0	157.5	88.0	94.4
38.0	13.1	6.5	15.0	13.5	15.0	83.3	45.3
39.0	13.1	6.5	37.5	13.5	157.5	94.3	93.0
40.0	13.1	9.0	60.0	13.5	157.5	94.6	94.1
41.0	13.1	9.0	37.5	25.0	157.5	94.5	86.2
42.0	20.0	6.5	15.0	13.5	157.5	88.3	89.8
43.0	13.1	6.5	60.0	13.5	300.0	94.5	96.3
44.0	13.1	4.0	37.5	13.5	300.0	87.3	96.7
45.0	13.1	6.5	15.0	25.0	157.5	80.7	89.1
46.0	6.3	6.5	15.0	13.5	157.5	78.1	87.6

3.2.2 Evaluation of the data

The validity of experimental data in optimization of operation parameters on the response variable was evaluated by fitting the data in a second-order model in the form of quadratic polynomial equation given by Equation 3.4 as proposed by Khedmati et al., (2017).

(3.4)

In equation 4, Y is the response variables (fluoride and arsenic reduction in percentage), b_0, b_i, b_{ii}, and b_{ij} are constant coefficients of intercept, linear, quadratic and interactive terms, respectively and Xi and Xj represent the four independent variables (current density, initial pH, treatment time, and initial concentrations).

3.2.3 Development of the regression model and model validation

The removal efficiency of the electrocoagulation depends on interaction of various parameters namely current density, initial pH, treatment time and initial concentration of arsenic and that of fluoride in this study. Thus, experiments were performed to study the combined effect of these factors on concurrence removal of arsenic and fluoride. The experiments on different combination of parameters together with the observed removal efficiencies are listed in Table 3.1. The coefficients of the response function are shown in equation 3.4, while the t-values and P-values values to assess the validity of the model prediction for simultaneous fluoride and arsenic removal efficiencies are presented in Table 3.2. The actual equations of the second order polynomial equations for the removal efficiencies of fluoride and arsenic are given by equation 3.5 and 3.6, respectively:

$$RedF\% = 50.06074 + 2.32193J + 0.15762pH + 0.635691t + 0.947744F + 0.018938As + 0.043211J*pH + 0.002694J*t + 0.003162J*F + 0.003177J*As + 0.004439pH*t + 0.013217pH*F + 0.004263pH*As - 0.002048t*F + 0.000241t*As - 0.000342F*As - 0.079254J^2 - 0.044261pH^2 - 0.00683t^2 - 0.026649F^2 - 0.000144As^2 \quad (3.5)$$

$$RedAs\% = 33.00636 - 0.139812J + 0.106762t - 0.496947F + 0.506654As - 0.004882J*pH + 0.005289J*t + 0.048847J*F + 0.00004J*As + 0.04349pH*t + 0.017403pH*F - 0.009904pH*As - 0.009904pH*As + 0.000316t*F + 0.000025t*As - 0.00137F*As - 0.013303J^2 0.332651pH^2 + 0.004548t^2 - 0.007014F^2 - 0.000913As^2 \quad (3.6)$$

Table 3.2: ANOVA and regression results for the response surface quadratic model for fluoride and arsenic reduction by combined Fe-Al electrocoagulation reactor

	Fluoride response		Arsenic response		
Source	F-value	p-value	F-value	p-value	
Model	06.31	< 0.0001	28.190	< 0.0001	Significant
A-J	33.32	< 0.0001	5.0600	0.0336	
B-pH	0.0118	0.9142	3.4500	0.0752	
C-t	38.25	< 0.0001	7.2900	0.0123	
D-F	12.91	0.0014	2.2200	0.1488	
E-As	03.47	0.0745	348.48	< 0.0001	
Lack of Fit	0.3774	0.9461	1.68	0.2964	Not significant
R^2	0.83		0.96		

Adj R^2	0.70	0.92
Pred R^2	0.51	0.84
Adeq Prec	8.90	16.79

The models for the simultaneous removal of arsenic and fluoride presented low p-values of ≤ 0.0001 and large F-values of 6.31 and 28.19, respectively implies that at least one of the terms in each model has a significant effect on the response. The current density (A), treatment time (B) and initial concentration (C) of fluoride and arsenic D are found to be significant to both models, all exhibiting low p-values ≤ 0.005. Meanwhile all their interaction terms were insignificant to the models. The lack of fit p-values of 0.94 for fluoride and 0.29 for arsenic were observed which made lack of fit not significant to both models. The square terms of initial concentration of fluoride ($D^2 \leq 0.0013$) and initial arsenic concentration (not shown) were highly significant to the fluoride removal model while the square of initial arsenic concentration ($E^2 < 0.0001$) was also significant term to arsenic removal.

The model presented a high regression coefficient (R^2) of 0.96 to arsenic reduction and 0.83 to fluoride reduction, showing that both models can highly predict the response. The models also have shown the appropriate and adequate signal to noise ratio of 8.9 and 16.8 for fluoride and arsenic reduction, respectively. The difference between predicted and adjusted correlated coefficient is ≤ 0.2 showing good agreement between the two terms. However, in each case the adjusted R^2 (0.70 and 0.92) is higher than the predicted R^2 (0.50 and 0.84) for fluoride and arsenic, respectively indicating that the factors added to modify the models have improved models. Hence, the response surface model developed in this study for predicting fluoride removal efficiency was considered to be satisfactory.

Figure 3.1a and b show the normal percentage probability of residual against the normal plot of residuals for fluoride and arsenic removal, respectively. Both plots form fairly straight line with an *S*-shape indicating positive correlation between probability and normal removal, ascertaining the assumption that both models were relatively satisfactory. The predicted and actual plots also confirm alignment between the residual and predicted concurrent fluoride and arsenic reduction Figure 3.2a and b suggesting that the models could well predict within the range of operation parameters. Therefore, it can be concluded that the quadratic models of the response surface

developed in this study correlating fluoride and arsenic removal with process variables are best suited to explain the experimental data of a combined Fe-Al EC process.

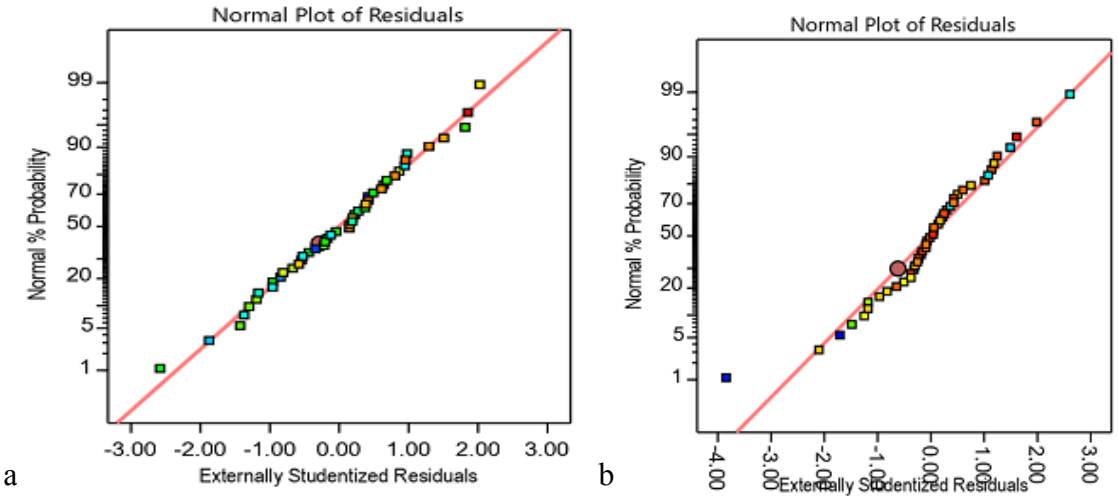

Figure 3.1: Normal probability plots for Al-Fe EC on a. fluoride reduction b. arsenic reduction

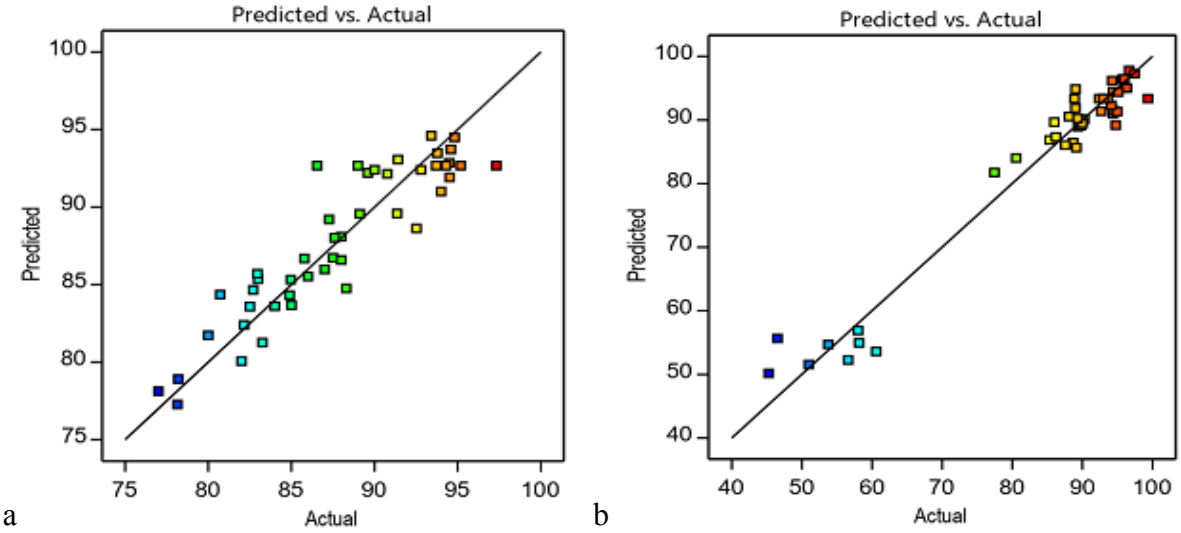

Figure 3.2: Plots for predicted against actual results for Al-Fe EC (a) fluoride removal (b) arsenic reduction

3.2.4 Physical changes observed during experiments

During water treatment in this study at pH 7.5 the changes of color, bubble evolution and formation of particles were observed. The color of the solution changes from clear to brown (iron iii oxide hydroxide, insoluble) then dark grey and finally faint grey Figure 3.3. This is attributed to the dissolution of iron electrodes followed by formation of various complexes of hydrated iron ions in water. The pale grey color that turns into dark grey as shown by equation reaction 3.7 is

an indication of formation of Fe^{2+} complexes of and (Parga et al., 2005; Taylor et al., 2009). The latter dark grey precipitate is a result of replacement of two water molecule by the strong ligand, hydroxide that builds up in solution as a results of water hydrolysis (Parga et al., 2005). Also, the darkness may indicate high concentration of Fe^{2+} in the solution. The color of the solution then changes into brown represented by equation reaction 3.8, which is a results of proton transfer during oxidation of Fe^{2+} to Fe^{3+} by the dissolved oxygen or that of the water molecules forming the precipitate of hydrated octahedral iron (iii) hydroxide(Parga et al., 2005; Murugananthan et al., 2004). On the other hand, aluminum dissolution led to the formation of white flocs $Al(OH)_3$ reaction equation 3.9 (Taylor et al., 2009). However, this white floc was not visible as it was either dominated by grey and brown colors of Fe^{2+} and Fe^{3+} complexes or made the two colors brighter. Meanwhile the bubble observed on top of the solution and near cathodes was a results of electrolysis of water producing hydrogen. (Kobya et al., 2006).

(3.7)

Brown (3.8)

(3.9)

a  b  c 

Figure 3.3: Photos showing color changes during arsenic and fluoride remediation at pH 7.5, 9.9 $mAcm^{-2}$ (a) Before treatment starts (b) First color change observed (c) Final color observed

3.2.5 Effect of operation parameters on simultaneous removal of fluoride and arsenic

Generally, the most important parameters, which affect the performance of electrocoagulation process, are initial pH of solution, initial concentration of pollutant, current density and reaction time.

3.2.5.1 Effect of current density and treatment time

The current density and treatment time both have the linear effect on the coagulant dosage thus affecting the removal of arsenic and fluoride similarly. According to Faraday's law equation

3.10, it is clear that Al^{3+} or Fe^{2+} dose released from anode depend on the electrolysis time and current density applied. In this case there is simultaneous increase in reduction of both arsenic and fluoride as the current density and treatment time increases. An increase in current density and treatment time lead to the increase in dissolution of Al^{3+} and Fe^{2+} ions and liberation of OH^- resulting into higher coagulants dosage, bubble production and growth of flocs. At the lowest J = 6.5 $mAcm^{-2}$ there is a lowest removal of both arsenic ~ 84.30% and fluoride ~90.20% which is attributed to the insufficient coagulant dosage released in the reactor Figure 3.4a and b. As current density and treatment time increase, the increase in percentage reduction of both fluoride and arsenic is observed with maximum efficiencies reaching 95% and 99%, respectively.

However, beyond 17.5 $mAcm^2$ and 22.50 $mAcm^2$ and ≥ 51minutes there is drop in percentage reduction on both fluoride and arsenic removal, respectively. At these points there is less amount of fluoride and arsenic remained in the solution thus, lowering the removal rate. Furthermore, at this point there is resistance to particle mobility due to accumulation of high amount of coagulant and increased gas production near the surface of electrodes causing IR drop at higher current density (Kobya et al., 2011; Nasrullah et al., 2012). The IR drop restricting fluoride uptake is observed when the charge loading () is 74 F/m^3 and for arsenic reduction it was 95 F/m^3. The drop in removal of both fluoride and arsenic after 51 minutes is ascertained by the fact that once the coagulant is saturated, further mixing of the reaction results into desorption of weakly attached fluoride and arsenic on the surface oxy-(hydroxide) adsorbent (Nasrullah et al., 2012).

(3.10)

Where: W is the theoretical total amount of aluminum and iron produced by current I (A) passed for a period of time t (s), M_{Al} and M_{Fe} is molecular mass (Al; 26.98 g/mol: Fe; 55.84 g/mol), N_T is total number of electrons transferred (Al; 3: Fe; 2), F is Faradays constant (96,485 C/mol). V is the volume water treated (600 cm^3).

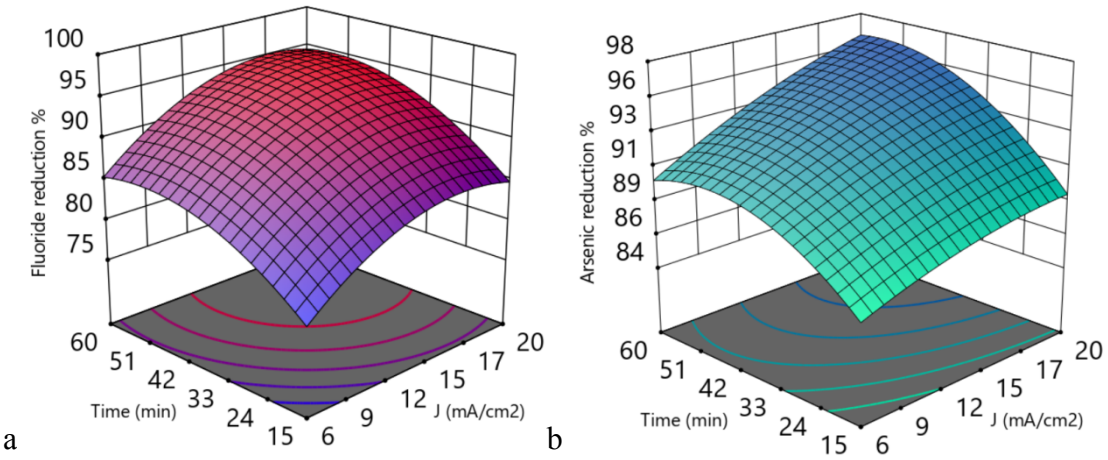

Figure 3.4: Response surface of experimental data showing interacting effect of treatment time and current density of Al-Fe electrocoagulation on (a) fluoride reduction (b) arsenic reduction

3.2.5.2 Effect of initial pH of the water sample

In this study initial pH appears to affect removal of fluoride and arsenic in different ways Figure 3.5. The arsenic removal increases slightly in acidic media from pH 4 and reaches maximum of 93.7% at pH ~ 5.5, beyond this point, it decreases to 89.4% at pH 9. Meanwhile there is insignificant changes on the fluoride removal within the range of applied initial pH all being ~92% however, the highest removal of 92.6% was attained at pH ~7. In aqueous solution arsenite species are present in the form of H_3AsO_3, H_2AsO_3 and $HAsO_3$ (Rosales et al., 2018), while fluoride is present in HF and F^- form (Thakur & Mondal, 2017). Moreover, during electrocoagulation there is a change in oxidation state of arsenite to arsenate which exist as AsO_4^{3-}, $HAsO_4^{2-}$ and $H_2AsO_4^-$ (Mohan & Pittman, 2007). Speciation of arsenic and fluoride changes with pH of solution and redox potential, similarly, to the aluminum and iron ions speciation. It must be noted that during dissolution of iron and aluminum electrodes the ionic species of ferric and aluminum (in acidic; Fe^{3+}, $Fe(OH)^{2+}$, $Fe(OH)_2^+$ $Fe(OH)_3$, Al^{3+}, $Al(OH)^{2+}$, $Al(OH)_2^+$ $Al(OH)_3$ and in basic $Fe(OH)_4^-$ $Al(OH)_4^-$, are formed (Rincón & La Motta, 2014).

High removal of arsenic at pH (5 – 6) suggests adsorption of dominant species $H_2AsO_4^-$ by charge neutralization on the positive surface of the oxy(hydroxides) is responsible for arsenic removal (Thakur & Mondal, 2017), sweep coagulation and co-precipitation can also be responsible for high arsenic removal in acidic medium, same as reported by (Thakur & Mondal, 2017). Meanwhile drop in the arsenic removal in basic medium proposes increase in repulsion between the negative arsenate ($HAsO_4^{2-}$) and dominant coagulant species $Fe(OH)_4^-$, and $Al(OH)_4^-$

(Thakur & Mondal, 2017). The small percentage of arsenate removed at pH ≥ 7 is due to sweep coagulation or particles entrapment of the neutral and negatively charged arsenic species to $Fe(OH)_4^-$ and $Al(OH)_4^-$ particles (Vasudevan et al., 2010).

The high removal of fluoride in neutral pH (6.5 - 7.5) suggests that amorphous oxy-hydroxide of aluminum and iron contributed to most of the fluoride reduction. These amorphous are neutral and dense and are dominant coagulant at the neutral pH suggesting that chemisorption of the F^- species on the oxy-hydroxide amorphous of aluminum and iron coagulants. Furthermore, the insignificant change to fluoride removal in the applied initial pH range (4 - 9) can be attributed to the buffer capacity of aluminum oxy-hydroxide that dominates in the uptake of fluoride. At pH ≥ 8 both fluoride and coagulants are negatively charged which means that smaller removed fluoride is due to sweep coagulation and co-precipitation (Vasudevan et al., 2010). Moreover, in both reactors at pH < 5 and pH > 8, the Fe^{2+} and Al^{3+} from anode tend to dissolve in solution causing a low formation of coagulant and subsequent low removal of both fluoride and arsenic.

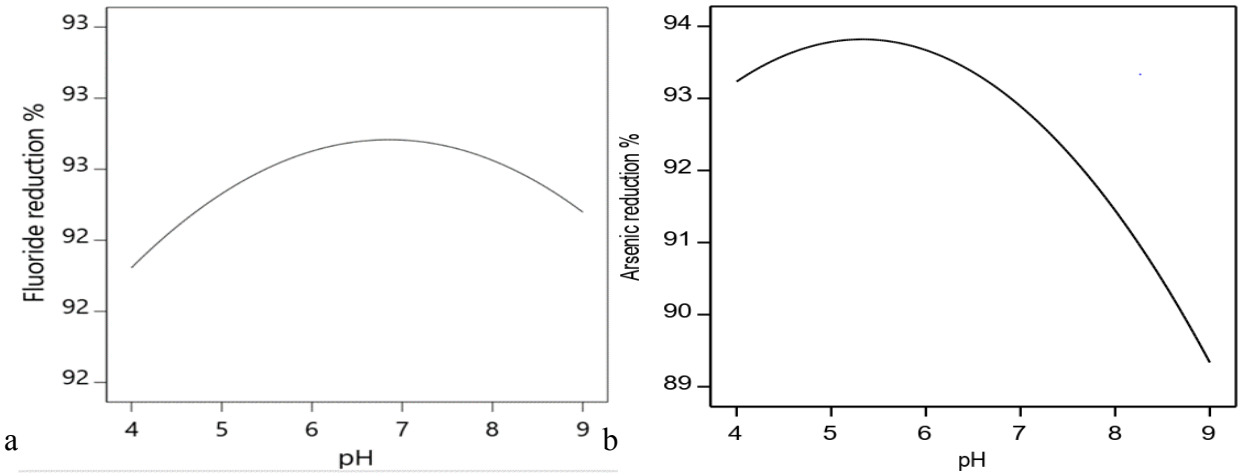

Figure 3.5: Plots showing effect of initial pH of the sample on (a) fluoride removal (b) arsenic removal, by Al-Fe electrocoagulation reactor

3.2.5.3 Effect of variation of initial fluoride concentration and arsenic concentration

Figure 3.6a and b reveal that the percentage reduction in fluoride and arsenic increases with increase in their respective initial concentrations. The fluoride attained 93% reduction while arsenic reached 98% at initial concentration of 16.5 mg/L and 200 µg/L, respectively beyond which there is drop in percentage reduction to both pollutants. At a lower level of F ≤ 16.5 mg/L and As ≤ 200 µg/L the ratio of pollutant to the produced adsorbent is ≤ 1 enhancing pollutants reduction linearly. However, at initial concentration (F ≥ 16 mg/L; As ≥ 200 µg/L) there is

decrease in reduction of both pollutants. The decrease in removal is due to competition for complexation sites which limit fluoride and arsenic removal and subsequence further stirring tend to lead to desorption (Vasudevan et al., 2010).

On the other hand, the effect of one pollutant on the removal of another is also observed Figure 3.7a and b. The increase in arsenic concentration has significant limitation to fluoride removal at a high concentration, while fluoride insignificantly reduce arsenic removal with increase of initial concentration (all ≥ 92 - 94%; As reduction). At As ≤ 182 µg/L there is an increase in fluoride reduction, however above this level clearly fluoride removal dropped. This is ascertained by the fact that at higher levels of arsenite there is competition for adsorption site diminishing fluoride removal. The arsenate may also replace hydroxyl group of the iron and aluminum lowering available sites for fluoride uptake. It can also be ascertained by the preferential adsorption of high amount of available ions in the solution as compared to less amount of ions as the dose of coagulant remain the same in electrocoagulation.

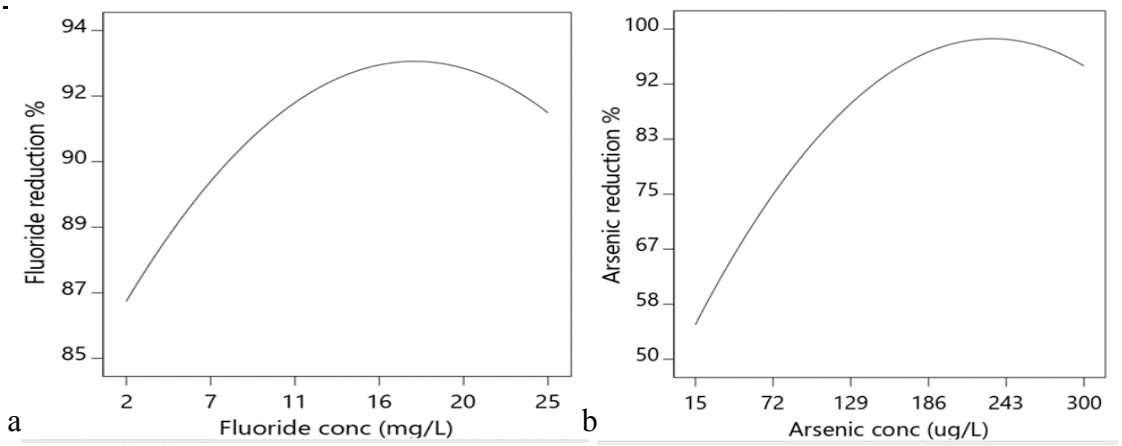

Figure 3.6: Plots showing effect of initial concentration of fluoride and initial concentration of arsenic on (a) fluoride reduction (b) arsenic reduction by Al-Fe electrocoagulation reactor

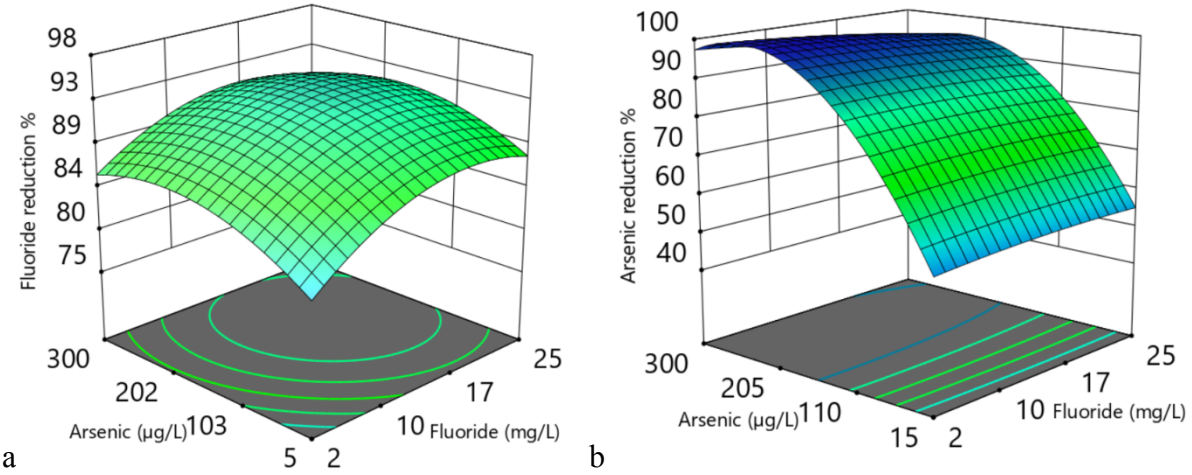

Figure 3.7: Response surface of experimental data showing interacting effect of initial concentration of arsenic and initial concentration of fluoride on (a) fluoride reduction (b) arsenic reduction by Al-Fe EC reactor

3.2.6 Optimization of operation parameters on simultaneous removal of fluoride and arsenic

The main objective of optimization was to determine the optimum values of variables for fluoride and arsenic removal with Al-Fe electrocoagulation from the model obtained using experimental data. The operating parameters were chosen so as to maximize fluoride and arsenic reduction at the minimal current density while initial pH of the sample, initial fluoride concentration and treatment time were left at a range. Several sets of experiments were suggested by the model and two of them were performed for verification. The two water samples tested for the performance of optimized operation condition had TDS of 350 mg/L and electrical conductivity of 600 µS/cm.

Table 3.3: Experimental and predicted results on a few selected solutions suggested for optimization test

S/N	J	pH	Time	F_o	F_t	As_o	As_t	Pred. F%	Pred. As%
1	9.90	7.50	50.00	16.00	1.12	200	9.67	91.70	95.20
2	12.00	7.90	50.00	16.00	1.32	220	10.20	94.10	96.30

Basing on the experimental results shown in Table 3.3, the Al-Fe electrocoagulation achieved better reduction of initial fluoride concentration of 16 mg/L to 1.12 mg/L and initial arsenic concentration of 200 µg/L to 9.67 µg/L both satisfying WHO minimum fluoride and arsenic level for drinking water at a current density of 9.9 $mAcm^{-2}$, initial pH 7.50 in 50 minutes. Thus,

the quantity of charge at optimum operation condition was calculated as (). The observed results at this optimum condition were 93.00% and 96.2% for fluoride and arsenic, corresponding to 0.50 mg and 6.40 µg removal per unit charge of electric current, respectively.

3.2.7 Cost analysis of water treatment at optimal operational parameters

The feasibility of the treatment process to a large scale depends on the cost of treatment process. The preliminary economic evaluation of the treatment cost in USD/m^3 for the present study was on the cost of electrode materials (C.E), electrical energy consumption (C.En) and (D) chemical cost calculated using Equation 3.11 (Daneshvar, Oladegaragoze, & Djafarzadeh, 2006).

(3.11)

Where: C.E electrode consumption cost (Kg/h); C.En energy consumption cost (kWh/m^3).

The working volume (V) of the EC was 0.0006 m^3, the potential difference applied 7 V, current density 9.90 $mAcm^{-2}$ (I = 0.8 A) and runtime 50 minutes. The total consumption for iron and aluminum electrodes in 50 min were found to be 0.00041 Kg or 0.69 Kg/m^3, while the whole sale price of electrodes a. (Al = 1.2 $/Kg: Fe = 0.9 $/Kg), b. industrial electricity price in Ethiopia is 0.04 $/kWh and the chemical cost D (cost of salt = 0.04 $/$m^3$).

Thus, the total electrical energy consumption and electrode consumption were calculated as 7.78 kWh/m^3 and 0.69 Kg/m^3, using equations 3.12 and 3.14, respectively (Daneshvar et al., 2006).

(3.12)

Thus, at optimized operation condition the amount of coagulant (total aluminum and iron consumed) per F and As removed, Al/Fe:F and Al/Fe:As of 27.55 mg/mg and 2.15 mg/µg, respectively was estimated to cost 0.99 $/$m^3$

3.3 Conclusion

- This study reported for the first efficiency of the hybrid Al-Fe as the only sacrificial electrode on the simultaneous reduction of arsenic and fluoride from contaminated water.
- Experimental design was carried out based on BBD of the response surface methodology to evaluate the effects of process variables and their interactions to achieve optimum condition.

- Under optimized condition of current density of 9.90 $mAcm^{-2}$, pH 7.5, reaction time of 50 minutes and initial concentration of arsenic 200 µg/L and that of fluoride 16 mg/L the technology achieved 93.00% and 96.20% reduction of fluoride and arsenic, respectively.
- The operating cost for the remediation of arsenic and or fluoride in Ethiopia was calculated to be 0.99 $\$/m^3$.
- Meanwhile the current density and treatment time were the most significant factors on the removal of both fluoride and arsenic.
- The optimized operation parameter of hybrid Al-Fe EC successfully reduced the concentration of both fluoride and arsenic to a level recommended by WHO for a drinking purpose and can be applied for remediation of both pollutants in groundwater of east Africa Rift valley zone.

3.4 References

Alarcón-Herrera, M. T., Bundschuh, J., Nath, B., Nicolli, H. B., Gutierrez, M., Reyes-Gomez, V. M., … Sracek, O. (2013). Co-occurrence of arsenic and fluoride in groundwater of semi-arid regions in Latin America: Genesis, mobility and remediation. Journal of Hazardous Materials, 262, 960–969. https://doi.org/10.1016/j.jhazmat.2012.08.005

Chatterjee, D., Halder, D., Majumder, S., Biswas, A., Nath, B., Bhattacharya, P., … Hazra, R. (2010). Assessment of arsenic exposure from groundwater and rice in Bengal Delta Region, West Bengal, India. Water Research, 44(19), 5803–5812.

Chen, G. (2004). Electrochemical technologies in wastewater treatment. Separation and Purification Technology, 38(1), 11–41.

Currell, M., Cartwright, I., Raveggi, M., & Han, D. (2011). Controls on elevated fluoride and arsenic concentrations in groundwater from the Yuncheng Basin, China. Applied Geochemistry, 26(4), 540–552. https://doi.org/10.1016/j.apgeochem.2011.01.012

Daneshvar, N., Oladegaragoze, A., & Djafarzadeh, N. (2006). Decolorization of basic dye solutions by electrocoagulation: an investigation of the effect of operational parameters. Journal of Hazardous Materials, 129(1–3), 116–122.

Dhadge, V. L., Medhi, C. R., Changmai, M., & Purkait, M. K. (2018). House hold unit for the treatment of fluoride, iron, arsenic and microorganism contaminated drinking water.

Chemosphere, 199, 728–736.

Dissanayake, C. B. (1991). The fluoride problem in the groundwater of Sri Lanka—environmental management and health. International Journal of Environmental Studies, 38(2–3), 137–155.

Emamjomeh, M. M., & Sivakumar, M. (2009). Fluoride removal by a continuous flow electrocoagulation reactor. Journal of Environmental Management. https://doi.org/10.1016/j.jenvman.2008.06.001

Esayas, S., Mattle, M. J., & Feyisa, L. (2009). Household water treatment : Defluoridation of drinking water by using bone char technology in Ethiopia.

Fawell, J., Bailey, K., Chilton, J., Dahi, E., & Magara, Y. (2006). Fluoride in drinking-water. IWA publishing.

Federation, W. E., & Association, A. P. H. (2005). Standard methods for the examination of water and wastewater. American Public Health Association (APHA): Washington, DC, USA.

Flora, S. J. S., Mittal, M., & Mishra, D. (2009). Co-exposure to arsenic and fluoride on oxidative stress, glutathione linked enzymes, biogenic amines and DNA damage in mouse brain. Journal of the Neurological Sciences, 285(1–2), 198–205.

Gomez, M. L., Blarasin, M. T., & Martínez, D. E. (2009). Arsenic and fluoride in a loess aquifer in the central area of Argentina. Environmental Geology, 57(1), 143–155.

Guzmán, A., Nava, J. L., Coreño, O., Rodríguez, I., & Gutiérrez, S. (2016). Arsenic and fluoride removal from groundwater by electrocoagulation using a continuous filter-press reactor. Chemosphere, 144, 2113–2120. https://doi.org/10.1016/j.chemosphere.2015.10.108

Hernández, J. H. (2018). Simultaneous removal of fluoride and arsenic from groundwater by electrocoagulation using a filter-press flow reactor with a three-cell stack. Separation and Purification Technology. https://doi.org/10.1016/j.seppur.2018.02.018

Jabir, N. R., Firoz, C. K., Baeesa, S. S., Ashraf, G. M., Akhtar, S., Kamal, W., … Tabrez, S. (2015). Synopsis on the linkage of Alzheimer's and Parkinson's disease with chronic

diseases. CNS Neuroscience & Therapeutics, 21(1), 1–7.

Jiang, S., Su, J., Yao, S., Zhang, Y., Cao, F., Wang, F., … Xi, S. (2014). Fluoride and arsenic exposure impairs learning and memory and decreases mGluR5 expression in the hippocampus and cortex in rats. PLoS One, 9(4), e96041.

Karim, M. D. M. (2000). Arsenic in groundwater and health problems in Bangladesh. Water Research, 34(1), 304–310.

Khedmati, M., Khodaii, A., & Haghshenas, H. F. (2017). A study on moisture susceptibility of stone matrix warm mix asphalt. Construction and Building Materials, 144, 42–49. https://doi.org/10.1016/j.conbuildmat.2017.03.121

Kobya, M., Gebologlu, U., Ulu, F., Oncel, S., & Demirbas, E. (2011). Electrochimica Acta Removal of arsenic from drinking water by the electrocoagulation using Fe and Al electrodes. Electrochimica Acta, 56(14), 5060–5070. https://doi.org/10.1016/j.electacta.2011.03.086

Kobya, M., Hiz, H., Senturk, E., Aydiner, C., & Demirbas, E. (2006). Treatment of potato chips manufacturing wastewater by electrocoagulation. Desalination, 190(1–3), 201–211.

Levy, D. B., Schramke, J. A., Esposito, K. J., Erickson, T. A., & Moore, J. C. (1999). The shallow groundwater chemistry of arsenic, fluorine, and major elements: Eastern Owens Lake, California. Applied Geochemistry, 14(1), 53–65. https://doi.org/10.1016/S0883-2927(98)00038-9

Mahlknecht, J., Steinich, B., & Navarro De León, I. (2004). Groundwater chemistry and mass transfers in the Independence aquifer, central Mexico, by using multivariate statistics and mass-balance models. Environmental Geology, 45(6), 781–795. https://doi.org/10.1007/s00254-003-0938-3

Mansouri, K., Ibrik, K., Bensalah, N., & Abdel-Wahab, A. (2011). Anodic dissolution of pure Aluminum during electrocoagulation process: Influence of supporting electrolyte, initial pH, and current density. Industrial & Engineering Chemistry Research, 50(23), 13362–13372.

Mohan, D., & Pittman, C. U. (2007). Arsenic removal from water/wastewater using adsorbents-

A critical review. Journal of Hazardous Materials, Vol. 142, pp. 1–53. https://doi.org/10.1016/j.jhazmat.2007.01.006

Moussa, D. T., El-Naas, M. H., Nasser, M., & Al-Marri, M. J. (2017). A comprehensive review of electrocoagulation for water treatment: Potentials and challenges. Journal of Environmental Management, 186, 24–41.

Murugananthan, M., Raju, G. B., & Prabhakar, S. (2004). Removal of sulfide , sulfate and sulfite ions by electro coagulation. 109(May 2003), 37–44. https://doi.org/10.1016/j.jhazmat.2003.12.009

Nasrullah, M., Singh, L., & Wahid, Z. A. (2012). Treatment of Sewage by Electrocoagulation and the Effect of High Current Density. Energy and Environmental Engineering Journal, 1(1), 27–31.

Osterwalder, L., Johnson, C. A., Yang, H., & Johnston, R. B. (2014). Multi-criteria assessment of community-based fluoride-removal technologies for rural Ethiopia. Science of The Total Environment, 488, 532–538.

Parga, J. R., Cocke, D. L., Valverde, V., Gomes, J. A. G., Kesmez, M., Moreno, H., … Mencer, D. (2005). Characterization of electrocoagulation for removal of chromium and arsenic. Chemical Engineering & Technology: Industrial Chemistry Plant Equipment Process Engineering Biotechnology, 28(5), 605–612.

Rango, T., Vengosh, A., Dwyer, G., & Bianchini, G. (2013). Mobilization of arsenic and other naturally occurring contaminants in groundwater of the main ethiopian rift aquifers. Water Research, 47(15), 5801–5818. https://doi.org/10.1016/j.watres.2013.07.002

Rao, M. V, & Tiwari, H. (2006). Amelioration by melatonin of chromosomal anomalies induced by arsenic and/or fluoride in human blood lymphocyte cultures. Fluoride, 39(4), 255.

Rincón, G. J., & La Motta, E. J. (2014). Simultaneous removal of oil and grease, and heavy metals from artificial bilge water using electro-coagulation/flotation. Journal of Environmental Management, 144, 42–50.

Rosales, M., Coreño, O., & Nava, J. L. (2018). Removal of hydrated silica, fluoride and arsenic from groundwater by electrocoagulation using a continuous reactor with a twelve-cell stack.

ECSN. https://doi.org/10.1016/j.chemosphere.2018.07.113

Saeed, M., Yasir, M., Rehman, A., Farooqi, A., & Malik, R. N. (2020). Jo ur na l P re. Environmental Research, 110168. https://doi.org/10.1016/j.envres.2020.110168

Taylor, P., Ghernaout, D., Ghernaout, B., Boucherit, A., Naceur, M. W., & Khelifa, A. (2009). Desalination and Water Treatment Study on mechanism of electrocoagulation with iron electrodes in idealised conditions and electrocoagulation of humic acids solution in batch using Aluminum electrodes. 37–41. https://doi.org/10.5004/dwt.2009.668

Thakur, L. S., & Mondal, P. (2017). Simultaneous arsenic and fl uoride removal from synthetic and real groundwater by electrocoagulation process : Parametric and cost evaluation. Journal of Environmental Management, 190, 102–112. https://doi.org/10.1016/j.jenvman.2016.12.053

Vasudevan, S., Lakshmi, J., & Sozhan, G. (2009). Studies on a Mg-Al-Zn alloy as an anode for the removal of fluoride from drinking water in an electrocoagulation process. Clean - Soil, Air, Water. https://doi.org/10.1002/clen.200900031

Vasudevan, S., Lakshmi, J., & Sozhan, G. (2010). Studies on the removal of arsenate by electrochemical coagulation using aluminum alloy anode. Clean - Soil, Air, Water, 38(5–6), 506–515. https://doi.org/10.1002/clen.201000001

Wan, W., Pepping, T. J., Banerji, T., Chaudhari, S., & Giammar, D. E. (2011). Effects of water chemistry on arsenic removal from drinking water by electrocoagulation. Water Research, 45(1), 384–392. https://doi.org/10.1016/j.watres.2010.08.016

Zhao, X., Zhang, B., Liu, H., & Qu, J. (2011). Simultaneous removal of arsenite and fluoride via an integrated electro-oxidation and electrocoagulation process. Chemosphere, 83(5), 726–729. https://doi.org/10.1016/j.chemosphere.2011.01.055

CHAPTER FOUR

Effects of Co-existing Ions on Simultaneous Removal of Fluoride and Arsenic from Water by Hybrid Al-Fe Electrocoagulation

This chapter is based on the submitted manuscript

Nyangi, M. J., Chebude, Y., Kilulya, K. F., & Andrew, M. Effects of co-existing ions on simultaneous removal of fluoride and arsenic from water by hybrid Al-Fe electrocoagulation (under review).

Abstract

The effects of co-existing ions in water such as Ca^{2+}, Mg^{2+}, NO_3^-, SO_4^{2-} and HCO^- on the simultaneous removal of F^- (16 mg/L) and As^{3+} (200 µg/L) using hybrid Al-Fe electrocoagulation were evaluated by Box-Behnken design. Experiments were conducted at operation conditions of J = 9.9 mA/cm^2, pH = 7.5 and 50 min. The analysis of variance results for all variables confirmed the predicted models by the experimental design R^2: 0.69 and 0.72 % for F- and As^{3+}, respectively which ensured a fairly satisfactory adjustment of the quadratic models with the experimental data. The results showed that Ca^{2+} (0.5-100 mg/L) enhanced F- removal, while SO_4^{2-} (> 80 mg/L) and NO_3^- (> 75 mg/L) suppressed the F- removal. On the other hand, NO_3^- (0.5-100 mg/L), SO_4^{2-} (> 50 mg/L), Mg^{2+} (> 50 mg/L), and Ca^{2+} (> 50 mg/L) reduced As^{3+} removal. The combination of Mg^{2+} (< 70 mg/L) and Ca^{2+} appears to increase the fluoride removal while the combination of other ions had antagonistic effects on the removal of both F- and As^{3+}. Carbonates showed an insignificant influence on the removal of both pollutants. The effect of individual co-existing ions was found to depend on the type and concentration of individual co-ion. In a real groundwater (F^- = 7.6 mg/L, As^{3+} = 220 mg & co-existing ions), the removal of F- and As^{3+} were found to be 91 and 98% respectively, similar to that in absence of co-existing ions.

Keywords; Arsenic, fluoride, electrocoagulation, Box Behnken design, co-existing ions

4.0 Introduction

Fluoride and arsenic are the most notable chemical threat at the global scale, particularly in East Africa Rift valley (Rango et al., 2013), as they become the major challenge in ensuring access to quality water in the zone (Dehghani et al., 2018). It is approximated that 90% of population of people living in East African Rift valley is affected by dental and skeletal fluorosis due to consumption of groundwater containing elevated levels of fluoride (≥ 1.5) (Fawell et al., 2006). On the other hand; the long term consumption of arsenic (> 10 µg/L) containing water leads to a range of health complications such as skin, lungs and bladder cancers (Chatterjee et al., 2010;Karim, 2000). This means that remediation of fluoride and arsenic from contaminated water is of paramount for the public safety against such deseases.

One of the advanced technologies that has demonstrated to be effective in remediation of fluoride and arsenic from contaminated water is electrocoagulation (Hernández, 2018; Nyangi et al., 2020). The electrocoagulation (EC) method allows an *in-situ* production of the metal oxy-(hydroxide) coagulant through electro-dissolution of electrodes (Moussa et al., 2017). It is easy to operate, cost effective in case of material availability and possibility of complete automation of the process (Moussa et al., 2017). The removal mechanism through EC is postulated to be through coagulation, precipitation, adsorption and charge neutralization (Garcia-Segura et al., 2017; Chen 2004). Moreover, the removal mechanism is said to be influenced by pH, redox potential, electrode material and water composition (Linares-Hernández et al., 2009; Martín-Domínguez et al., 2018; Demirbas & Kobya, 2017; Canizares et al., 2009).

However, the performance of the EC technology appears to be affected by the presence of co-existing ions in natural groundwater such as calcium, nitrate, magnesium, sulphate, carbonate and bicarbonate ions (Mohan & Pittman, 2007; Meng et al., 2000; Vasudevan et al., 2010). The presence of such ions and their combinations may have significant effects on water conductivity, current efficiency, the rate of anode dissolution and pH change, all of which control the performance of an EC (Moussa et al., 2017). There are contradictory reports on the ways these ions affect EC performance. For example, sulphate is reported to slow down removal rate of arsenic (You & Han, 2015) and fluoride (Hu et al., 2003), when the concentration is at ≥ 100 mg/L, however at < 10 mg/L the removal increases. This was attributed to the inhibition to dissolution of electrodes caused by buildup of an inert film that prevent current from crossing the cell leading to lower defluoridation efficiency (Hu et al., 2003). Likewise, Wan et al., (2011)

found insignificant effect from nitrate and sulphate on the removal of arsenic in both laboratory and field tests by Fe-EC. This was further proved by García-Lara & Montero-Ocampo (2010) when they managed to achieve 99% removal of arsenic, using Al-EC, from groundwater in the presence of sulphate, carbonate and other ions. Moreover, in the presence of magnesium 1 - 10 mg/L, the arsenic removal is reported to increase, but at 100 mg/L he observed the decrease in the removal due to the inhibition of coagulant formation by formation of magnesium hydroxide and increased zeta potential (You & Han, 2015).

Many studies on electrocoagulation technology have reported the effects of operation parameters, inter-electrode distance, efficiency, and removal mechanism (Moussa, El-naas, et al., 2017); however, there is a limited knowledge about the effect of individual and combined co-existing ions on the performance of electrocoagulation. The aim of the present work was to investigate the effect of individual and combined co-existing ions (Ca^{2+}, Mg^{2+}, NO_3^-, SO_4^{2-} and carbonates) on the removal of fluoride and arsenic using hybrid Al-Fe EC.

4.1 Methodology

4.1.1 Material preparation

Standard stock solutions of 1000 µg/L arsenic and 1000 mg/L fluoride were prepared using distilled water according to the standard procedure (Federation & Association, 2005). Likewise, the stock concentration solution of Ca^{2+}, Mg^{2+}, NO_3^-, SO_4^{2-} and carbonates (all 1000 mg/L), were prepared according to the standard procedure (Federation & Association, 2005). Then appropriate concentrations were obtained using dilution law. Meanwhile, Al and Fe electrodes plates (Al; 15 cm × 2 cm × 0.05 cm and Fe; 15 cm × 2 cm × 0.05 cm) were pre-cleaned by rubbing with sandpaper, rinsed in 2 M NaOH and 2 M HCl to remove particles that may present on the surface then washed with distilled water.

4.1.2 Design of experiment

The design of experiment was performed using Box Behnken design of the response surface methodology (RSM). The RSM can be used to assess the relative significance of several factors in the complex interaction (Tak et al., 2015; Kobya et al., 2013). This study evaluated the influence of the independent variables (co-existing ions (CEI)); Ca^{2+}, Mg^{2+}, NO_3^-, SO_4^{2-} and CO_3^{2-}) on removal of dependent variables (fluoride and arsenic) using hybrid Al-Fe EC. The set of experiments set by the Design-Expert 11 is shown in Table 4.1 and 4.2.

Table 4.1: Experimental range and levels of independent process variables

Operational parameters			Range of actual coded variables		
Factor	Ion	Unit	Low	Medium	High
A	Calcium	mg/L	0.5	50.25	100
B	Bicarbonate	mg/L	0.5	50.25	100
C	Carbonate	mg/L	0.5	50.25	100
D	Nitrate	mg/L	0.5	50.25	100
E	Sulphate	mg/L	0.5	50.25	100
F	Magnesium	mg/L	0.5	50.25	100

4.1.3 Experimental setup

The batch mode reactor of 800 cm^3 glass cell with active volume 600 cm^3 was used in this study. The sacrificial electrode (aluminum and iron; one each) were connected to other two as cathode in a mono-polar parallel mode (MP-P) at inter electrode distance of 1.5 cm. Then the end poles of electrodes were connected to the positive and negative terminals in a direct current (DC) power source. The potential was maintained at 7 V, current density at 9.9 mA/cm^{-2} and treatment time 50 min. Thus, the amount of aluminum-iron oxyhydroxide coagulant generated was estimated to be 0.40 g by Faraday's law using Equation 4.1.

Where: W is the theoretical total amount of aluminum and iron produced by current I (A) passed for a period of time t (s), M_{Al} and M_{Fe} is molecular mass (Al; 26.98 g/mol: Fe; 55.84 g/mol), N_T is total number of electrons transferred (Al; 3: Fe; 2), F is Faradays constant (96,485 C/mol). V is the volume of water treated (600 cm^3).

4.1.4 Sample analyses

Prior to analyses, treated water samples were filtered using (Whatman filter paper 0.45 μm) and analyzed for fluoride and arsenic. The analysis of treated water samples for fluoride and arsenic were carried using ion selective electrode ISE and ICP-OES, respectively. The percentage of fluoride and arsenic removal was calculated (Equation 4.2).

(4.2)

Where: Co and Ct are initial and final concentration at time (mg/L), respectively for fluoride and arsenic.

4.1.5 Statistical analysis

Experimental data shown in Table 4.2 were analyzed using Design-Expert version 11 program including ANOVA and regression to obtain the effects of interaction between the co-existing ions and the response. Two-dimensional, contour plots and three-dimensional curves of the response surfaces were developed using the same program to explain the interactions among variables and their effect to the fluoride and arsenic removal. However, the data for individual co-existing ions were extracted from the Design Expert and plotted using MS Excel for better visibility. The quality of polynomial fit of the model was checked by the determination of coefficient (R^2), and its statistical significance was checked by the Fisher F-test in the same program. Model terms were evaluated by the p value (probability) with 95% confidence level. The response variable that represented removal efficiency was fitted by a second-order model in the form of quadratic polynomial equation (Equation 4.3) (Thakur & Mondal, 2016).

(4.3)

Where: Y is the response variables (fluoride and arsenic reduction in percentage), b_0, b_i, b_{ii}, and b_{ij} are constant coefficients of intercept, linear, quadratic and interactive terms, respectively and Xi and Xj represent the five independent variables (initial concentration of calcium, magnesium, nitrate, sulphate, bicarbonate and carbonate).

4.2 Results and discussion

The results of the effect of interaction between co-existing ions on the removal of arsenic and fluoride in a hybrid Fe-Al EC is presented in Table 4.2. It was observed that the efficiency of Al-Fe EC on the arsenic removal decreased when all six ions co-exist. For example, in experiment 36, the As^{3+} removal declined to 57.30 from 96.25%, which could be attributed to the high CEI: As^{3+} ratio (1200 mg/mg) that tend to limit arsenic access to the surface of adsorbent. On the other hand, both antagonism and synergism interaction effects were observed on the removal of F^-. The experiment number 39 and 45 demonstrated highest synergism effects removal of fluoride, the removal had increased to 96.69 % from 91.76%. Meanwhile, the most antagonistic effect was noted at experiment 10 where the removal felt to 52%. This, may signify that beside the competition for the adsorption sites other factors depending on the type of individual common ion could have significant effect on the Al and Fe dissolution as discussed in the sections to follow.

Table 4.2: Effect of co-ions on the removal of fluoride and arsenic in the EC process using hybrid Al-Fe electrodes

S/N	mass	Ca^{2+}	HCO_3^-	CO_3^{2-}	NO_3^-	SO_4^{2-}	Mg^{2+}	Ft	Ast	F%	As%
1	0.41	0.50	0.50	50.25	0.50	50.25	50.25	3.71	0.03	76.81	86.00
		100.0									
2	0.41	0	0.50	50.25	0.50	50.25	50.25	1.83	0.02	88.56	90.75
			100.0								
3	0.41	0.50	0	50.25	0.50	50.25	50.25	2.43	0.02	84.81	90.00
		100.0	100.0								
5	0.41	0	0	50.25	0.50	50.25	50.25	1.56	0.01	90.25	94.50
					100.0						
6	0.41	0.50	0.50	50.25	0	50.25	50.25	1.46	0.03	90.88	83.95
		100.0			100.0						
7	0.41	0	0.50	50.25	0	50.25	50.25	1.48	0.04	90.75	81.65
			100.0		100.0						
8	0.41	0.50	0	50.25	0	50.25	50.25	1.41	0.03	91.19	83.45
		100.0	100.0		100.0						
9	0.41	0	0	50.25	0	50.25	50.25	2.03	0.05	87.31	73.35
10	0.41	50.25	0.50	0.50	50.25	0.50	50.25	7.61	0.03	52.44	83.25
			100.0								
11	0.41	50.25	0	0.50	50.25	0.50	50.25	2.02	0.03	87.38	84.45
				100.0							
12	0.41	50.25	0.50	0	50.25	0.50	50.25	1.68	0.04	89.50	82.50
			100.0	100.0							
13	0.41	50.25	0	0	50.25	0.50	50.25	1.17	0.04	92.69	81.50
						100.0					
14	0.41	50.25	0.50	0.50	50.25	0	50.25	1.44	0.04	91.00	82.45
			100.0			100.0					
15	0.41	50.25	0	0.50	50.25	0	50.25	1.58	0.04	90.13	81.30
				100.0		100.0					
16	0.41	50.25	0.50	0	50.25	0	50.25	1.09	0.03	93.19	84.20
			100.0	100.0		100.0					
17	0.41	50.25	0	0	50.25	0	50.25	1.42	0.04	91.13	81.00
18	0.41	50.25	50.25	0.50	0.50	50.25	0.50	3.13	0.03	80.44	83.00

				100.0							
19	0.41	50.25	50.25	0	0.50	50.25	0.50	3.14	0.03	80.38	85.50
					100.0						
20	0.41	50.25	50.25	0.50	0	50.25	0.50	1.34	0.04	91.63	81.30
				100.0	100.0						
21	0.41	50.25	50.25	0	0	50.25	0.50	1.45	0.06	90.94	68.50
							100.0				
22	0.41	50.25	50.25	0.50	0.50	50.25	0	0.63	0.04	96.06	82.05
				100.0			100.0				
23	0.41	50.25	50.25	0	0.50	50.25	0	2.64	0.04	83.50	81.40
					100.0		100.0				
24	0.41	50.25	50.25	0.50	0	50.25	0	2.03	0.04	87.31	80.25
				100.0	100.0		100.0				
25	0.41	50.25	50.25	0	0	50.25	0	3.37	0.03	78.94	83.00
26	0.41	0.50	50.25	50.25	0.50	0.50	50.25	2.70	0.04	83.13	82.15
		100.0									
27	0.41	0	50.25	50.25	0.50	0.50	50.25	1.38	0.04	91.38	79.30
					100.0						
28	0.41	0.50	50.25	50.25	0	0.50	50.25	2.28	0.04	85.75	81.80
		100.0			100.0						
29	0.41	0	50.25	50.25	0	0.50	50.25	2.32	0.07	85.50	66.00
						100.0					
30	0.41	0.50	50.25	50.25	0.50	0	50.25	3.35	0.03	79.06	82.65
		100.0				100.0					
31	0.41	0	50.25	50.25	0.50	0	50.25	1.32	0.04	91.75	78.90
					100.0	100.0					
32	0.41	0.50	50.25	50.25	0	0	50.25	1.55	0.04	90.31	82.30
		100.0			100.0	100.0					
33	0.41	0	50.25	50.25	0	0	50.25	0.94	0.07	94.13	63.95
34	0.41	50.25	0.50	50.25	50.25	0.50	0.50	1.28	0.07	92.00	65.40
			100.0								
35	0.41	50.25	0	50.25	50.25	0.50	0.50	1.94	0.05	87.88	73.05
						100.0					
36	0.41	50.25	0.50	50.25	50.25	0	0.50	1.07	0.09	93.31	57.35

			100.0			100.0					
37	0.41	50.25	0	50.25	50.25	0	0.50	3.55	0.06	77.81	72.50
							100.0				
38	0.41	50.25	0.50	50.25	50.25	0.50	0	4.11	0.04	74.31	81.50
			100.0				100.0				
39	0.41	50.25	0	50.25	50.25	0.50	0	0.51	0.03	96.81	83.45
						100.0	100.0				
40	0.41	50.25	0.50	50.25	50.25	0	0	1.90	0.04	88.13	80.95
			100.0			100.0	100.0				
41	0.41	50.25	0	50.25	50.25	0	0	2.97	0.09	81.44	53.50
42	0.41	0.50	50.25	0.50	50.25	50.25	0.50	0.93	0.03	94.19	84.50
		100.0									
43	0.41	0	50.25	0.50	50.25	50.25	0.50	1.65	0.06	89.69	72.50
				100.0							
44	0.41	0.50	50.25	0	50.25	50.25	0.50	3.20	0.07	80.00	66.50
		100.0		100.0							
45	0.41	0	50.25	0	50.25	50.25	0.50	0.64	0.03	96.00	83.50
							100.0				
46	0.41	0.50	50.25	0.50	50.25	50.25	0	2.10	0.06	86.88	67.75
		100.0					100.0				
47	0.41	0	50.25	0.50	50.25	50.25	0	1.57	0.05	90.19	76.95
				100.0			100.0				
48	0.41	0.50	50.25	0	50.25	50.25	0	1.60	0.04	90.00	82.50
		100.0		100.0			100.0				
49	0.41	0	50.25	0	50.25	50.25	0	1.75	0.04	89.06	79.00
50	0.41	50.25	50.25	50.25	50.25	50.25	50.25	1.51	0.01	90.56	93.00

Removal of F^- and As^{3+} in the absence of common ions were found to be 91.76% and 96.25%, respectively (Chapter 3).

4.2.1 Development of regression model and model validation

The removal efficiency of the electrocoagulation on fluoride and arsenic can be affected by interaction of co-existing ions in water. In this study the ions of calcium, magnesium, carbonate, bicarbonate, sulfate and nitrate were investigated for their effect on the performance of hybrid Al-Fe EC. The experiments on combination of different initial concentrations of these ions

together with the observed removal efficiencies are shown in Table 4.2. The coefficients of the response function are shown in equation 4.3, while the t-values and P-values to assess the validity of the model prediction for removal efficiencies of fluoride and arsenic are presented in Table 4.3. The actual equations of the second order polynomial equations for the removal efficiencies of fluoride and arsenic are given by equation 4.4 and 4.5, respectively: These equations were then used for prediction of the removal efficiencies at any combination of the initial concentration of these ions.

Both models presented low p-values ≤ 0.002 and 0.0025 for the removal of fluoride and arsenic, respectively. Moreover, they presented large F-values of 2.18 for fluoride and 3.19 for arsenic, which indicated that at least one of the terms in each model had a significant effect on the response. In this case the calcium and carbonate were the most significant ions that affected the removal of fluoride and arsenic, respectively (both $p < 0.05$). Other important significant terms were square terms, E^2 and F^2 for arsenic, and interaction BF for both fluoride and arsenic. Meanwhile, the lack of fit p-values of 0.11 for fluoride and 0.08 for arsenic were observed which made lack of fit not significant to both models. On the other hand, the models presented fair regression coefficients (R^2) of 0.69 to fluoride removal and 0.72 to arsenic removal.

Table 4.3: ANOVA results for the responses on fluoride and arsenic removal

	Fluoride		Arsenic		
Source	F-value	p-value	F-value	p-value	
Model	2.180	0.025	3.180	0.002	significant
A-Calcium	5.720	0.024	1.280	0.268	
B-Bicarbonate	0.599	0.446	0.073	0.790	
C-Carbonate	0.023	0.881	0.001	0.983	
D-Nitrate	3.190	0.086	8.740	0.007	
E-Sulphate	0.983	0.331	2.180	0.152	
F-Magnesium	0.291	0.594	1.740	0.199	
AF	0.538	0.470	0.002	0.967	
BF	8.110	0.009	8.140	0.008	
DE	1.840	0.187	0.010	0.923	
E^2	0.531	0.473	22.030	< 0.0001	

F^2	1.950	0.175	32.680	< 0.0001	
Lack of Fit	3.130	0.105	3.530	0.083	not significant

R^2 (F) = 0.69: R^2 (As) = 0.72

4.2.2 Model validation

The predicted against the actual plots (Figure 4.1) confirmed alignment between the residual and predicted fluoride and arsenic reduction segmenting that the models could well predict within the range of initial concentration of ions applied. Figure 4.2 shows the normal percentage probability of residual against the normal plot of residuals for fluoride and arsenic removal, respectively. Both plots form fairly straight line with an *S*-shape indicating positive correlation between probability and normal removal, ascertaining the assumption that both models were relatively satisfactory Therefore, it can be concluded that the quadratic models of the response surface developed in this study correlating fluoride and arsenic removal with process variables are best suited to explain the experimental data of a combined Al-Fe EC process.

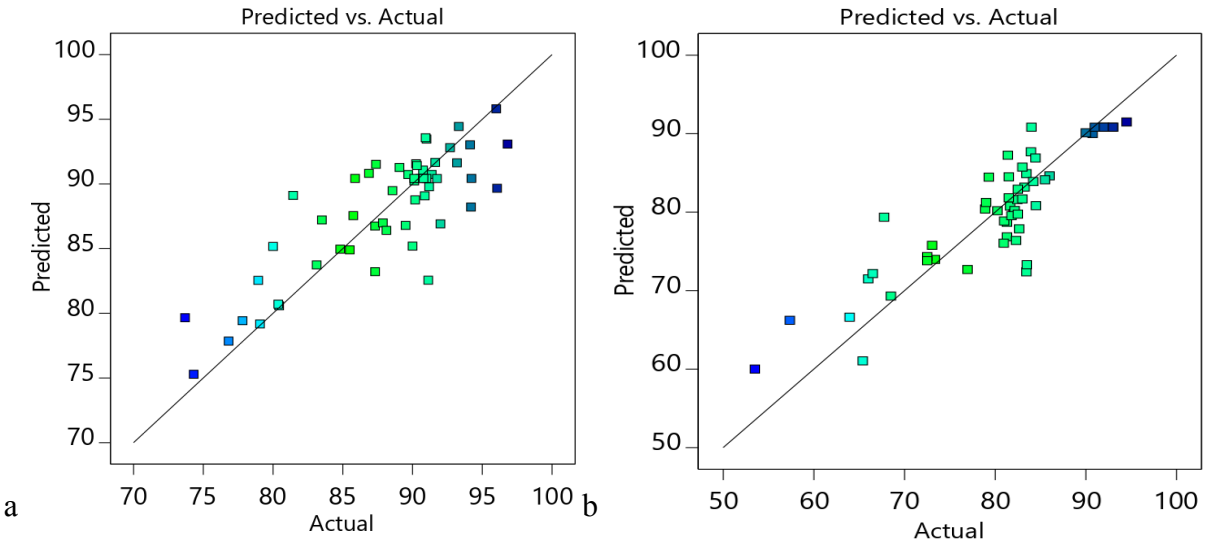

Figure 4.1: Comparison of predicted and actual values for (a) fluoride (b) arsenic reduction in the EC process.

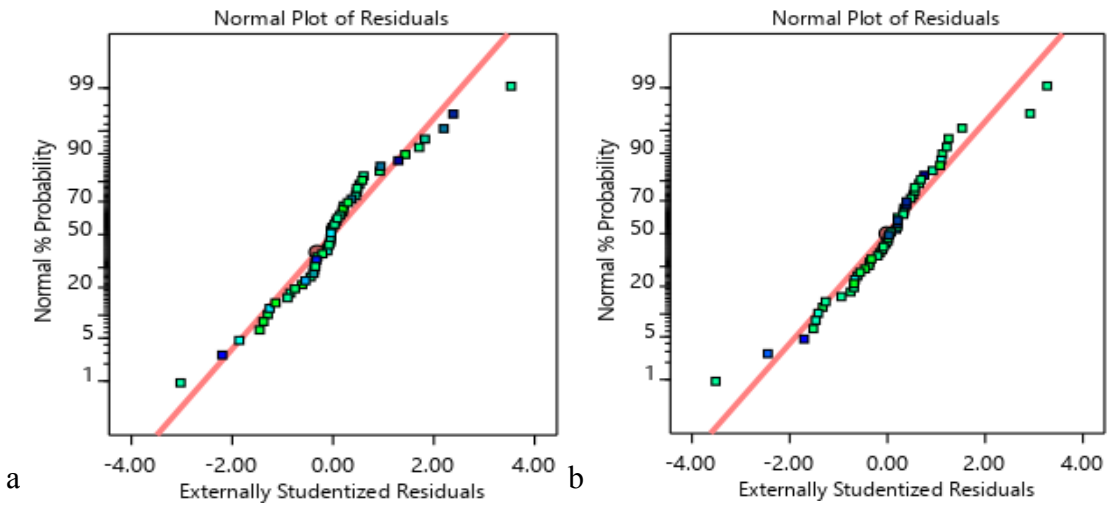

Figure 4.2: Comparison of normal probability and external studentized residual (a) fluoride (b) arsenic

4.2.3 Model equations

The following are the coded equations generated by the models for the removal of fluoride (Equation 4.4) and removal of arsenic (Equation 4.5). These equations were then used to calculate the removal of fluoride and arsenic at a desired initial concentration of each co-existing ions to evaluate their effect on the performance of EC.

F % = 90.4284 + 2.14844 * A + 0.695208 * B + -0.135521 * C + 1.60417 * D + 0.890521 * E + -0.484375 * F + -1.25781 * AB + 2.03125 * AC + -2.41016 * AD + 1.0625 * AE + -1.14063 * AF + -1.46063 * BC + -1.60156 * BD + -3.77328 * BE + 4.42969 * BF + 0.445313 * CD + -2.24188 * CE + -0.644531 * CF + 2.10938 * DE + -4.38281 * DF + 0.898437 * EF + 0.773826 * A^2 + -1.05419 * B^2 + 0.211535 * C^2 + -2.57774 * D^2 + -0.999507 * E^2 + -1.91378 * F^2 (4.4)

As % = 90.8333 + -1.38333 * A + -0.329167 * B + -0.0270833 * C + -3.6125 * D + -1.80417 * E + 1.6125 * F + -1.00625 * AB + 2.0375 * AC + -3.075 * AD + -0.43125 * AE + 0.0875 * AF + -0.53125 * BC + -2.06875 * BD + -1.65313 * BE + -6.0375 * BF + -1.4875 * CD + 0.64375 * CE + 2.2625 * CF + -0.20625 * DE + 2.3125 * DF + -2.7375 * EF + -4.45764 * A^2 + -0.436806 * B^2 + 0.946528 * C^2 + -0.482639 * D^2 + -8.76181 * E^2 + -10.6722 * F^2 (4.5)

4.2.4 Effect of individual co-existing ion on the removal of arsenic and fluoride

The effects of each individual ion on the removal of fluoride and arsenic were evaluated statistically using the quadratic model of the BBD by keeping the initial concentrations of other co-existing ions at their mean concentration (50.25 mg/L).

4.2.4.1 Magnesium

An increase of magnesium from 0.5 to 50 mg/L indicated insignificant increase of fluoride removal from 88 to 90 % (Figure 4.3a). However, at concentration > 50 mg/L magnesium, the removal of fluoride slightly declined to 86%. Similar trend was observed to the arsenic removal although the changes were more pronounced. Arsenic uptake had increased from 78 to 92% at 0.5 - 50 mg/L magnesium. In both cases the fluoride and arsenic removal declined to 85 and 80%, respectively at 100 mg/L of magnesium. This is attributed to the fact that at higher magnesium concentrations, magnesium combines more with available hydroxyl ion generated at the cathode to form solid magnesium hydroxide (Equation 4.6) (Tolonen et al., 2015). The formation of solid $Mg(OH)_2$, decreases production of solid AIOH, the main coagulant, and subsequent removal of both fluoride and arsenic tend to decline as observed at > 50 mg/L to both systems. Appropriate amounts of magnesium have positive effect on fluoride and arsenic removal; in this study, at ~50 mg/L corresponding to Mg:F (~ 3.2 mg/mg) and Mg:As (~0.25 mg/µg) per 0.41 g of coagulant have positive effect on fluoride and arsenic removal. Above these ratios, magnesium can lead to a decreased removal of both fluoride and arsenic.

(4.6)

4.2.3.1 Calcium

An increase in calcium concentration appears to significantly increase the uptake of fluoride through cooperative adsorption (Figure 4.3b). Cooperative effects is the one which adsorption of a particular adsorbate is enhanced by the previous adsorbed ion (Liu, 2015) . The fluoride removal had significantly increased from 89.00 to 94.00% with an increase of 0.5 mg/L to 100 mg/L of $[Ca^{2+}]$. Addition of Ca^{2+} permit formation of $Ca(OH)_2$ that tend to increase equilibrium shift towards solid phase by forming solid CaF_2 when F^- replaces the hydroxyl of $Ca(OH)_2$ as shown by Equation 4.7. Furthermore, since Ca^{2+} (1) is more electropositive than both Fe^{2+} (1.83) and Al^{3+} (1.61) then it tends to increase the positive surface charge of the adsorbent when added in a system (*the electronegativity values shown in bracket*). This enhances the removal of F^- by electrostatic force interactions in the whole range of calcium concentration added as observed in Figure 4.3b. On the other hand, at a lower concentration of calcium $[Ca^{2+}] < 25$ mg/L there is a slight increase in arsenic removal in a range of 87-91% (Figure 3b). However, at higher level of $[Ca^{2+}] > 50$ mg/L there was significant decrease in arsenic removal 90 to 83%, the decline in arsenic removal may be attributed to the higher Ca^{2+}/As ratio > 250 mg/µg in the reactor,

restricting arsenic mass transfer to the AlOH surface sites that lead a decrease in arsenic removal (Kobya et al., 2017).

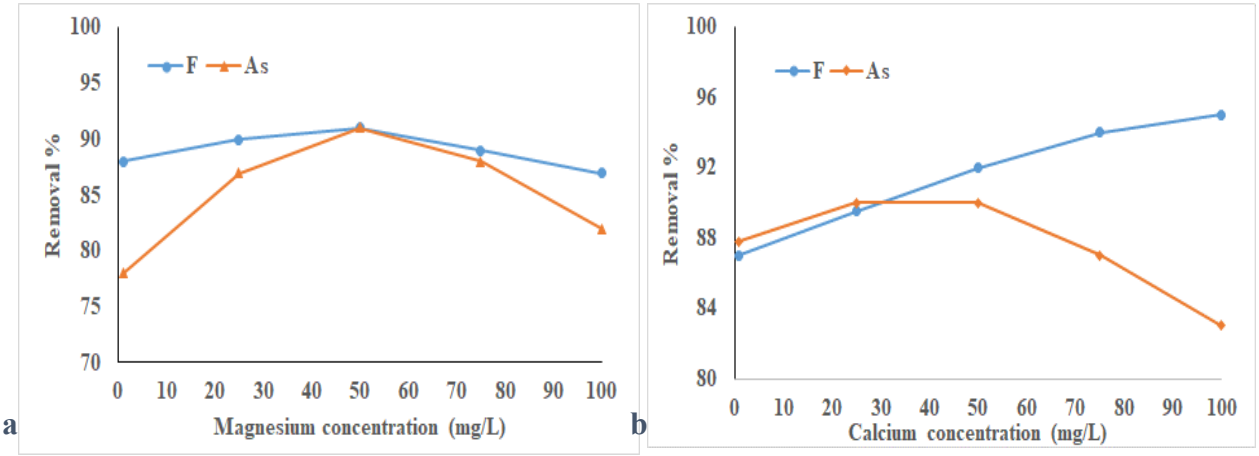

Figure 4.3: Effect of (a) magnesium concentration on (b) calcium concentration on the removal of fluoride and arsenic by hybrid Al-Fe electrocoagulation

4.2.3.3 Nitrate

There was a significant increase on the removal of fluoride from 85 to 92% as the nitrate concentration increases from 0.5 – 75 mg/L (Figure 4.4a). However, at > 75 mg/L of nitrate, F^- removal declined to 88% which is ascertained by the high concentration of NO_3^- that tend to compete with F- for the adsorption sites. Additionally, higher [NO_3^-] > 75 mg/L may permit formation of soluble nitrates of iron and aluminum thereby reducing formation of solid AlOH coagulant. For the arsenic removal, the removal efficiency was observed to decline from 94 to 87% with an increase in NO_3^- levels from 0.5 to 100 mg/L (Figure 4.4a). This could be attributed to the high ratio between NO_3^-/As^{3+} (2.5 mg/µg - 200 mg/µg) in the solution where the relatively high amount of nitrate could limit mass transfer of arsenic and lower the adsorption of arsenic on AlOH. Moreover, as the concentration of NO_3 ion increases, NO_3^- tend to attach on the surface of electrodes resulting into the formation of passive layer leading to a decrease in the current density and subsequence removal of arsenic (Amani-ghadim et al., 2011). Therefore, following the negative effect on the removal of arsenic by nitrate in the whole concentration range of NO_3^-

applied the amount of NO_3^- should be kept low < 0.5 mg/L regardless of initial concentration of arsenic.

4.2.3.4 Sulphate

The effect of sulphate ions (SO_4^{2-}) on the removal of fluoride and arsenic is presented in Figure 4.4b. At a concentration range of 0 - 80 mg/L SO_4^{2-}, there was a slight enhancement of fluoride removal. For instance, fluoride removal insignificantly increased from 88% to 91% while arsenic significantly increased from 83 to 90% on increasing in sulphate concentration from 0.5 to 50 mg/L. At a lower concentration, the SO_4^{2-} ions facilitate an increase in the conductivity of the solution and current efficiency thus, improving the removal rate. However, at 50 mg/L < [SO_4^{2-}] > 80 mg/L, there was a decrease on the removal of fluoride and arsenic, respectively, which is attributed to the increase of the inhibition to the localized corrosion of aluminum and iron electrode, due to the build-up of massive sulphate on the electrode surface. When the corrosion of Al^{3+} and Fe^{2+} electrodes is inhibited, the coagulant dosage for effective fluoride and arsenic adsorption decreases as well, leading to a decrease in Al-Fe EC efficiency. Moreover, the ion exchange reaction between F^- and SO_4^{2-} at SO_4^{2-} > 50 mg/L according to Equation 4.8 is also another possible reaction slowing down removal of fluoride (Zuo et al., 2008). This implies that for the effective performance of Al-Fe EC the concentration of SO_4^{2-} should not exceed 60 mg/L.

(4.8)

4.2.3.5 Carbonates

Both carbonate (not shown here) and bicarbonate appear to have similar but insignificant effects on the efficiency of electrocoagulation on F^- removal at 0.5-100 mg/L. As observed in Figure 4.4c the removal of fluoride and arsenic remains almost the same regardless an increase in carbonate concentration. This implies that the dissolution of Al^{3+} and Fe^{2+}, the surface charge of AIOH, the movement of fluoride and arsenic in the reactor were not affected at the carbonate's concentration in the range (1-100 mg/L).

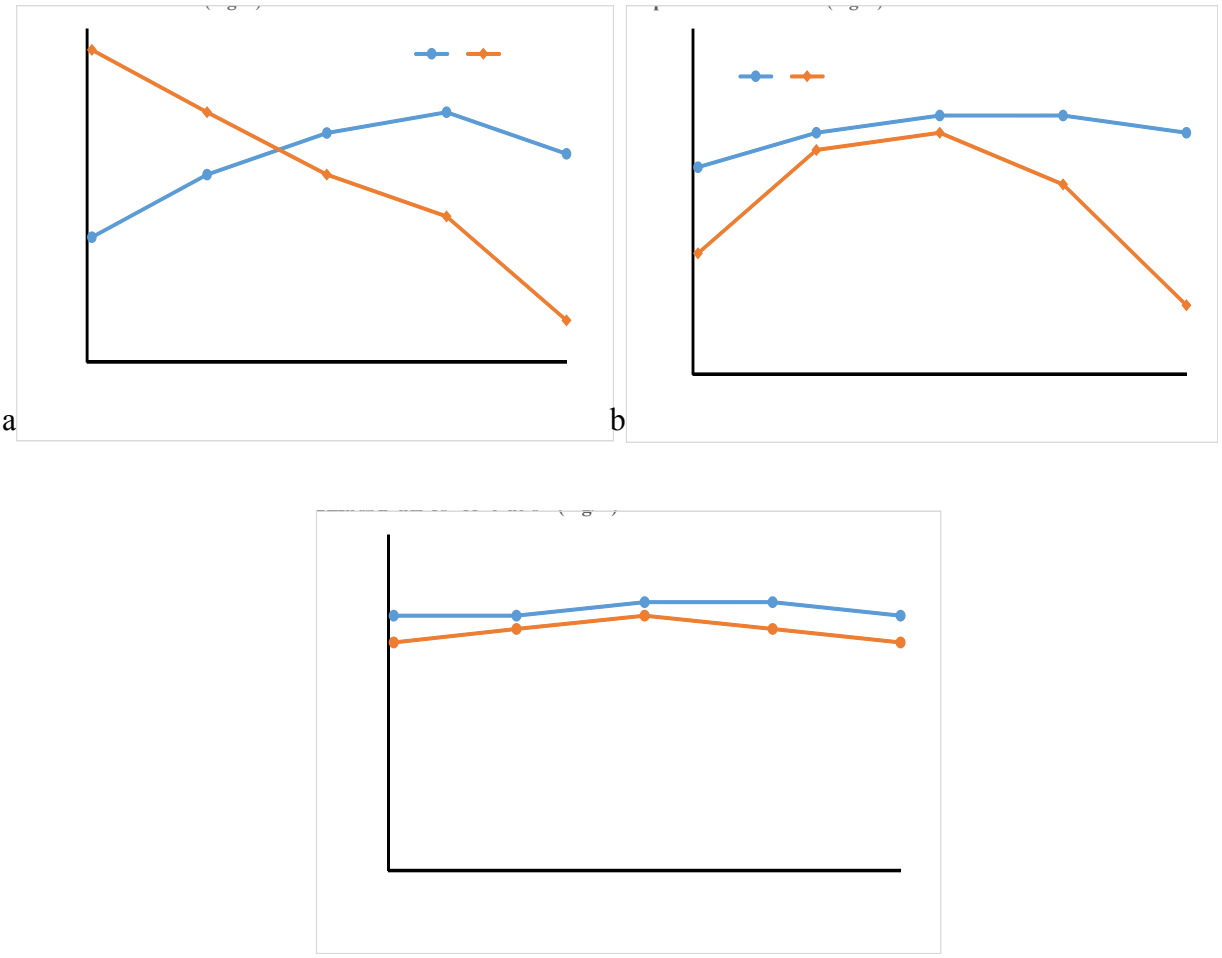

Figure 4.4: The effect of (a) nitrate concentration (b) sulphate concentration (c) bicarbonate concentration on the removal of fluoride and arsenic by hybrid Al-Fe electrocoagulation

4.2.5 Combining effects of co-existing ions on the performance of Al-Fe EC

4.2.5.1 Nitrate and carbonate

When nitrate and carbonate interact, the maximum removal attained for fluoride and arsenic were 90% and 94%, respectively (Figure 4.5a and b). The maximum fluoride removal (90 %) was achieved at initial concentration of 80 mg/L of NO_3^- and 10 mg/L that of HCO_3^-. At this point the performance of an EC was similar to that in absence of ions. Moreover, the same maximum fluoride removal could be achieved by decreasing NO_3^- concentration and increasing HCO_3^- by following the middle circle line shown in Figure 8a. For the case of arsenic, the highest removal

was achieved at high carbonate [HCO_3^-] > 70 mg/L and low nitrate [NO_3^-] < 10 mg/L. On the other side increasing concentration of nitrate 10-100 mg/L at a fixed high concentration of carbonate (> 70 mg/L) the arsenic removal also tends to decrease reaching the lowest of 80 % removal. An increase in the total ions tend to lower the performance of an EC probably due to the hindrance to the mass transfer and accumulation of the ions on the surface of electrode which tend to lower the dissolution of Al^{3+} and Fe^{2+}.

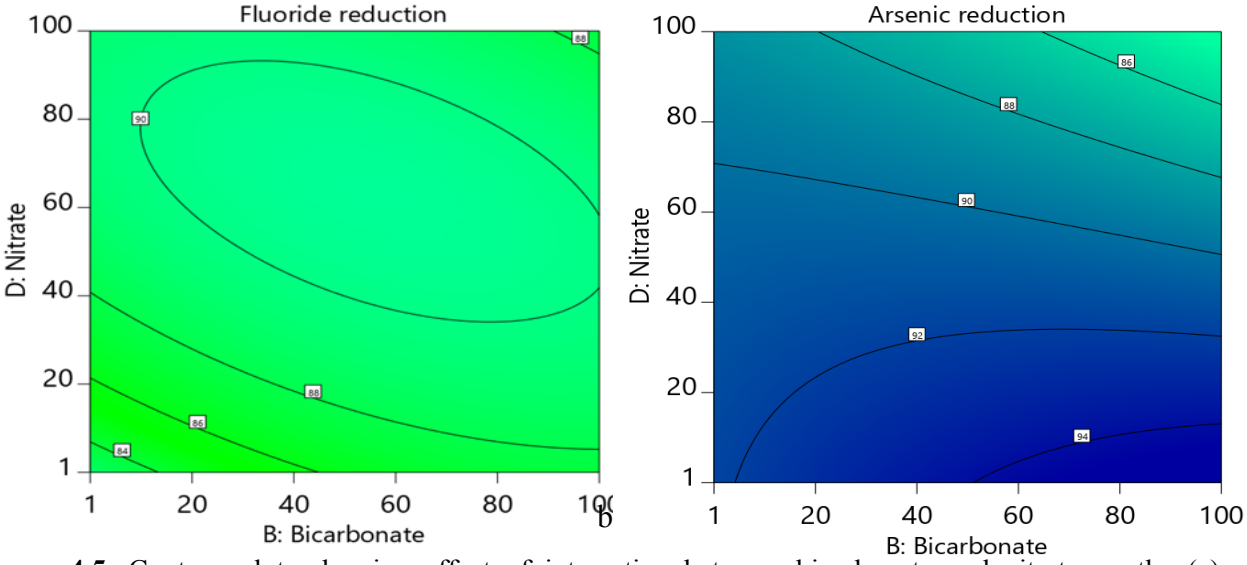

Figure 4.5: Contour plots showing effect of interaction between bicarbonate and nitrate on the (a) removal of fluoride (b) removal of arsenic

4.2.5.2 Nitrate and sulfate

The increase in sulphate ions appears to significantly lower the fluoride removal and the surface bent more towards higher SO_4^{2-} concentration (Figure 4.6a and b). Meanwhile, the increase in nitrate initially foster removal that eventually started to decline at concentration > 67 mg/L. At all concentration of SO_4^{2-}, removal was small in the presence of low NO_3^-, though when the NO_3^- was increased to 100 mg/L the removal efficiency was restored to 91%. This phenomenon is similar to that reported by Hu et al., (2003) that the presence of NO_3^- prevent inhibition to Al^{3+} and Fe^{2+} dissolution caused by SO_4^{2-}. On the other hand, at higher NO_3^- there was a low uptake of arsenic (Figure 9b). The highest arsenic removal of 86% was achieved at [NO_3^-] < 36 mg/L and 70 ≥ [SO_4^-] ≤ 28. When the two co-exist out of these concentration range removal efficiencies became low. At a very low concentration of ion; [NO_3^-] < 36 mg/L and [SO_4^-] < 28 mg/L, the conductivity of the solution could be low and reducing dissolution efficiency. When the concentration is higher it means the IR drop may occur and also the arsenic mass transfer to the surface of coagulant become limited (Nasrullah et al., 2012).

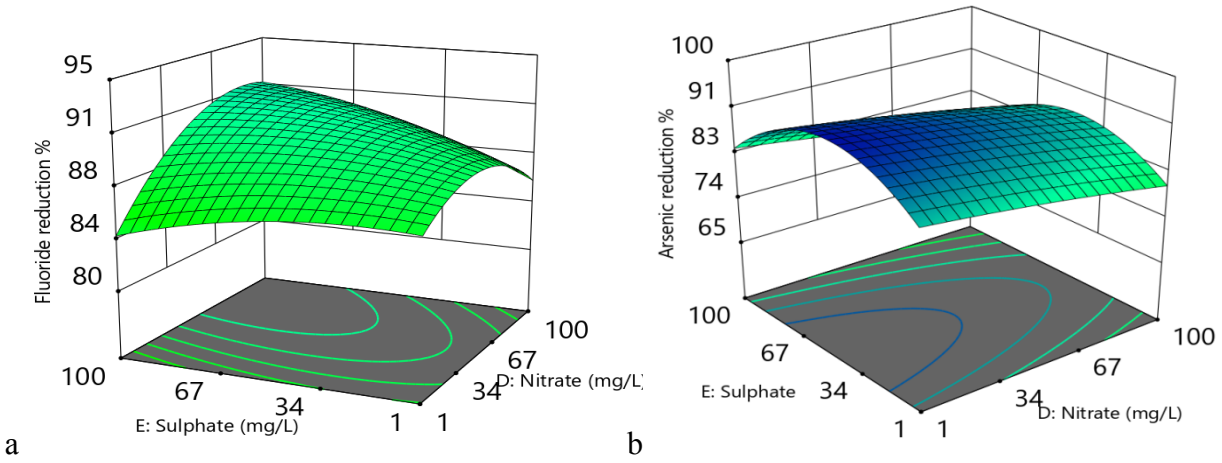

Figure 4.6: 3-D surface plots showing effect of interaction between sulphate and nitrate on (a) removal of fluoride (b) removal of arsenic

4.2.5.3 Sulfate and bicarbonate

The presence of sulphate and carbonate have been a major concern in ensuring supply of safe drinking water especially from groundwater sources (Su & Puls, 2001). The increase in both sulphate and bicarbonate appears to have significant effects toward removal of fluoride (Figure 4.7a). In the low concentration of both sulphate and bicarbonate, the efficiency of an EC also appeared to be low probably due to the low conductivity of the solution. However, the maximum fluoride removal of 92 % was the highest when the sulphate ion was increased to 90 mg/L at constant bicarbonate (10 mg/L). Upon increase of bicarbonate at fixed SO_4^{2-} (90 mg/L) the removal efficiency declined to 88% at 90 mg/L of HCO_3^-. On the other hand, the increase in bicarbonate to 100 mg/L appears to have insignificant effect to the efficiency of the Al-Fe EC towards arsenic removal in the presence of sulphate. As noted in Figure 4.7b at highest concentration (100 mg/L) of one ion and another being kept low the maximum fluoride removal of 91 % was observed. Meanwhile, the increase on the sulphate ion initially increases the rate of arsenic removal regardless of bicarbonate, however at $[SO_4^-]$ > 80 mg/L removal started to decline. This reflects that at higher $[SO_4^{2-}]$ > 80 mg/L, regardless of bicarbonate there is a decline on electrode corrosion due to passivation of electrode surface (Wilkie & Hering, 1996). The arsenic removal is controlled by the concentration of sulphate while carbonate appears to have negligible influence.

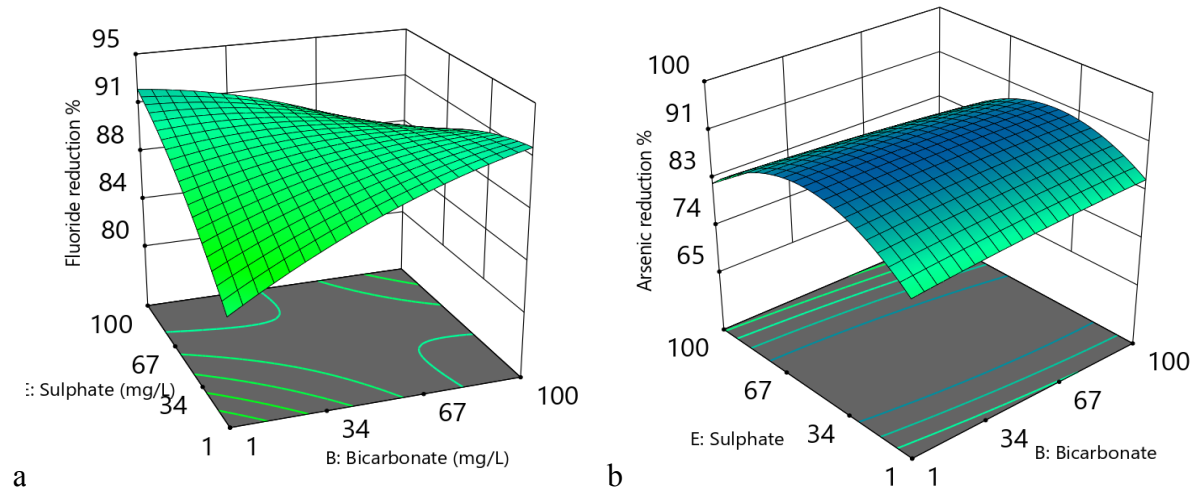

Figure 4.7: 3-D surface plots showing effect of interaction between bicarbonate and sulphate on the (a) removal of fluoride (b) removal of arsenic

4.2.5.4 Calcium and Magnesium

When calcium and magnesium co-exist, [Ca^{2+}] significantly increases fluoride removal with increase in concentration (1-100 mg/L). The removal had increased from 85 to 94 % at 100 mg/L of calcium. However, as seen in Figure 4.8a, the surface curve has bent down towards the magnesium axis, this means that the concentration of magnesium inhibited the uptake of fluoride. The efficiency of EC started to decline when the magnesium level reaches [Mg^{2+}] > 70 mg/L. The highest removal was attained at higher concentration of Ca^{2+} (100 mg/L) at a Mg^{2+} concentration ~70 mg/L. Therefore, for the effective removal of F^- (94%) the level of Mg^{2+} concentration should be < 70 mg/L and Ca^{2+} ~100 mg/L. On the other hand, the removal of arsenic was low but increased with [Mg^{2+}] to a maximum removal of 89 % when Mg^{2+} ~ 40 mg/L. At magnesium concentration > 40 mg/L the arsenic removal started to decline despite an increase in the level of Ca^{2+} (Figure 4.8b). Thus, the Al-Fe EC efficiency appears to be dependent on the concentration of magnesium, therefore, the maximum level of magnesium that can permit effective removal of both fluoride and arsenic is ~70 mg/L in the presence of any amount of Ca^{2+} (1-100 mg/L).

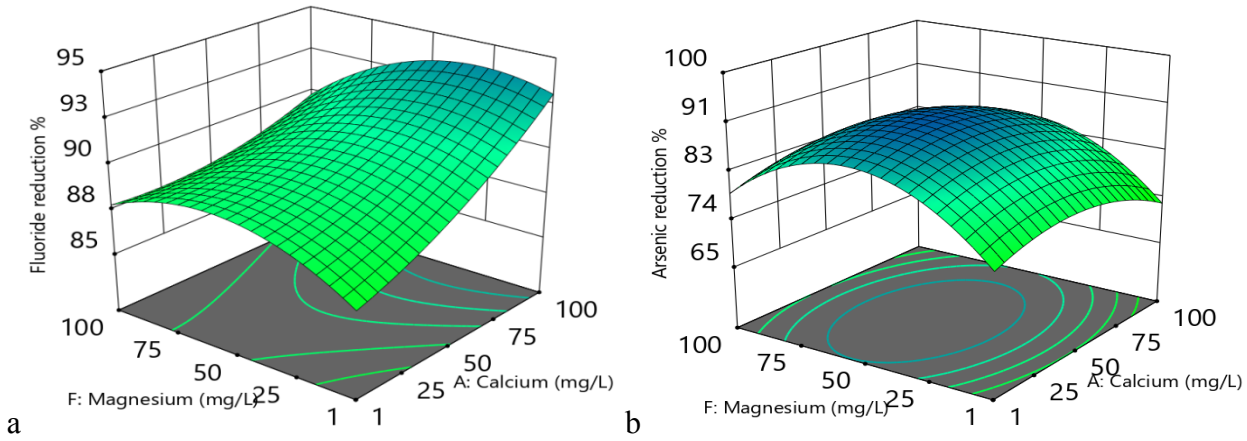

Figure 4.8: 3-D surface plots showing effect of interaction between magnesium and calcium on the (a) reduction of fluoride (b) reduction of arsenic

4.3 Optimal level of co-existing ions for effective performance of hybrid Al-Fe EC for simultaneous removal of fluoride and arsenic

To find the optimal concentration level of each that the Al-Fe EC will still perform to the maximum the common ions were left at their range (0.5 – 100 mg/L) and the reduction of fluoride and arsenic were maximized in the BBD design model. Results revealed that at Ca^{2+} = 100 mg/L; HCO_3- = 97 mg/L; CO_3^- = 100 mg/L; NO_3^- = 0.5 mg/L; SO_4^{2-} = 17 mg/L; and Mg^{2+} = 64 mg/L, the model predicted that of 96.85 % and 92.17 % fluoride and arsenic removal could be achieved. The experiment was set and performed at the suggested initial concentration of co-ions and managed to reduce fluoride and arsenic by 93.55% and 94.21%, respectively. Thus, the performance of hybrid Fe-Al electrocoagulation at J = 9.9 mA/cm^{-2}, pH = 7.5, t = 50 min in the presence of common ions was closer to the performance in the absence of common ion as reported in our previous study. This may be due to opposite effect contributed by the common ions as described leading to the cancellation of the overall effects to the performance of an EC.

4.4 Simultaneous removal of arsenic and fluoride from real groundwater.

Thus, the performance of hybrid Fe-Al electrocoagulation at J = 9.9 mA/cm^{-2}, pH = 7.5, t = 50 min in the presence of common ions was closer to the performance in the absence of CEI as reported in a previous chapter (Chapter Three). In this report the Al-Fe hybrid achieved removal

of 16 mg/L and 200 µg/L initial concentration of fluoride and arsenic by 94 and 96 %, respectively in the absence of CEI. The performance of Al-Fe EC is here tested in a real groundwater characterized by (As = 220 µg/L and F = 7.6 mg/L) + co-existing ions (Ca^{2+} = 0.5; Na^{+} = 306; NO^{3-} = 18; SO_4^{2-} = 53, HCO_3^{-} = 102 mg/L pH 7.5 and EC = 2160 S/m) collected from Ziway, Ethiopia and achieved 91 and 98% fluoride and arsenic reduction, respectively. Another water sample collected from Arusha, Tanzania also characterized by (F = 22 mg/L) + co-existing ions (Ca^{2+} = 12; Na^{+} = 104; NO^{3-} = 51; SO_4^{2-} = 32, HCO_3^{-} = 160 mg/L, pH 7.2, and EC = 824 S/m) achieved 93 % fluoride reduction. The performance appears to be similar as that in the absence of CEI. This may be due to the different/opposite effects caused by the individual co-existing ions as described leading to the cancellation of the overall effects to the performance of an EC.

4.5 Conclusion

In this study, Box Behnken statistical design of the RSM was used to evaluate the effect of co-existing ions to the performance of hybrid Al-Fe EC on the simultaneous removal of fluoride and arsenic. The proposed models fitted fairly with the experimental data. It can be concluded from this study that the type and initial concentration of ion except that of carbonates had influence on the simultaneous removal of fluoride and arsenic. The calcium ion is important to improve the removal of fluoride possibly by increasing positive surface charge of the AlOH while it has negative effect on the arsenic removal at higher concentration. Sulphate and nitrate on the other hand tend to reduce the efficiency of arsenic removal which is attributed to the formation of a passive film layer on the anode electrode and reducing corrosion of anode. The effect of magnesium on the removal of both fluoride and arsenic depend on the concentration levels, where it reduces removal efficiency when at higher concentration. The carbonates are found to have insignificant influence on the removal efficiency to both fluoride and arsenic. Thus, the individual effects of co-existing ion are found to depend on the kind of ion as well as on their concentration levels. The hybrid Al-Fe EC can still effectively remove fluoride and arsenic to its capacity in a real groundwater due to opposite effects contributed by naturally occurring anions and cations in water.

4.6 References

Abejón, A., Garea, A., & Irabien, A. (2015). Arsenic removal from drinking water by reverse osmosis: Minimization of costs and energy consumption. Separation and Purification

Technology, 144, 46–53. https://doi.org/10.1016/j.seppur.2015.02.017

Al-ghouti, M. A., & Da, D. A. (2020). Guidelines for the use and interpretation of adsorption isotherm models : A review. Journal of Hazardous Materials, 393(February), 122383. https://doi.org/10.1016/j.jhazmat.2020.122383

Alarcón-Herrera, M. T., Bundschuh, J., Nath, B., Nicolli, H. B., Gutierrez, M., Reyes-Gomez, V. M., … Sracek, O. (2013). Co-occurrence of arsenic and fluoride in groundwater of semi-arid regions in Latin America: Genesis, mobility and remediation. Journal of Hazardous Materials, 262, 960–969. https://doi.org/10.1016/j.jhazmat.2012.08.005

Amani-ghadim, A. R., Aber, S., Olad, A., & Ashassi-sorkhabi, H. (2011). Electrochimica Acta Influence of anions on Reactive Red 43 removal in electrochemical coagulation process. Electrochimica Acta, 56(3), 1373–1380. https://doi.org/10.1016/j.electacta.2010.10.089

Amani-Ghadim, A. R., Aber, S., Olad, A., & Ashassi-Sorkhabi, H. (2013). Optimization of electrocoagulation process for removal of an azo dye using response surface methodology and investigation on the occurrence of destructive side reactions. Chemical Engineering and Processing: Process Intensification. https://doi.org/10.1016/j.cep.2012.10.012

Araújo, C. S. T., Almeida, I. L. S., Rezende, H. C., Marcionilio, S. M. L. O., Léon, J. J. L., & de Matos, T. N. (2018). Elucidation of mechanism involved in adsorption of Pb (II) onto lobeira fruit (Solanum lycocarpum) using Langmuir, Freundlich and Temkin isotherms. Microchemical Journal, 137, 348–354.

Ayawei, N., Ekubo, A. T., Wankasi, D., & Dikio, E. D. (2015). Adsorption of congo red by Ni/Al-CO3: Equilibrium, thermodynamic and kinetic studies. Oriental Journal of Chemistry, 31(3), 1307–1318.

Balasubramanian, N., Kojima, T., Basha, C. A., & Srinivasakannan, C. (2009). Removal of arsenic from aqueous solution using electrocoagulation. Journal of Hazardous Materials, 167(1–3), 966–969.

Canizares, P., Jiménez, C., Martínez, F., Rodrigo, M. A., & Sáez, C. (2009). The pH as a key parameter in the choice between coagulation and electrocoagulation for the treatment of wastewaters. Journal of Hazardous Materials, 163(1), 158–164.

Catalano, J. G., Park, C., Fenter, P., & Zhang, Z. (2008). Simultaneous inner-and outer-sphere arsenate adsorption on corundum and hematite. Geochimica et Cosmochimica Acta, 72(8), 1986-2004.

Chandra Srivastava, V., Deo Mall, I., & Mani Mishra, I. (2006). Modelling individual and competitive adsorption of cadmium (II) and zinc (II) metal ions from aqueous solution onto bagasse fly ash. Separation Science and Technology, 41(12), 2685–2710.

Chatterjee, D., Halder, D., Majumder, S., Biswas, A., Nath, B., Bhattacharya, P., … Hazra, R. (2010). Assessment of arsenic exposure from groundwater and rice in Bengal Delta Region, West Bengal, India. Water Research, 44(19), 5803–5812.

Chen, G. (2004). Electrochemical technologies in wastewater treatment. Separation and Purification Technology, 38(1), 11–41.

Chithra, K., & Balasubramanian, N. (2010). Modeling electrocoagulation through adsorption kinetics. Journal of Modelling and Simulation of Systems, 1(2), 124–130.

Choy, K. K., Porter, J. F., & McKay, G. (2000). Langmuir isotherm models applied to the multicomponent sorption of acid dyes from effluent onto activated carbon. Journal of Chemical & Engineering Data, 45(4), 575-584.

Daniel, R., & Prabhakara Rao, A. V. S. (2012). An efficient removal of arsenic from industrial effluents using electro-coagulation as clean technology option. International Journal of Environmental Research, 6(3), 711–718.

Davis, H. T., Valencourt, L. R., & Johnson, C. E. (1975). Transport processes in composite media. Journal of the American Ceramic Society, 58(9 10), 446–452.

Davoudinejad, M., & Ghorbanian, S. A. (2013). Modeling of adsorption isotherm of benzoic compounds onto GAC and introducing three new isotherm models using new concept of Adsorption Effective Surface (AES). Sci Res Essays, 8(46), 2263–2275.

Choy, K. K., Porter, J. F., & McKay, G. (2000). Langmuir isotherm models applied to the multicomponent sorption of acid dyes from effluent onto activated carbon. Journal of Chemical & Engineering Data, 45(4), 575-584.

Demirbas, E., & Kobya, M. (2017). Operating cost and treatment of metalworking fluid wastewater by chemical coagulation and electrocoagulation processes. Process Safety and Environmental Protection, 105, 79–90.

Dissanayake, C. B. (1991). The fluoride problem in the groundwater of Sri Lanka—environmental management and health. International Journal of Environmental Studies, 38(2–3), 137–155.

Elwakeel, K. Z., Atia, A. A., & Guibal, E. (2014). Fast removal of uranium from aqueous solutions using tetraethylenepentamine modified magnetic chitosan resin. Bioresource Technology, 160, 107–114.

Fawell, J., Bailey, K., Chilton, J., Dahi, E., & Magara, Y. (2006). Fluoride in drinking-water. IWA publishing.

Federation, W. E., & Association, A. P. H. (2005). Standard methods for the examination of water and wastewater. American Public Health Association (APHA): Washington, DC, USA.

García-Lara, A. M., & Montero-Ocampo, C. (2010). Improvement of arsenic electro-removal from under groundwater by lowering the interference of other ions. Water, Air, and Soil Pollution, 205(1–4), 237.

Garcia-Segura, S., Eiband, M. M. S. G., de Melo, J. V., & Martínez-Huitle, C. A. (2017). Electrocoagulation and advanced electrocoagulation processes: A general review about the fundamentals, emerging applications and its association with other technologies. Journal of Electroanalytical Chemistry, 801, 267–299.

Girish, C. R. (2018). Multicomponent adsorption and the Interaction between the adsorbent And the adsorbate: A review. Interaction, 14, 15.

Girish, C. R. (2018). Simultaneous adsorption of pollutants onto the adsorbent review of interaction mechanism between the pollutants and the adsorbent. International Journal of Engineering and Technology, 7, 3613-3622.

Gomes, J. A. G., Daida, P., Kesmez, M., Weir, M., Moreno, H., Parga, J. R., … Peterson, E. (2007). Arsenic removal by electrocoagulation using combined Al–Fe electrode system and

characterization of products. Journal of Hazardous Materials, 139(2), 220–231.

Hamdaoui, O., & Naffrechoux, E. (2007). Modeling of adsorption isotherms of phenol and chlorophenols onto granular activated carbon: Part I. Two-parameter models and equations allowing determination of thermodynamic parameters. Journal of Hazardous Materials, 147(1–2), 381–394.

Hashim, K. S., Shaw, A., Al Khaddar, R., Pedrola, M. O., & Phipps, D. (2017). Iron removal, energy consumption and operating cost of electrocoagulation of drinking water using a new flow column reactor. Journal of Environmental Management, 189, 98–108.

Hernández, J. H. (2018). Simultaneous removal of fluoride and arsenic from groundwater by electrocoagulation using a filter-press flow reactor with a three-cell stack. Separation and Purification Technology. https://doi.org/10.1016/j.seppur.2018.02.018

Ho, Y.-S., & McKay, G. (2000). The kinetics of sorption of divalent metal ions onto sphagnum moss peat. Water Research, 34(3), 735–742.

Holt, P. K., Barton, G. W., Wark, M., & Mitchell, C. A. (2002). A quantitative comparison between chemical dosing and electrocoagulation. Colloids and Surfaces A: Physicochemical and Engineering Aspects, 211(2–3), 233–248.

Hu, C Y, Lo, S. L., & Kuan, W. H. (2003). Effects of co-existing anions on fluoride removal in electrocoagulation (EC) process using aluminum electrodes. Water Research, 37(18), 4513–4523.

Hu, Ching Yao, Lo, S. L., & Kuan, W. H. (2007). Simulation the kinetics of fluoride removal by electrocoagulation (EC) process using aluminum electrodes. Journal of Hazardous Materials. https://doi.org/10.1016/j.jhazmat.2006.11.010

Karim, M. D. M. (2000). Arsenic in groundwater and health problems in Bangladesh. Water Research, 34(1), 304–310.

Khader, Y., & Mckay, G. (1992). Prediction of Binary Component Isotherms for Adsorption on Heterogeneous Surfaces. Journal of Chemical Technology Biotechnology, 53, 345–352.

Khatibikamal, V., Torabian, A., Janpoor, F., & Hoshyaripour, G. (2010). Fluoride removal from

industrial wastewater using electrocoagulation and its adsorption kinetics. Journal of Hazardous Materials, 179(1–3), 276–280. https://doi.org/10.1016/j.jhazmat.2010.02.089

Kobya, M., Demirbas, E., Gebologlu, U., Oncel, M. S., & Yildirim, Y. (2013). Optimization of arsenic removal from drinking water by electrocoagulation batch process using response surface methodology. Desalination and Water Treatment, 51(34–36), 6676–6687.

Kobya, M., Gebologlu, U., Ulu, F., Oncel, S., & Demirbas, E. (2011). Electrochimica Acta Removal of arsenic from drinking water by the electrocoagulation using Fe and Al electrodes. Electrochimica Acta, 56(14), 5060–5070. https://doi.org/10.1016/j.electacta.2011.03.086

Kobya, M., Sık, E., Demirbas, E., Goren, A. Y., & Oncel, M. S. (2017). Effect of Ca , Mg , Fe and Mn cations on arsenic removal from groundwater by electrocoagulation process using iron ball anodes

Kumar, P. S., Ramalingam, S., Kirupha, S. D., Murugesan, A., Vidhyadevi, T., & Sivanesan, S. (2011). Adsorption behavior of nickel (II) onto cashew nut shell: Equilibrium, thermodynamics, kinetics, mechanism and process design. Chemical Engineering Journal, 167(1), 122–131.

Lagergren, S. K. (1898). About the theory of so-called adsorption of soluble substances. Sven. Vetenskapsakad. Handingarl, 24, 1–39.

Larous, S., & Meniai, A. H. (2012). Removal of copper (II) from aqueous solution by agricultural by-products-sawdust. Energy Procedia, 18, 915–923.

Lattanzi, A. M., Pecha, M. B., Bharadwaj, V. S., & Ciesielski, P. N. (2020). Beyond the effectiveness factor: Multi-step reactions with intraparticle diffusion limitations. Chemical Engineering Journal, 380, 122507.

Linares-Hernández, I., Barrera-Díaz, C., Roa-Morales, G., Bilyeu, B., & Ureña-Núñez, F. (2009). Influence of the anodic material on electrocoagulation performance. Chemical Engineering Journal, 148(1), 97–105.

Liu, S. (2015). Cooperative adsorption on solid surfaces. Journal of Colloid and Interface Science, 450, 224–238.

Mameri, N., Yeddou, A. R., Lounici, H., Belhocine, D., Grib, H., & Bariou, B. (1998). Defluoridation of septentrional sahara water of north africa by electrocoagulation. Water Research, 32(5), 1604–1612.

Martín-Domínguez, A., Rivera-Huerta, M. de L., Pérez-Castrejón, S., Garrido-Hoyos, S. E., Villegas-Mendoza, I. E., Gelover-Santiago, S. L., … Buelna, G. (2018). Chromium removal from drinking water by redox-assisted coagulation: Chemical versus electrocoagulation. Separation and Purification Technology, 200, 266–272.

Meng, X., Bang, S., & Korfiatis, G. P. (2000). Effects of silicate, sulfate, and carbonate on arsenic removal by ferric chloride. Water Research, 34(4), 1255–1261.

Mohan, D., & Pittman, C. U. (2007). Arsenic removal from water/wastewater using adsorbents-A critical review. Journal of Hazardous Materials, Vol. 142, pp. 1–53. https://doi.org/10.1016/j.jhazmat.2007.01.006

Moussa, D. T., El-naas, M. H., Nasser, M., & Al-marri, M. J. (2017). A comprehensive review of electrocoagulation for water treatment : Potentials and challenges. Journal of Environmental Management, 186, 24–41. https://doi.org/10.1016/j.jenvman.2016.10.032

Moussa, D. T., El-Naas, M. H., Nasser, M., & Al-Marri, M. J. (2017). A comprehensive review of electrocoagulation for water treatment: Potentials and challenges. Journal of Environmental Management, 186, 24–41.

Namasivayam, C., & Yamuna, R. T. (1995). Waste biogas residual slurry as an adsorbent for the removal of Pb (II) from aqueous solution and radiator manufacturing industry wastewater. Bioresource Technology, 52(2), 125–131.

Nasrullah, M., Singh, L., & Wahid, Z. A. (2012). Treatment of Sewage by Electrocoagulation and the Effect of High Current Density. Energy and Environmental Engineering Journal, 1(1), 27–31.

Nyangi, M. J., Chebude, Y., & Kilulya, K. F. (2020). Fluoride removal efficiencies of Al EC and Fe EC reactors : process optimization using Box – Behnken design of the surface response methodology. Applied Water Science, 1–11. https://doi.org/10.1007/s13201-020-01297-x

Nyangi, M. J., Chebude, Y., Kilulya, K. F., & Andrew, M. (2020). Simultaneous removal of fluoride and arsenic from water by hybrid Al-Fe electrocoagulation : process optimization through surface response method. Separation Science and Technology, 00(00), 1–11. https://doi.org/10.1080/01496395.2020.1837877

Padilla-Ortega, E., Leyva-Ramos, R., & Flores-Cano, J. V. (2013). Binary adsorption of heavy metals from aqueous solution onto natural clays. Chemical Engineering Journal, 225, 535–546.

Pérez-Marín, A. B., Zapata, V. M., Ortuno, J. F., Aguilar, M., Sáez, J., & Lloréns, M. (2007). Removal of cadmium from aqueous solutions by adsorption onto orange waste. Journal of Hazardous Materials, 139(1), 122–131.

Plazinski, W., & Rudzinski, W. (2009). Kinetics of adsorption at solid/solution interfaces controlled by intraparticle diffusion: a theoretical analysis. The Journal of Physical Chemistry C, 113(28), 12495–12501.

Rango, T., Bianchini, G., Beccaluva, L., & Tassinari, R. (2010). Geochemistry and water quality assessment of central Main Ethiopian Rift natural waters with emphasis on source and occurrence of fluoride and arsenic. Journal of African Earth Sciences, 57(5), 479–491.

Rango, T., Vengosh, A., Dwyer, G., & Bianchini, G. (2013). Mobilization of arsenic and other naturally occurring contaminants in groundwater of the main ethiopian rift aquifers. Water Research, 47(15), 5801–5818. https://doi.org/10.1016/j.watres.2013.07.002

Rocha-Amador, D., Navarro, M. E., Carrizales, L., Morales, R., & Calderón, J. (2007). Decreased intelligence in children and exposure to fluoride and arsenic in drinking water. Cadernos de Saúde Pública, 23, S579–S587.

Saeed, M., Rehman, M. Y. A., Farooqi, A., & Malik, R. N. (2020). Co-exposure effects of arsenic and fluoride on intelligence and oxidative stress in school-aged children: a cohort study. Environmental Research, 110168.

Sampranpiboon, P., Charnkeitkong, P., & Feng, X. (2014). Equilibrium isotherm models for adsorption of zinc (II) ion from aqueous solution on pulp waste. WSEAS Transactions on Environment and Development, 10, 35–47.

Shen, F., Chen, X., Gao, P., & Chen, G. (2003). Electrochemical removal of fluoride ions from industrial wastewater. Chemical Engineering Science, 58(3–6), 987–993.

Sivarajasekar, N., & Baskar, R. (2019). Adsorption of Basic Magenta II onto H2SO4 activated immature Gossypium hirsutum seeds: Kinetics, isotherms, mass transfer, thermodynamics and process design. Arabian Journal of Chemistry, 12(7), 1322–1337.

Su, C., & Puls, R. W. (2001). Arsenate and arsenite removal by zerovalent iron: effects of phosphate, silicate, carbonate, borate, sulfate, chromate, molybdate, and nitrate, relative to chloride. Environmental Science & Technology, 35(22), 4562–4568.

Tak, B. yul, Tak, B. sik, Kim, Y. ju, Park, Y. jin, Yoon, Y. hun, & Min, G. ho. (2015). Optimization of color and COD removal from livestock wastewater by electrocoagulation process: Application of Box-Behnken design (BBD). Journal of Industrial and Engineering Chemistry. https://doi.org/10.1016/j.jiec.2015.03.008

Thakur, L. S., & Mondal, P. (2016). Techno-economic evaluation of simultaneous arsenic and fluoride removal from synthetic groundwater by electrocoagulation process: optimization through response surface methodology. Desalination and Water Treatment, 57(59), 28847–28863. https://doi.org/10.1080/19443994.2016.1186564

Tian, Y., Wu, M., Liu, R., Wang, D., Lin, X., Liu, W., … Huang, Y. (2011). Modified native cellulose fibers—A novel efficient adsorbent for both fluoride and arsenic. Journal of Hazardous Materials, 185(1), 93–100.

Tolonen, E.-T., Rämö, J., & Lassi, U. (2015). The effect of magnesium on partial sulphate removal from mine water as gypsum. Journal of Environmental Management, 159, 143–146.

Varank, G., Demir, A., Yetilmezsoy, K., Top, S., Sekman, E., & Bilgili, M. S. (2012). Removal of 4-nitrophenol from aqueous solution by natural low-cost adsorbents Removal of 4-nitrophenol from aqueous solution by natural low-cost adsorbents. NISCAIR.

Vasudevan, S., Lakshmi, J., & Sozhan, G. (2009). Studies on a Mg-Al-Zn alloy as an anode for the removal of fluoride from drinking water in an electrocoagulation process. Clean - Soil, Air, Water. https://doi.org/10.1002/clen.200900031

Vasudevan, S., Lakshmi, J., & Sozhan, G. (2010). Studies on the removal of arsenate by electrochemical coagulation using aluminum alloy anode. Clean - Soil, Air, Water, 38(5–6), 506–515. https://doi.org/10.1002/clen.201000001

Veneranda, M., Aramendia, J., Bellot-gurlet, L., Castro, K., Madariaga, J. M., Veneranda, M., … Castro, K. (2018). FTIR spectroscopic semi-quantification of iron phases : A new method to evaluate the protection ability index (PAI) of archaeological artefacts corrosion systems Corrosion Science, 133, 68–77. https://doi.org/10.1016/j.corsci.2018.01.016

Wan, W., Pepping, T. J., Banerji, T., Chaudhari, S., & Giammar, D. E. (2011). Effects of water chemistry on arsenic removal from drinking water by electrocoagulation. Water Research, 45(1), 384–392. https://doi.org/10.1016/j.watres.2010.08.016

Wang, H., Wang, T., Zhang, B., Li, F., Toure, B., Omosa, I. B., … Pradhan, M. (2014). Water and wastewater treatment in Africa–current practices and challenges. CLEAN–Soil, Air, Water, 42(8), 1029–1035.

Wang, J., & Guo, X. (2020). na l P re of. Journal of Hazardous Materials, 122156. https://doi.org/10.1016/j.jhazmat.2020.122156

Wilkie, J. A., & Hering, J. G. (1996). Adsorption of arsenic onto hydrous ferric oxide: effects of adsorbate/adsorbent ratios and co-occurring solutes. Colloids and Surfaces A: Physicochemical and Engineering Aspects, 107, 97–110.

Wu, Y., Wen, Y., Zhou, J., Cao, J., Jin, Y., & Wu, Y. (2013). Comparative and competitive adsorption of Cr (VI), As (III), and Ni (II) onto coconut charcoal. Environmental Science and Pollution Research, 20(4), 2210–2219.

You, H. J., & Han, I. S. (2015). Effects of Dissolved Ions and Natural Organic Matter on Electrocoagulation of As (III) in Groundwater. Biochemical Pharmacology, (Iii). https://doi.org/10.1016/j.jece.2015.12.034

Zhao, X., Zhang, B., Liu, H., & Qu, J. (2011). Simultaneous removal of arsenite and fluoride via an integrated electro-oxidation and electrocoagulation process. Chemosphere, 83(5), 726–729. https://doi.org/10.1016/j.chemosphere.2011.01.055

Zhou, X., & Zhou, X. I. N. (2014). The Unit Problem in the Thermodynamic Calculation of

Adsorption Using the Langmuir Equation. Chemical Engineering Communications 201(11), 1459–1467.

Zhu, J., Zhao, H., & Ni, J. (2007). Fluoride distribution in electrocoagulation defluoridation process. Separation and Purification Technology. https://doi.org/10.1016/j.seppur.2007.01.030

Zuo, Q., Chen, X., Li, W., & Chen, G. (2008). Combined electrocoagulation and electroflotation for removal of fluoride from drinking water. 159, 452–457. https://doi.org/10.1016/j.jhazmat.2008.02.039

CHAPTER FIVE

Adsorption Isotherms and Kinetics Study of Fluoride and Arsenic Removal in Single and Binary Component Systems using Hybrid Al-Fe Electrocoagulation

This chapter is based on the published manuscript

Nyangi, M. J., Chebude, Y., Kilulya, K. F., & Minu, A. (2021). Removal of fluoride and arsenic from groundwater by hybrid Al–Fe electrocoagulation: Adsorption isotherm and kinetics study of single and binary component systems. Remediation, 1–13. https://doi.org/10.1002/rem.21677

Abstract

This study reports on the adsorption isotherm and kinetics of arsenic and/or fluoride by the hybrid iron-aluminum electrocoagulation in a batch reactor. The experiments were performed at a condition of current density J = 9.9 $mAcm^{-2}$; time = 50 min; and pH = 7.5, at variable initial concentrations. The flocs surfaces were characterized using Fourier Transform Infrared Spectroscopy (FTIR) and X-Ray powder diffraction (XRD) that revealed presence of $AlAsO_4$•2(H_2O), AlF_2OH and FeOOAs. Adsorption of fluoride and arsenic in both systems followed Freundlich and Langmuir models. The adsorption processes for fluoride and arsenic were spontaneous and physical in nature with monolayer maximum adsorption capacities of 76.36 mg/g and 1.14 mg/g, respectively in single systems. In a binary component system, the adsorption capacity of arsenic was 0.06 mg/g while that of arsenic became 75.60 mg/g as evaluated using extended Langmuir and extended Freundlich models. Moreover, the kinetics of fluoride and/or arsenic adsorption followed the pseudo second order model. The remediation of fluoride and arsenic from water by Al-Fe oxyhydroxide were found to be through ionic exchange and electrostatic attraction, respectively.

Key terms: Adsorption, fluoride, arsenic, electrocoagulation, groundwater, remediation

5.1 Introduction

In recent years, the co-existence of arsenic and fluoride in groundwater has surfaced as a worldwide environmental issue (Alarcón-Herrera et al., 2013). This is because long term consumption of arsenic (> 10 μg/L) containing water leads to a range a wide range of health effects such as cancer of skin, lungs, and bladder (Chatterjee et al., 2010). On the other hand, the excess intake of fluoride is known to cause dental and skeleton fluorosis (Tian et al., 2011). It is also reported that combined exposure of these two chemicals may lead to both endemic fluorosis and arsenicosis (Alarcón-Herrera et al., 2013). Thus, it has become necessary to remove these toxicants from potable water. For many years, fluoride and arsenic have been removed individually from contaminated waters by chemical coagulation, ion exchange, adsorption, membrane processes, nano-filtration, and electrochemical technologies (Khair et al., 2014).

Notwithstanding, the issues of cost, sludge disposal, high chemical demand, and material availability have been a challenge for the applicability of these technologies in rural communities. High operating costs, skilled labour requirements, and concentrated sludge generation are major drawbacks associated with the membrane filtration technologies (Alarcón-Herrera et al., 2013; Wu et al., 2013). In recent years, electrocoagulation (EC) is reported to be effective for individual removal of arsenic and fluoride (Hashim et al., 2017). EC is more efficient, produces less sludge, is cost effective, and environmentally benign compared to chemical coagulation (Holt et al., 2002). Usually aluminum and iron electrodes are frequently used due to their availability and ability to remove arsenic and fluoride effectively from water. During the EC process, the anode dissolutes and releases the ions of Al^{3+} and Fe^{2+} that then react with the hydroxyl ion resulting from water hydrolysis at the cathode to form coagulants. The coagulants are consequently transformed into a series of polymeric species, depending on water pH and current density (Kobya et al., 2011).

The removal mechanism of arsenic and/ or fluoride by EC is not well understood as it involves complex soluble and insoluble components. Various researchers have proposed different mechanisms involved in aluminum or iron EC. For the arsenic removal, Balasubramanian et al. (2009) reported the monolayer deposition of arsenic on a homogenous adsorbent surface. Also displacement of hydroxyl of the hydroxides by arsenic is another reported possible mechanism

(Daniel & Rao, 2012). Several researchers described the mechanism of the fluoride removal by EC (Daniel & Rao, 2012; Mameri et al., 1998; Wang et al., 2007). For example, the removal of fluoride by EC is found to involve both coprecipitation and adsorption of fluoroaluminum on already formed fluoroaluminum particles (Zhu et al., 2007). Similarly, Khatibikamal et al. (2010) studied the adsorption kinetics of fluoride removal in treated industrial wastewater from the steel industry using a batch EC reactor with aluminum electrodes and reported second order kinetics governing the removal rate (Khatibikamal et al., 2010).

However, in a multicomponent water system with both the presence of fluoride and arsenic, it is necessary to study the influence of competetive interactions among the pollutants on the overall adsorption process. The adsorption of a pollutant may be affected by other components because of the changes in properties such as surface charge, structure, size, the functional groups of the components, porosity and active sites present on the adsorbent surface (Wu et al., 2013). Thus, it is necessary to establish the relationships between the adsorption capacity of a component and the concentration of other pollutants present with the assistance of multicomponent isotherm models.

To the best of literature review, there is no study reported on the isotherm equilibrium and kinetics of the simultaneous removal of fluoride and arsenic by using a hybrid iron-aluminum EC. Therefore, the aim of this study was to investigate the simultaneous removal mechanism of fluoride and arsenic in a hybrid Al-Fe EC system and compare their adsorption isotherms and kinetics in single and binary component systems.

5.1 Adsorption isotherm and kinetic models

5.1.1 Adsorption isotherm for a single component system

An equilibrium isotherm expresses the relation between the amounts of adsorbate removed from solution at equilibrium by a unit of mass of adsorbent at constant temperature. In this study, experimental equilibrium data were fitted by three isotherm models, Freundlich, Langmuir, and Fowler-Guggenheim (F-G) models. The linear forms of each model equation and plot parameters are provided in Table 5.1.

The Freundlich isotherm is derived by assuming that the adsorbent has a heterogeneous surface with a non-uniform distribution of heat of adsorption over the surface (Equation 5.0) (Davis et al., 1975). The Langmuir theory, on the other hand, assumes that the sorption takes place at specific homogeneous sites within the adsorbent (Equation 5.1) (Pérez-Marín et al., 2007). Moreover, the Fowler-Guggenheim (F-G) model hypothesized the possibility of lateral interaction between adsorbates that can take place at constant energy (Equation 5.2) (Hamdaoui & Naffrechoux, 2007). Here the type of interaction is predicted from interaction energy between adsorbed molecules (*W)*. It is repulsive when *W* is negative and attractive when *W* is positive (Davoudinejad & Ghorbanian, 2013). Meanwhile, the feasibility and spontaneity of the reaction was computed by using the Langmuir equilibrium constant K_L value that can be utilized to calculate the Gibbs free energy (ΔG) of the adsorption reaction using Equation 5.3.

$$\Delta G = -RT\ln K_L \quad (1.3)$$

Where; R is universal gas constant (8.14 J/mol); K_L = Langmuir equilibrium constant; T is room temperature (298 K).

5.1.2 Adsorption isotherm for a binary component system

Multicomponet isotherms models are used to calculate the value of one component adsorbed per unit weight of adsorbent in the presence of another component at equilibrium. The data from binary mixture in this study were evaluated using the extended Langmuir equation (5.4) and extended Freundlich models (Equation 5.5). An extended Langmuir isotherm (EL) was developed by assuming the presence of equal competition between the ions (adsorbates) for the same active sites on the homogenous surface of the adsorbent. However, this model utilizes a parameter from a mono-parameter system to predict their behavior in a multisystem as it assumed that there is no interaction between adsorbates (Sivarajasekar & Baskar, 2019). On the other hand, an extended Freundlich model uses the idea of correlative approach where single and multicomponent equilibrium data for each species on the heterogeneous layer of the adsorbent are integrated to yield correlative constants in the adsorption isotherm data for multicomponent systems (Padilla-Ortega, Leyva-Ramos, & Flores-Cano, 2013).

Table 5.1: Adsorption isotherm model equations for single and binary component systems

Model	Linear form	Plot
Single adsorption equations		
Langmuir		Ce (5.0)
Freundlich		vs (5.1)
F-G		Ø (5.2)
Binary adsorption equations		
Extended Langmuir		Extended Freundlich
(5.4)	and (5.5)	

Where; Ce is equilibrium concentration in solution (mg/L); qe equilibrium concentration in solid phase (mg/g); qm monolayer maximum adsorption capacity (mg/g); K_{FG}, K_F, and K_L equilibrium constants for F-G, Freundlich, and Langmuir, respectively; Θ is fraction of adsorbent coverage; W is interaction energy between adsorbed molecules (kJ/mol); *x*, *y* and *z* binary Freundlich adsorption correlation constants, q' maximum adsorption capacity of adsorbate in a binary system (mg/g); K_{Li} and K_{Fi} Langmuir and Freundlich equilibrium constants for species *i* and *j* in a binary mixture.

5.1.3 Adsorption kinetics

The adsorption kinetic data are normaly used to evaluate adsorption rate, perfomance of adsorbent, and the mass transfer. This information helps in designing an adsorption system. The mass transfer kinetic involves three steps. First external diffusion where adsorbate tranfers through the liquid film around adsorbent. Second internal diffusion which describes the diffusion of the adsorbate in the pores of the adsorbent. Lastly, adsorption of the adsorbate on the active sites of the adsorbent. The first step is fast and cannot describe the rate dependence of adsorption (Wang & Guo, 2020), which means the second and third steps can be evaluated to understand the kinetic nature of adsorption (Wang & Guo, 2020).

To investigate the kinetic adsorption process, various kinetic models were studied using pseudo-first-order (PFO) and pseudo second order (PSO) kinetics, while intraparticle diffusion and

Bangham's kinetics models were applied to investigate the mechanism of arsenic and fluoride diffusion into an adsorbent. The most accurate model among these models is selected according to the linear regression correlation coefficient values R^2.

The PFO model as proposed by Lagergren (1898)(Lagergren, 1898) is represented by Equation 5.6:

(5.6)

Where: K_1 (min^{-1}) is the rate constant of adsorption, q_t and q_e are the adsorbed amounts (in mg/g) at a given time t and at equilibrium, respectively.

The PSO model as described by Ho & McKay (2000) is represented by Equation 5.7:

(5.7)

Where: k_2 is the rate constant of the PSO equation (in g/mg min^{-1}); q_t and q_e are the adsorbed amounts (in mg/g) at a given time t and at equilibrium, respectively. The q_e and k_2 can be calculated from the slope and intercept of plot of t/q_t versus t.

The intra-particle diffusion model or pore diffusion mechanism describes the transport of species from the surface to the interior pores of the particle (Plazinski & Rudzinski, 2009). The linear expression of this kinetic model can be estimated by the following Equation 5.8 proposed by Plazinski & Rudzinski, (2009).

(5.8)

Where: K_W is the measure of diffusion coefficient (mg/g.$min^{0.5}$) and C is the intraparticle diffusion constant (mg/g). K_w and C can be obtained from the slope and intercept of the plot of q_t versus $t^{0.5}$.

When the plot is a straight line, it implies that the adsorption process is controlled by intra-particle diffusion only. However, if the graph shows multi-linear plots, it means that several steps are involved in the diffusion process (Plazinski & Rudzinski, 2009). Here it is assumed that the external resistance to mass transfer surrounding the particles is significant only in the early stages of adsorption: this is represented by the first sharper line. The second linear portion is the slow adsorption signifying adsorption of adsorbate into internal pores of adsorbent.

The Bangham model is used to investigate the adsorbate pore diffusion activities on the surface intra-pores of the adsorbent. The linear form of the model can be expressed by Equation 5.9 (Varank et al., 2012):

(5.9)

Where: α is Bangham model constant, Co is the initial concentration of adsorbate (mg/L), V is the volume of solution (mL), M is the mass of adsorbent (g/L), q_t is the quantity of adsorbate adsorbed (mg/g) at time t, α (<1) and Kj are constants which can be obtained from slope and intercept of the plot against log t, respectively.

5.2 Methodology

5.2.1 Material prepartion

Standard 1,000 µg/L arsenic and 1,000 mg/L fluoride stock solution were prepared according to the water and wastewater analysis standard procedure (Federation & Association, 2005). Meanwhile, aluminum and iron electrodes plates (Fe; 15 cm × 2 cm × 0.05 cm; and Al; 15 cm × 2 cm × 0.05 cm) were pre-cleaned by rubbing with sandpaper, rinsed in NaOH (2 M) and HCl (2 M) to remove any particles that may be present on the surface, and then washed with distilled water. The electrodes were dried at 103 ºC.

5.2.2 Electrocoagulation reactor setup

A batch mode reactor was used to carry out treatment of water samples as well as adsorption isotherm and kinetic studies through hybrid Al-Fe EC in 800 cm^3 glass cells where the active volume was 600 cm^3. The aluminum and iron electrodes were connected in a mono-polar parallel mode (MP-P) at inter electrode distance of 1.5 cm. Two electrodes one of each type (total area, 80 cm^2 (4 surfaces x 10 x 2 cm, dipped in water)) were connected as sacrificial electrodes to make a total surface area to volume ratio (S) of 0.13 cm^{-1}. The end poles of the electrodes were connected to the positive and negative terminals in a direct current (DC) power source as shown in Figure 5.1.

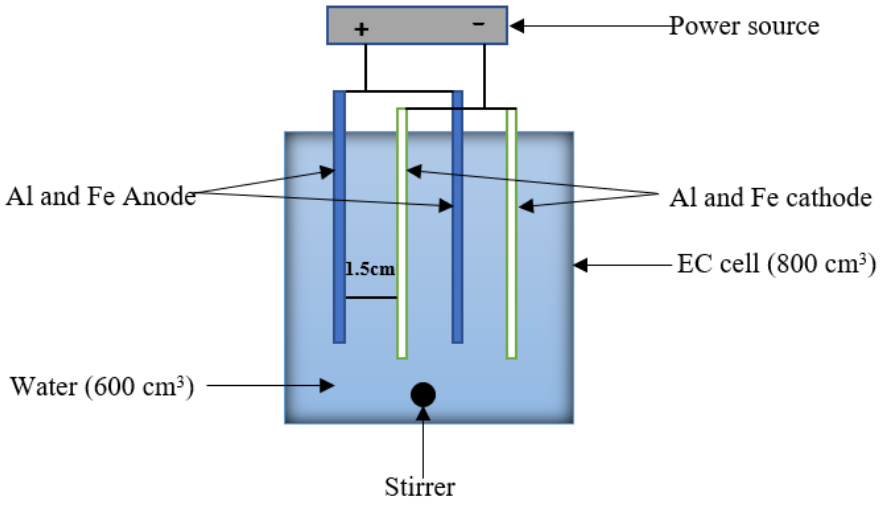

Figure 5.1: Schematic laboratory scale cell assembly for electrocoagulation experiments

5.2.3 Adsorption equilibrium procedure

The adsorption equilibriums for single component systems were measured at initial fluoride concentrations of 3, 6, 12, and 24 mg/L and initial arsenic concentration of 0.015, 0.075, 0.150, and 0.300 mg/L. In the binary ions systems, the adsorption equilibriums were measured for each initial concentration of fluoride ranging between 6-30 mg/L with the arsenic concentrations varied in a range 0.075-0.3 mg/L. The adsorption reactions were conducted with a constant mass of adsorbent by allowing reactions to proceed at J = 9.9 mAcm^{-2}; pH 7.5; t = 50 minutes to ensure the equilibrium is attained. The amount of adsorbent produced was estimated to be 0.41 g using Faraday's law (Equation 5.10**)** (Nyangi et al., 2020):

Where: m is the theoretical amount of adsorbent produced (g); I electric current passed (A); t treatment time (s); M_{Al} and M_{Fe} are molecular mass (Al; 26.98 g/mol: Fe; 55.84 g/mol), N_T is total number of electrons transferred (Al; 3: Fe; 2), F is Faraday's constant (96,485 C/mol), and V is the volume of treated water (600 cm^3).

5.2.4 Adsorption kinetics procedure

The experiments were performed at initial concentrations of arsenic and fluoride of 14 mg/L and 160 mg/L, respectively, to study their kinetics in both single component and binary component systems. The treatment time was varied at a range of 15-60 minutes while the current density

was varied at a range of J = 6.5-12 $mAcm^{-2}$ to ensure a constant amount of adsorbent (0.41 g) was produced with respect to time. 15 mL samples were quickly taken from the reactor every 15 minutes for arsenic and fluoride analysis.

5.2.5 Sample analyses

The analysis of water samples for fluoride and arsenic were carried out using ion selective electrode (ISE) and inductive coupled plasma optical emission spectroscopy ICP-OES, respectively. The percentages of fluoride and arsenic removal were calculated using Equation 5.11. Analyses of co-existing ions were performed using Atomic Emission Spectroscopy (AES) for cations (Na^+, K^+, Ca^{2+}, Mg^{2+}) and ion chromatography for anions (F^-, Cl^-, NO_3^-, SO_4^{2-}), while HCO_3^- was analyzed using a titration technique. Moreover, the residues of the floc samples were analyzed using X-ray powder diffraction (XRD) and Fourier transform infrared spectroscopy (FT-IR). The analyses of flocs were performed in the Chemistry Department at Addis Ababa University. Nonlinear regression analysis method (MS Excel) was used to obtain the least square fit for all the models. The amount of fluoride and/or arsenic at equilibrium and at a time (t) was calculated using Equation 5.12 and 5.13, respectively as proposed by Chithra & Balasubramanian (2010):

(5.11)

(5.12)

(5.13)

Where: C_o, C_e, and C_t are concentrations (mg/L) of fluoride/arsenic at initial, equilibrium, and time t, rsepectively; m is the mass of adsorbent (g); and V is the volume of water sample (L).

5.3 Results and discussion

5.3.1 Characteristics of floc produced

FT-IR analyses were performed in the range 4,000–450 cm^{-1} using Spectrum 65 FT-IR (PerkinElmer) spectrometer to analyze the floc. The infrared spectrum, shown in Figure 5.2a, exhibited a broad band with two significant splits at 3,450 and 3,600 cm^{-1} reflecting the presence of O-H of hydroxide/oxy-hydroxide stretching vibrations (Gomes et al., 2007). Another important peak that appeared at ~ 1,650 cm^{-1} reflects water bending stretch (Gomes et al., 2007). The two peaks observed at 1,020 cm^{-1} and 790 cm^{-1} characterize lepidocrocite ($Fe^{3+}OOH$)

(Veneranda et al., 2018) and As^{3+}-O stretching (Gomes et al., 2007). The absence of the peak for arsenate As(V) (874 cm^{-1}) indicates that in this case there was no oxidation of arsenite to arsenate. Finally, the peak at 520 cm^{-1} indicates the presence of Al-F stretch which can be due to the exchange of ions between fluoride and hydroxyl of aluminum.

The XRD spectrogram of a floc produced as presented in Figure 5.2b demonstrated amorphous or poor crystalline phases. The peaks resulted from aluminum electrode show the presence of $AlAsO_4$•$2(H_2O)$ (Theta 2(Θ) = 20, 36 and 53), $Al(OH)_3$ (2Θ = 28, 40, 45a and 53), AlOOH (2Θ = 19 and 28), and AlF_2OH (28, 45 and 53) (Gomes et al., 2007). The presence of $AlAsO_4$•$2(H_2O)$ and AlF_2OH signify that aluminum oxyhydroxide is involved in the removal of both As and F through co-precipitation or entrapped within the aluminum hydroxide complex as stipulated in reactions 1 and 2. On the other hand, the dissolution of iron electrode has led to the formation of iron oxides of Fe_3O_4, (2Θ = 35, 61) and lepidocrocite, FeOOH (2Θ = 36, 47) (Gomes et al., 2007) (Veneranda et al., 2018) suggesting there was oxidation of Fe^{2+} to Fe^{3+} and Fe^{4+} during EC. The presence of lepidocrocite is further proof of the involvement of lepidocrocite on the adsorption of arsenic as predicted by FTIR data. Thus, the FTIR and XRD analyses indicate that the removal of both fluoride and arsenic by hybrid Al-Fe EC could be through ionic exchange between hydroxyl of the Aluminum hydroxide and both fluoride and arsenic while the iron coagulant phases could remove arsenic by adsorption on the surface of iron oxyhydroxide.

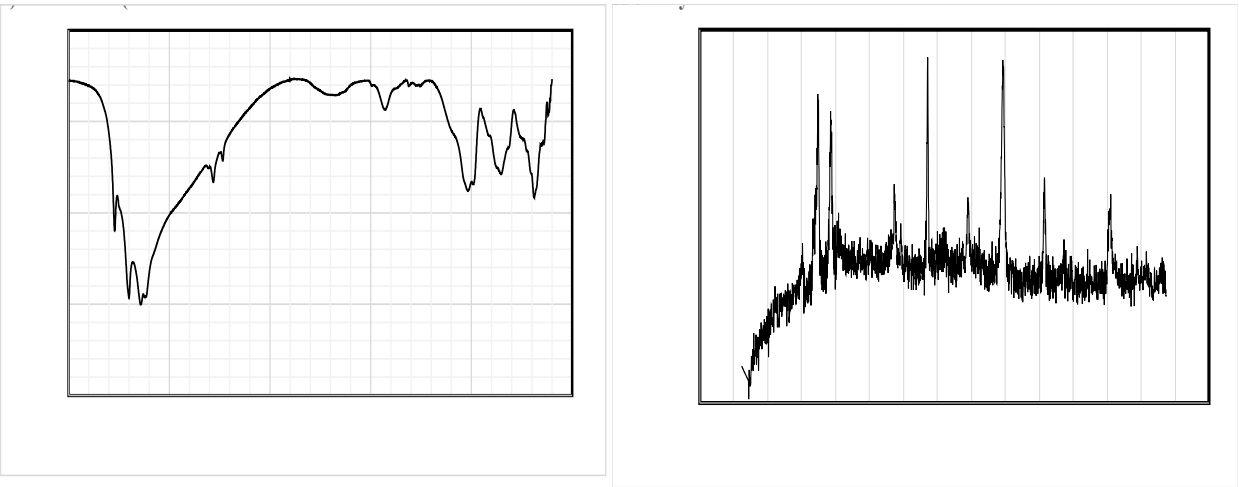

Figure 5.2: Characterization of floc obtained from Al-Fe EC at (J = 6.25 mA/cm^{-2}, F= 16 mg L, As = 200 µg/L, pH 7, running time 50 min; (a) FTIR spectrogram and (b) XRD spectrogram.

5.3.2 Single and binary adsorption of fluoride and arsenic ions

The changes in equlibrium concentration during adsorption of fluoride and arsenic in a single and binary systems are represented in Table 5.2 and Figures 5.3a and 5.3b, respectively. A rapid uptake of both fluoride and arsenic at their low initial concentration was observed. For example, in single system at 0.3 mg/L and 0.015 mg/L of arsenic, the removal of 0.82 and 0.76 for fluoride and arsenic were attained. However, the fraction removal appears to increase with the initial concentration of fluoride and arsenic (Figure 5.3a and 5.3b). The removal of fluoride and arsenic have increased from 0.82 to 0.88 and from 0.76 to 0.96 at 0-24 mg/L and 0-0.3 mg/L, respectively. The rapid adsorption at low concentration is attributed to the low resistance in mass tranfer between liquid and solid phase as well as higher available free sites on the Al/Fe hydroxides adsorbent for F and As adsorption (Larous & Meniai, 2012).

In a binary component mixture of fluoride and arsenic the same trend as in single systems were observed; however, the removal of fluoride appears to insignificantly increase with increase in arsenic concentration while that of arsenic significantly decreased when the concentration of fluoride increased. For example, the removal fraction of 24 mg/L of fluoride appeared to increase to 0.94 from 0.86 when the arsenic concentration increased from 0.08 to 0.23 mg/L. However, at 0.3 mg/L of arsenic the removal declined to 0.90 mg/L indicating attainment of saturation and further stirring leads to desorption of fluoride (Lattanzi et al., 2020). On the other hand, the 0.15 mg/L of arsenic removal significantly decreased from 0.91 to 0.79 when the fluoride concentration is increased in the range of 6-30 mg/L. To study the reasons for the different interactive effects taking place on the surface of adsorbent in a binary system the changes in affinities (K_F) were studied (Table 5.2). In both cases (removal of fluoride and arsenic) the affinities appeared to increase with the increase in concentration of another ion. The affinity (K_F) and heterogeneity (1/n) towards fluoride changes from 0.161-0.193 L/mg and 0.79-0.63 at an arsenic concentration between (0.015-0.3 mg/L) and the K_F and 1/n of arsenic has increased from 45-819 L/mg and 1.26-2.60 at fluoride (6-30 mg/L). The higher the K_F the more the strength of the interaction between adsorbent-adsorbate while the lower value of 1/n suggests favorability of the adsorbtion (Al-ghouti & Da, 2020).

Table 5.2: Adsorption of fluoride and arsenic in single and binary component systems

	Adsorption of Fluoride						Adsorption of Arsenic					
	F	As	CeF	Ad F	1/n	K_F	F	As	Ce As	Ad As	1/n	K_F
1	3.0	0.000	0.57	0.81	0.96	0.123	0.0	0.015	0.001	0.93	0.97	16
2	6.0	0.000	0.95	0.84	0.96	0.123	0.0	0.075	0.006	0.92	0.97	16
3	12.0	0.000	1.55	0.87	0.96	0.123	0.0	0.150	0.012	0.92	0.97	16
4	24.0	0.000	3.02	0.87	0.96	0.123	0.0	0.300	0.017	0.94	0.97	16
5	3.0	0.075	0.47	0.84	0.79	0.161	6.0	0.015	0.002	0.86	1.26	45
6	6.0	0.075	0.80	0.87	0.79	0.161	6.0	0.075	0.009	0.88	1.26	45
7	12.0	0.075	1.36	0.89	0.79	0.161	6.0	0.150	0.014	0.91	1.26	45
8	24.0	0.075	2.56	0.89	0.79	0.161	6.0	0.300	0.018	0.94	1.26	45
9	3.0	0.150	0.42	0.86	0.69	0.171	12.0	0.015	0.005	0.66	1.66	106
10	6.0	0.150	0.73	0.88	0.69	0.171	12.0	0.075	0.013	0.82	1.66	106
11	12.0	0.150	1.20	0.90	0.69	0.171	12.0	0.150	0.022	0.85	1.66	106
12	24.0	0.150	1.90	0.92	0.69	0.171	12.0	0.300	0.032	0.89	1.66	106
13	3.0	0.225	0.40	0.88	0.63	0.179	24.0	0.015	0.007	0.53	2.00	360
14	6.0	0.225	0.70	0.88	0.63	0.179	24.0	0.075	0.020	0.73	2.00	360
15	12.0	0.225	1.13	0.91	0.63	0.179	24.0	0.150	0.019	0.88	2.00	360
16	24.0	0.225	1.57	0.93	0.63	0.179	24.0	0.300	0.041	0.86	2.00	360
17	3.0	0.300	0.52	0.83	0.63	0.193	30.0	0.015	0.007	0.52	2.60	819
18	6.0	0.300	0.80	0.87	0.63	0.193	30.0	0.075	0.022	0.71	2.60	819
19	12.0	0.300	1.32	0.89	0.63	0.193	30.0	0.150	0.023	0.85	2.60	819
20	24.0	0.300	2.46	0.90	0.63	0.193	30.0	0.300	0.053	0.82	2.60	819

2

The small increase in the fluoride uptake in the binary component could be due to the fact that the surface charge of the Al-Fe hydroxide becomes slightly more positive in the presence of arsenic, permiting electrostatic attraction towards F^- as revealed by the slight increase in the affinity (K_F) towards fluoride when the As concentration increases. The presence of electrostatic attraction during fluoride removal was also revealed in the FTIR flocs spectrum by the existence of Al-F bond (Figure 5.2a). Meanwhile. the decrease in the arsenic removal could be attributed to the competition for the adsorption sites with the fluoride (Vasudevan et al., 2009). Moreover, the higher concentration of fluoride than arsenic in the mixture also means that the fluoride-containing molecules could be limiting the access of arsenic to the adsorbent surface, therefore, despite strong affinity exhibited by the arsenic, its removal becomes reduced at higher fluoride concentrations.

[2] Ad is adsorption: CeF and CeAs are concentration of fluoride and arsenic at equilibrium (mg/L)

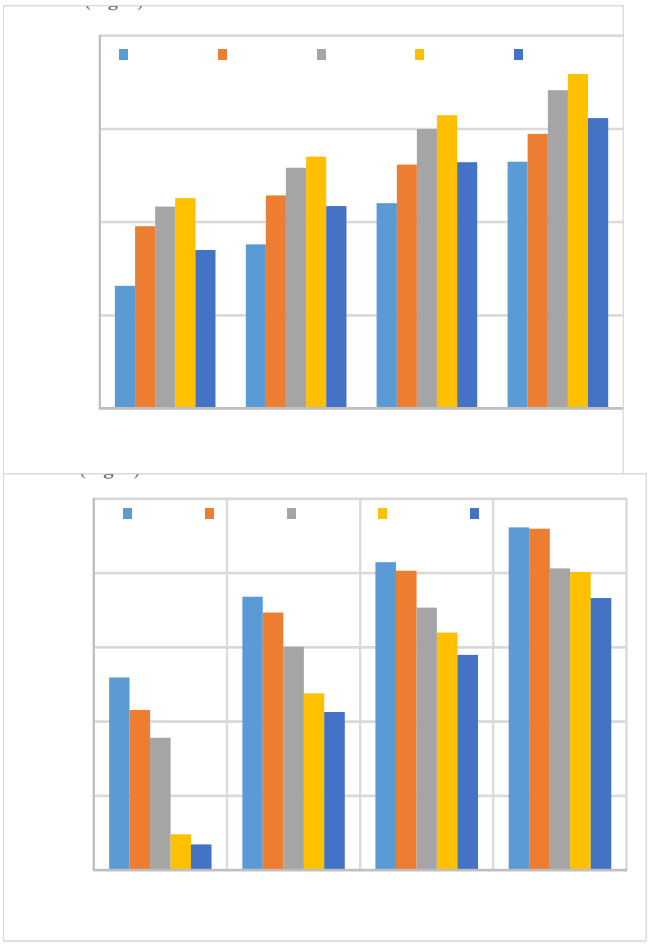

Figure 5.3: Effect of initial concentration on the removal of (a) fluoride in a single component and in the presence of arsenic 0.075-0.3 mg/L (b) arsenic in a single system and in the presence of 6-30 mg/L of fluoride at pH 7.5.

5.3.3 Adsorption isothermal study

5.3.3.1 Single component isotherm model

The best fit model of the experimental data to describe adsorption in single componet systems were identified using three different models: the Langmuir model, Freundlich model, and F-G model. Results of the parameter values are presented in Table 5.3 and Figure 5.4a-d. The Langmuir model attained high correlation factors $R^2 > 0.99$ for both F and As showing that the experimental data fitted well to the model. Both adsorption of fluoride and arsenic exhibited separation factor $R_L < 1$ (calculated from); (where Co (mg/L) initial concentration of F and As, K_L (L/mg) Langmuir adsorption constant)) which means that the individual adsorption of fluoride and arsenic on the surface of Al-Fe oxyhydroxide were favorable (Al-ghouti & Da, 2020). The

fluoride achieved higher maximum monolayer adsorption capacity (q_m) of 76.6 mg/g while that of arsenic is 1.14 mg/g. Higher adsorption capacity towards fluoride than arsenic is attributed to the higher initial concentration of fluoride used in this study (3-24 mg/L) which may also imply high driving force to the fluoride towards the adsorbent surface (Liu, 2015).

Thus, the adsorption of both fluoride and arsenic were not limited to a single layer as they both obeyed the Freundlich model (Araújo et al., 2018). Here, arsenic has shown stronger affinity, K_F = 18.5 L/mg, compared to that of fluoride, K_F = 0.12 L/mg, which is attributed to the formation of strong inner layer complexation sphere (Catalano et al., 2008). The affinity towards both fluoride and arsenic appears to increase with the increase of initial concentration of other ions (Tabe 2). This may suggests that F and As were adsorbed in different adsorption sites. It must be noted that during EC of hybrid Al-Fe the adsorbent produced is a mixture of hydroxide of aluminum and iron, indicating the presence of different affinity energies on the adsorbent surface. Adsorption of fluoride and arsenic on Al-Fe oxyhydroxides both presented the degree of heterogeneity $1/n < 1$ suggesting adsorption to be favorable as well (Ayawei et al., 2015).

To evaluate feasibility of the reaction, the equilibrium constant value from Langmuir was utilized to calculate the Gibbs free energy using the equation $\Delta G = -RTlnK'$ at 298 K. As described in (Zhou & Zhou, 2014), the equilibrium constant should be dimensionless in order to calculate the Gibbs free energy. Therefore, the Langmuir constant K_L (L/mg) is converted into standard equilibrium constant K' using equation $K' = K_L \times M \times 0.055$ (Zhou & Zhou, 2014) (M = molar mass of As and F). The values for ΔG are found to be -5.13 kJ/mol and -10.71 kJ/mol for fluoride and arsenic, respectively. The negative Gibbs energy in this range indicates that the adsorption of both fluoride and arsenic were physical in nature, and spontaneous and exothermic. The higher energy released during arsenic adsorption (ΔG = -10.71 kJ/mol) further proves the stronger affinity of arsenic to the adsorbent compared to that of fluoride which released less energy (ΔG = -5.13 kJ/mol). Moreover, the adsorption data (Table 5.3) shows weak correlation to the F-G model suggesting absence of lateral interaction between adjacent fluoride or arsenic on the surface of Al-Fe oxyhydroxide (Sampranpiboon et al., 2014).

Table 5.3: Parameter values from individual modelling for adsorption of arsenic and fluoride:

	Parameter	Fluoride	Arsenic
Langmuir	R^2	0.980	0.999
	q_m (mg/g)	76.36	1.14
	R_L	0.49	0.40
	K_L (L/mg)	0.12	18.19
Freundlich	R^2	0.977	0.984
	1/n	0.96	0.97
	K_F	0.123	15.85
F-G	R^2	0.99	0.95
	K_{FG}	0.03	0.17
	w	--	--

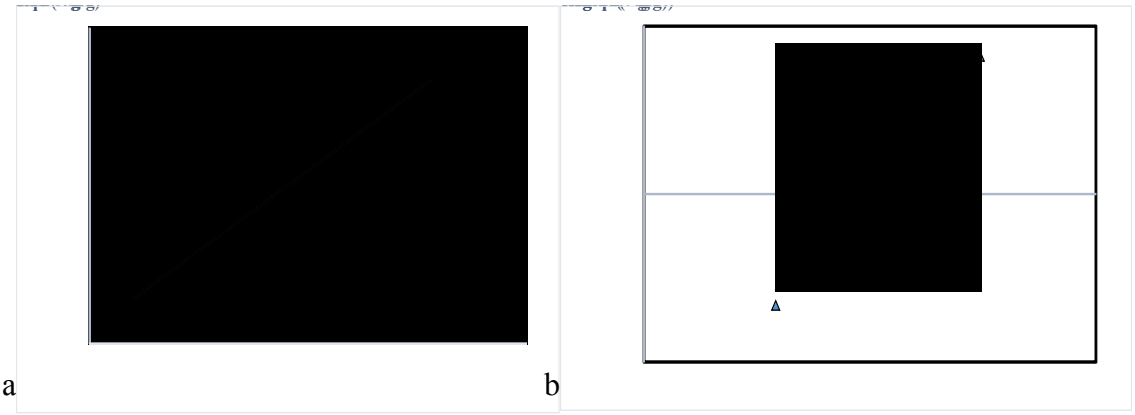

a b

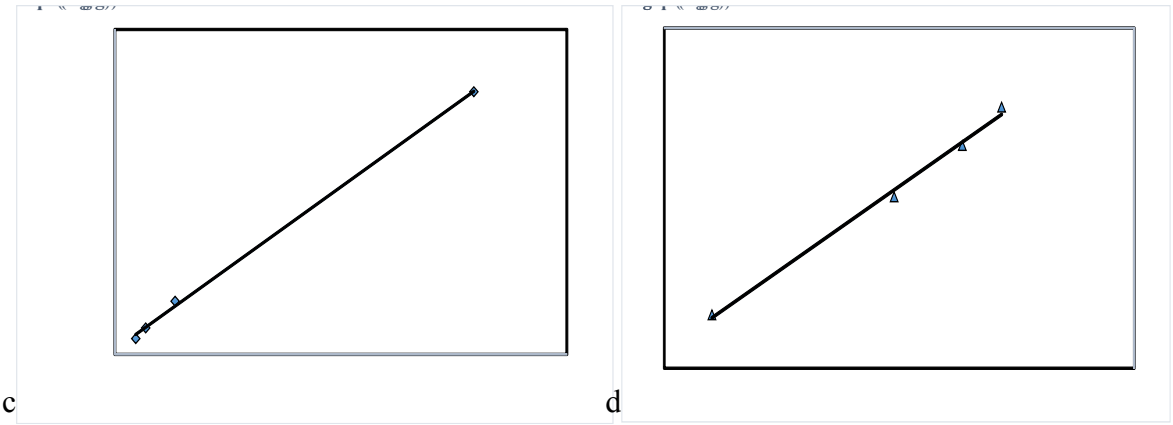

c d

Figure 5.4: Adsorption isotherm plots for (a) Langmuir isotherm for fluoride (b) Freundlich isotherm for arsenic (c) Langmuir isotherm for fluoride (d) Langmuir isotherm for arsenic

5.3.3.2 Binary mixture isotherm parameters

To deduce the interactive behavior between fluoride and arsenic, data from the binary mixture were evaluated using Extended Langmuir (Choy et al., 2000) and Extended Freundlich models (Khader & Mckay, 1992). The parametric values of the binary adsorption models are given in Table 5.4 and Figures 5.5(a-d). The adsorption equilibrium data for the simultaneous adsorption of fluoride and arsenic were evaluated using Extended Freundlich and Extended Langmuir models both showing correlation factors in a range (R^2 = 0.982 - 0.999). The adsorption in a binary system can show one of the three different kinds of interaction (μ). The interaction can be characterized by the adsorption capacity for one solute in a binary mixture to the adsorption capacity of the same solute in a single component solution (i.e., $\mu = q'/q_{m)}$, where q' is maximum monolayer adsorption capacity in a binary system, q_m is maximum monolayer capacity in a single system). When $\mu < 1$, the interaction is antagonism, when the effect of a single component in the mixture is dominant. If $\mu > 1$, adsorption behavior is called synergism in which the effect of the mixture is dominant; and if $\mu = 1$, there is no effect of the mixture on a single component adsorption and the adsorption behavior is non-interactive (Girish, 2018). In this study, the adsorption capacity towards fluoride was not affected as it remained almost the same (75.6 mg/g) while that towards arsenic was significantly reduced to 0.06 mg/g from 1.14 mg/g, corresponding to the interactive effect $\mu_F = 0.97$ and $\mu_{As} = 0.05$, respectively. This means that the presence of arsenic did not affect adsorption of fluoride while fluoride antagonistically lowered the arsenic adsorption (Girish, 2018).

The value of equilibrium constant (K_L) for fluoride adsorption slightly increased to 0.13 L/mg from 0.12 L/mg signifying that the Al-Fe oxyhydroxide surface, pores, surface charge, and zeta potential for fluoride adsorption were not affected when arsenic is present. Meanwhile, the K_L value for arsenic was significantly reduced to 14.06 from 18.19 L/mg indicating competition for adsorption sites induced by addition of fluoride. This could be attributed to the higher concentration ratio of fluoride/arsenic (mg/µg) in the mixture. Moreover, the negative Freundlich constants x = -0.88 for As adsorption reveals decrease in affinity of Al-Fe oxyhydroxide towards arsenic adsorption while the positive x = +0.2 signifies slight increase in affinity of Al-Fe oxyhydroxide towards fluoride (Amani-Ghadim et al., 2013). The other correlative factors y and z being positive also indicate adequacy of the extended Freundlich isotherm in describing adsorption in a binary mixture.

Table 5.4: Binary adsorption isotherm for simultaneous removal of fluoride and arsenic

Model	Parameter	Fluoride	Arsenic
Extended Langmuir	R^2	0.997	0.999
	q' (mg/g)	76.00	0.06
	K_{Li} (L/mg)	0.13	14.06
Extended Freundlich	R^2	0.982	0.995
	x	0.20	-0.88
	y	0.02	0.16
	z	0.13	0.35

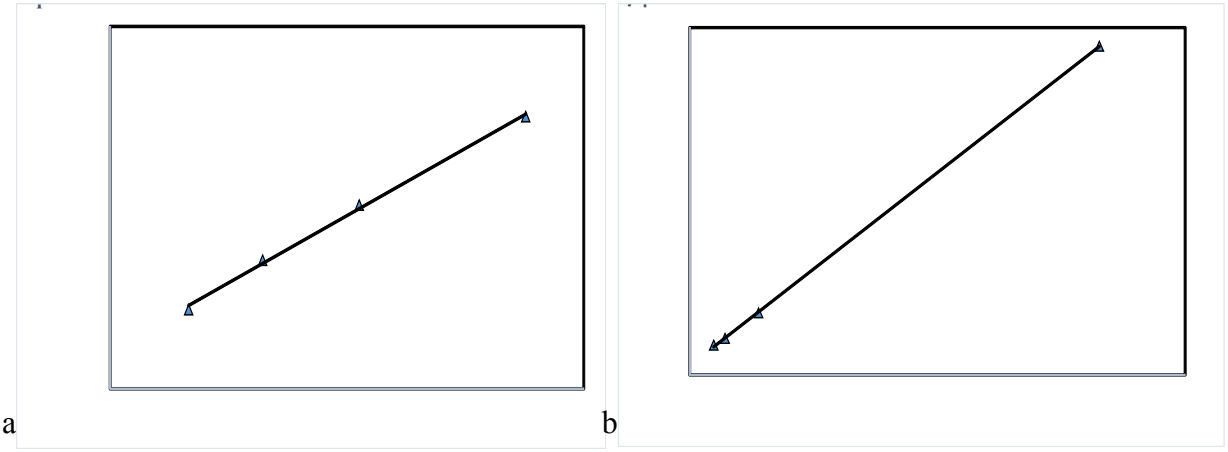

a b

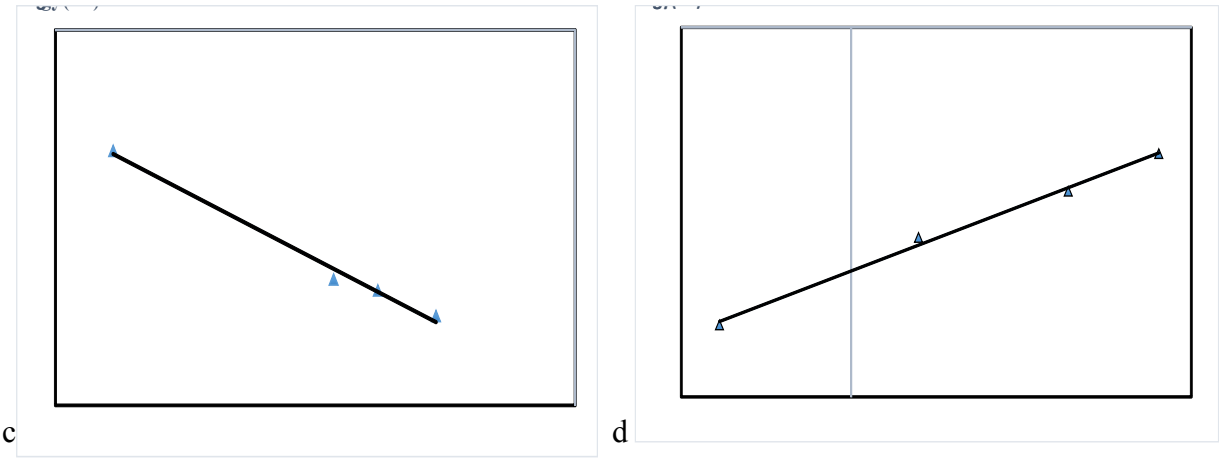

c d

Figure 5.5: Adsorption isotherm plots for (a) Extended Langmuir for fluoride (b) Extended Langmuir of arsenic (c) Extended Freundlich for fluoride (d) Extended Freundlich for arsenic.

5.3.3.3 Adsorption kinetics for fluoride and arsenic in a single and binary systems

Calculated parameters of the various kinetic models and the validation results have been reported in Table 5.5 and Figures 5.6(a-f), figures for Bangham kinetic model are not shown here. PSO kinetics presented highest correlation coefficient at $R^2 \geq 0.99$ for all systems. Furthermore, the calculated equilibrium constant values (q_e) for PSO are closer to the experimental equilibrium constants (q) for the amount of adsorbates (q) in the solid phase between the experimental values (qe) and calculated values (q) revealing that the adsorption of fluoride and arsenic in single and binary systems followed PSO (Table 5.5). The kinetics of the fluoride uptake increased in a binary system from 0.36 to 0.45 min^{-1}, while that of arsenic decreased from 0.67 to 0.5 min^{-1}. This means that the presence of fluoride could have hinder the rate of As towards adsorption sites, while arsenic on the other hand could have increased the adsorption surface charge enhancing the electrostatic force of attraction between fluoride and the Al-Fe oxyhydroxide surface.

The intra-particle diffusion model was used to describe the diffusion of fluoride and/or arsenic on the surface of Al-Fe oxyhydroxide. The data plots for both fluoride and arsenic in single and binary component systems are presented by straight lines with intercepts of linearity that did not pass through the origin (Figures 5.6e-f). This suggests that the rate of fluoride and arsenic diffusing from the solution onto the active sites of the Al-Fe oxyhydroxide at initial and final stages differs (Namasivayam & Yamuna, 1995). Moreover, it reflects the presence of some

degree of boundary layer control on the rate of adsorption (Elwakeel et al., 2014). The boundary layer of fluoride-Al-Fe oxyhydroxide slightly thickened from 14.75 to 15.86 mg/g causing a decrease on the rate of diffusion from 0.53 to 0.46 mg/g. On the other hand, the boundary layer of arsenic-Al-Fe oxyhydroxide decreased from 195 to 188 mg/g leading to a slight increase in the arsenic diffusion from 0.37 to 0.43. These results suggest an insignificant change in the rate of fluoride and arsenic diffusion to the surface of the adsorbent. Furthermore, diffusion of fluoride into the pores of the adsorbent surface deduced from the Bangham model also controlled the rate of fluoride and arsenic adsorption. The values of < 1 imply that adsorption of fluoride and arsenic into the pores of the Al-Fe oxyhydroxide proceeded at a low kinetic rate (Varank et al., 2012).

Table 5.5: Parameter values for pseudo first order, pseudo second order, intra-particle, and Bangham models

		Single system		Binary system	
	Parameter	Fluoride	Arsenic	Fluoride	Arsenic
Model	qe.	18.75	218	19.3	215
Pseudo first order	R^2	0.97	0.98	0.97	0.93
	q (mg/g)	6.17	57	12.93	179.46
	K_1 (min^{-1})	-0.06	-0.08	-0.11	-0.12
Pseudo second order	R^2	0.99	1.00	0.99	0.99
	q (mg/g)	19	250	20	250
	K_2 (g/mg.min)	0.36	0.67	0.45	0.50
Intraparticle	R^2	0.95	0.95	0.94	0.98
	C	14.75	195	15.86	188
	K_{in} (mg/gmin^0.5)	0.53	3.71	0.46	4.355
Bangham	R^2	0.98	0.98	0.98	0.99
		0.21	0.13	0.23	0.31
	K*j*	8.95	153.31	8.46	13.82

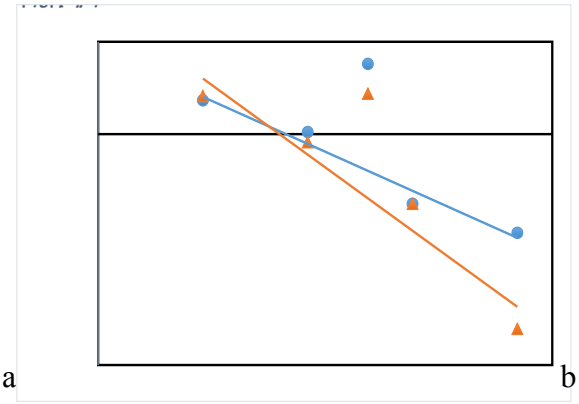

a

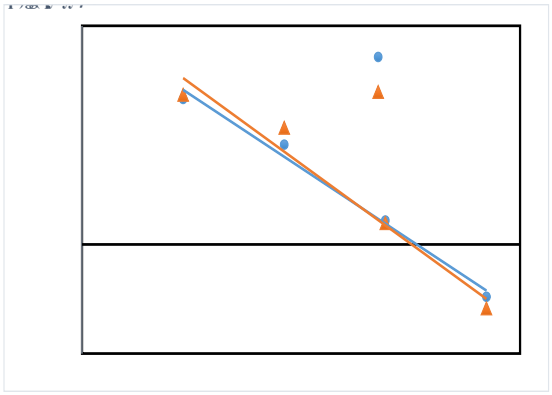

b

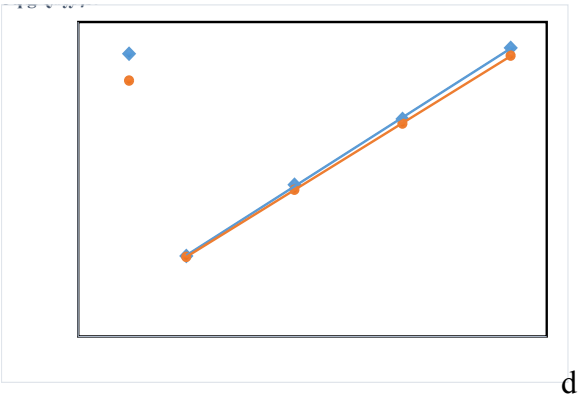

c

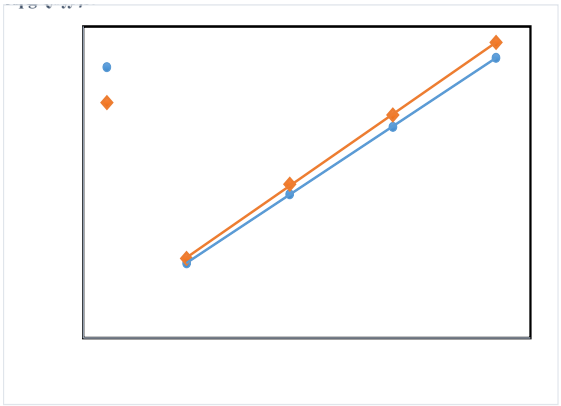

d

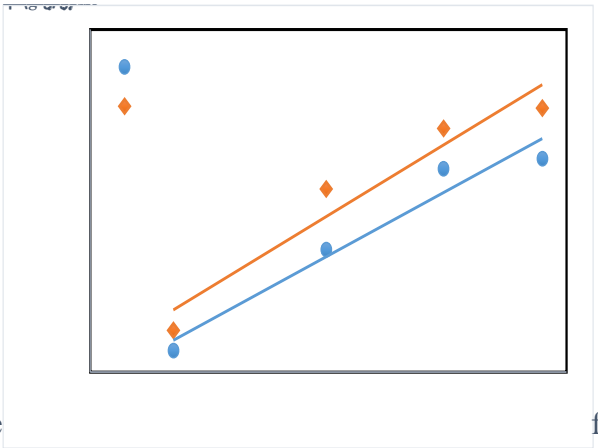

e

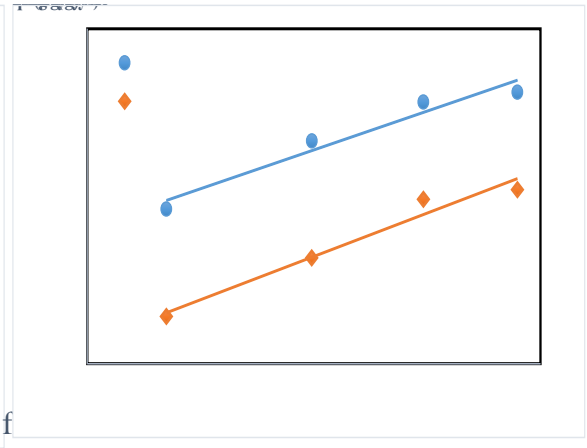

f

Figure 5.6: Linear plots for (a, b) pseudo first order (c, d) pseudo second order (e, f) intraparticle diffusion models for adsorption kinetics of fluoride and arsenic in a single and binary systems, respectively.

5.3.4 Suggested simultaneous removal mechanisms of fluoride and arsenic by Al-Fe electrocoagulation.

The analyses of the floc samples, and adsorption isotherm and kinetic models reveal that the simultaneous removal mechanisms of fluoride and arsenic proceeded in different ways (Figure 5.7). The aluminum coagulant phases are involved on the adsorption of both fluoride and arsenic through ionic exchange by replacing the OH^- of the $Al(OH)_3$ to form aluminum fluoro hydroxide and hydrated aluminum arseno hydroxide ($AlAsO_4 \bullet 2(H_2O)$) route 3 and 1 in Figure 7. On the other hand, the iron phase coagulant are found to adsorb arsenic through electrostatic attraction by deprotonating FeOOH to form FeOOAs as shown in route 2 in Figure 5.7.

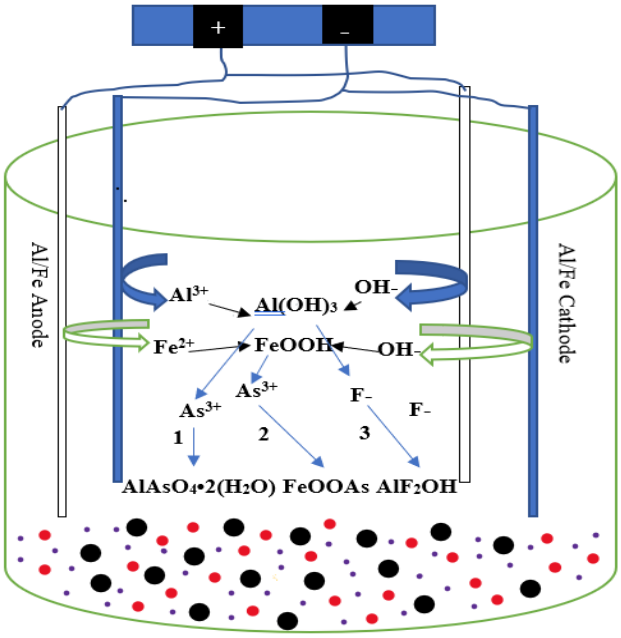

Figure 5.7: Schematic illustration of the fluoride and arsenic removal mechanisms by the hybrid Al-Fe electrocoagulation

5.4 Conclusion

In the laboratory scale experiments, the equilibrium data for the removal of As and F ions showed that the uptake of the ions from single component followed Freundlich and Langmuir isotherm models. Fluoride achieved the maximum monolayer adsorption capacity of 76.4 mg/g and arsenic 1.14 mg/g at condition of 9.9 $mAcm^{-2}$ and pH 7.5 in 50 minutes. Adsorption of both fluoride and arsenic were physical in nature and spontenous with arsenic demonstrating a stronger affinity constant (K_F = 18.2 L/mg) compared to that of fluoride (K_F = 0.12 L/mg). The presence of arsenic appears to have negligible effects on the fluoride adsorption while fluoride inhibited the arsenic adsorption capacitywhich declined to 0.06 mg/g. The kinetics of adsorption processes for both single and binary mixture can be modelled using PSO while diffusion of species on the surface was controlled not only by intraparicle diffusion but also by the active sites attachment. The removal of fluoride and arsenic were through different mechanisms, fluoride was removed through ion exhange while arsenic removal was dominated by electrostatic attraction.

5.8 References

Al-ghouti, M. A., & Da, D. A. (2020). Guidelines for the use and interpretation of adsorption isotherm models : A review. Journal of Hazardous Materials, 393, 122383. https://doi.org/10.1016/j.jhazmat.2020.122383

Alarcón-Herrera, M. T., Bundschuh, J., Nath, B., Nicolli, H. B., Gutierrez, M., Reyes-Gomez, V. M., … Sracek, O. (2013). Co-occurrence of arsenic and fluoride in groundwater of semi-arid regions in Latin America: Genesis, mobility and remediation. Journal of Hazardous Materials, 262, 960–969. https://doi.org/10.1016/j.jhazmat.2012.08.005

Amani-Ghadim, A. R., Aber, S., Olad, A., & Ashassi-Sorkhabi, H. (2013). Optimization of electrocoagulation process for removal of an azo dye using response surface methodology and investigation on the occurrence of destructive side reactions. Chemical Engineering and Processing: Process Intensification. https://doi.org/10.1016/j.cep.2012.10.012

Araújo, C. S. T., Almeida, I. L. S., Rezende, H. C., Marcionilio, S. M. L. O., Léon, J. J. L., & de Matos, T. N. (2018). Elucidation of mechanism involved in adsorption of Pb (II) onto lobeira fruit (Solanum lycocarpum) using Langmuir, Freundlich and Temkin isotherms.

Microchemical Journal, 137, 348–354.

Ayawei, N., Ekubo, A. T., Wankasi, D., & Dikio, E. D. (2015). Adsorption of congo red by Ni/Al-CO3: Equilibrium, thermodynamic and kinetic studies. Oriental Journal of Chemistry, 31(3), 1307–1318.

Balasubramanian, N., Kojima, T., Basha, C. A., & Srinivasakannan, C. (2009). Removal of arsenic from aqueous solution using electrocoagulation. Journal of Hazardous Materials, 167(1–3), 966–969.

Catalano, J. G., Park, C., Fenter, P., & Zhang, Z. (2008). Simultaneous inner- and outer-sphere arsenate adsorption on corundum and hematite. Geochimica et Cosmochimica Acta, 72, 1986–2004. https://doi.org/10.1016/j.gca.2008.02.013

Chatterjee, D., Halder, D., Majumder, S., Biswas, A., Nath, B., Bhattacharya, P., … Hazra, R. (2010). Assessment of arsenic exposure from groundwater and rice in Bengal Delta Region, West Bengal, India. Water Research, 44(19), 5803–5812.

Chithra, K., & Balasubramanian, N. (2010). Modeling electrocoagulation through adsorption kinetics. Journal of Modelling and Simulation of Systems, 1(2), 124–130.

Choy, K. K. H., Porter, J. F., & Mckay, G. (2000). Langmuir Isotherm Models Applied to the Multicomponent Sorption of Acid Dyes from Effluent onto Activated Carbon. Journal of Chemical Engineering Data 575–584.

Daniel, R., & Prabhakara Rao, A. V. S. (2012). An efficient removal of arsenic from industrial effluents using electro-coagulation as clean technology option. International Journal of Environmental Research, 6(3), 711–718.

Davis, H. T., Valencourt, L. R., & Johnson, C. E. (1975). Transport processes in composite media. Journal of the American Ceramic Society, 58(9 10), 446–452.

Davoudinejad, M., & Ghorbanian, S. A. (2013). Modeling of adsorption isotherm of benzoic compounds onto GAC and introducing three new isotherm models using new concept of Adsorption Effective Surface (AES). Sci Res Essays, 8(46), 2263–2275.

Duan, Q., Jiao, J., Chen, X., & Wang, X. (2018). Association between water fluoride and the level of children's intelligence: a dose–response meta-analysis. Public Health, 154, 87–97.

Elwakeel, K. Z., Atia, A. A., & Guibal, E. (2014). Fast removal of uranium from aqueous solutions using tetraethylenepentamine modified magnetic chitosan resin. Bioresource Technology, 160, 107–114.

Federation, W. E., & Association, A. P. H. (2005). Standard methods for the examination of water and wastewater. American Public Health Association (APHA): Washington, DC, USA.

Girish, C. R. (2018). Multicomponent adsorption and the Interaction between the adsorbent And the adsorbate: A review. Interaction, 14, 15.

Gomes, J. A. G., Daida, P., Kesmez, M., Weir, M., Moreno, H., Parga, J. R., … Peterson, E. (2007). Arsenic removal by electrocoagulation using combined Al–Fe electrode system and characterization of products. Journal of Hazardous Materials, 139(2), 220–231.

Hamdaoui, O., & Naffrechoux, E. (2007). Modeling of adsorption isotherms of phenol and chlorophenols onto granular activated carbon: Part I. Two-parameter models and equations allowing determination of thermodynamic parameters. Journal of Hazardous Materials, 147(1–2), 381–394.

Hashim, K. S., Shaw, A., Al Khaddar, R., Pedrola, M. O., & Phipps, D. (2017). Iron removal, energy consumption and operating cost of electrocoagulation of drinking water using a new flow column reactor. Journal of Environmental Management, 189, 98–108.

Ho, Y.-S., & McKay, G. (2000). The kinetics of sorption of divalent metal ions onto sphagnum moss peat. Water Research, 34(3), 735–742.

Holt, P. K., Barton, G. W., Wark, M., & Mitchell, C. A. (2002). A quantitative comparison between chemical dosing and electrocoagulation. Colloids and Surfaces A: Physicochemical and Engineering Aspects, 211(2–3), 233–248.

Khader, Y., & Mckay, G. (1992). Prediction of Binary Component Isotherms for Adsorption on

Heterogeneous Surfaces. Journal of Chemical Technology Biotechnology, 345–352.

Khair, A. M., Li, C., Hu, Q., Gao, X., & Wanga, Y. (2014). Fluoride and Arsenic Hydrogeochemistry of Groundwater at Yuncheng Basin , Northern China Geochemistry International, 52(10), 868–881. https://doi.org/10.1134/S0016702914100024

Khatibikamal, V., Torabian, A., Janpoor, F., & Hoshyaripour, G. (2010). Fluoride removal from industrial wastewater using electrocoagulation and its adsorption kinetics. Journal of Hazardous Materials, 179(1–3), 276–280. https://doi.org/10.1016/j.jhazmat.2010.02.089

Kobya, M., Ulu, F., Gebologlu, U., Demirbas, E., & Oncel, M. S. (2011). Treatment of potable water containing low concentration of arsenic with electrocoagulation: Different connection modes and Fe–Al electrodes. Separation and Purification Technology, 77(3), 283–293.

Lagergren, S. K. (1898). About the theory of so-called adsorption of soluble substances. Sven. Vetenskapsakad. Handingarl, 24, 1–39.

Larous, S., & Meniai, A. H. (2012). Removal of copper (II) from aqueous solution by agricultural by-products-sawdust. Energy Procedia, 18, 915–923.

Lattanzi, A. M., Pecha, M. B., Bharadwaj, V. S., & Ciesielski, P. N. (2020). Beyond the effectiveness factor: Multi-step reactions with intraparticle diffusion limitations. Chemical Engineering Journal, 380, 122507.

Liu, S. (2015). Cooperative adsorption on solid surfaces. Journal of Colloid and Interface Science, 450, 224–238.

Mameri, N., Yeddou, A. R., Lounici, H., Belhocine, D., Grib, H., & Bariou, B. (1998). Defluoridation of septentrional sahara water of north africa by electrocoagulation. Water Research, 32(5), 1604–1612.

Namasivayam, C., & Yamuna, R. T. (1995). Waste biogas residual slurry as an adsorbent for the removal of Pb (II) from aqueous solution and radiator manufacturing industry wastewater. Bioresource Technology, 52(2), 125–131.

Nyangi, M. J., Chebude, Y., Kilulya, K. F., & Andrew, M. (2020). Simultaneous removal of

fluoride and arsenic from water by hybrid Al-Fe electrocoagulation : process optimization through surface response method. Separation Science and Technology, 00(00), 1–11. https://doi.org/10.1080/01496395.2020.1837877

Padilla-Ortega, E., Leyva-Ramos, R., & Flores-Cano, J. V. (2013). Binary adsorption of heavy metals from aqueous solution onto natural clays. Chemical Engineering Journal, 225, 535–546.

Pérez-Marín, A. B., Zapata, V. M., Ortuno, J. F., Aguilar, M., Sáez, J., & Lloréns, M. (2007). Removal of cadmium from aqueous solutions by adsorption onto orange waste. Journal of Hazardous Materials, 139(1), 122–131.

Plazinski, W., & Rudzinski, W. (2009). Kinetics of adsorption at solid/solution interfaces controlled by intraparticle diffusion: a theoretical analysis. The Journal of Physical Chemistry C, 113(28), 12495–12501.

Sampranpiboon, P., Charnkeitkong, P., & Feng, X. (2014). Equilibrium isotherm models for adsorption of zinc (II) ion from aqueous solution on pulp waste. WSEAS Transactions on Environment and Development, 10, 35–47.

Shen, F., Chen, X., Gao, P., & Chen, G. (2003). Electrochemical removal of fluoride ions from industrial wastewater. Chemical Engineering Science, 58(3–6), 987–993.

Sivarajasekar, N., & Baskar, R. (2019). Adsorption of Basic Magenta II onto H2SO4 activated immature Gossypium hirsutum seeds: Kinetics, isotherms, mass transfer, thermodynamics and process design. Arabian Journal of Chemistry, 12(7), 1322–1337.

Tian, Y., Wu, M., Liu, R., Wang, D., Lin, X., Liu, W., … Huang, Y. (2011). Modified native cellulose fibers—A novel efficient adsorbent for both fluoride and arsenic. Journal of Hazardous Materials, 185(1), 93–100.

Varank, G., Demir, A., Yetilmezsoy, K., Top, S., Sekman, E., & Bilgili, M. S. (2012). Removal of 4-nitrophenol from aqueous solution by natural low-cost adsorbents Removal of 4-nitrophenol from aqueous solution by natural low-cost adsorbents. Indian Journal of

Chemical Technology, 19, 7-25

Vasudevan, S., Lakshmi, J., & Sozhan, G. (2009). Studies on a Mg-Al-Zn alloy as an anode for the removal of fluoride from drinking water in an electrocoagulation process. Clean - Soil, Air, Water. https://doi.org/10.1002/clen.200900031

Veneranda, M., Aramendia, J., Bellot-gurlet, L., Castro, K., Madariaga, J. M., Veneranda, M., … Castro, K. (2018). FTIR spectroscopic semi-quantification of iron phases : A new method to evaluate the protection ability index (PAI) of archaeological artefacts corrosion systems To cite this version : HAL Id : hal-01734761 evaluate the protection ability index (PAI) of archaeological artefacts. Corrosion Science, 133, 68–77. https://doi.org/10.1016/j.corsci.2018.01.016

Wang, J., & Guo, X. (2020). Adsorption kinetic models: Physical meanings, applications, and solving methods. Journal of Hazardous Materials, 122156. https://doi.org/10.1016/j.jhazmat.2020.122156.

Wang, S.-X., Wang, Z.-H., Cheng, X.-T., Li, J., Sang, Z.-P., Zhang, X.-D., … Wang, Z.-Q. (2007). Arsenic and fluoride exposure in drinking water: children's IQ and growth in Shanyin county, Shanxi province, China. Environmental Health Perspectives, 115(4), 643–647.

Wu, Y., Wen, Y., Zhou, J., Cao, J., Jin, Y., & Wu, Y. (2013). Comparative and competitive adsorption of Cr (VI), As (III), and Ni (II) onto coconut charcoal. Environmental Science and Pollution Research, 20(4), 2210–2219.

Zhou, X., & Zhou, X. I. N. (2014). The Unit Problem in the Thermodynamic Calculation of Adsorption Using the Langmuir Equation. Chemical Engineering Communications 201(11), 1459–1467.

Zhu, J., Zhao, H., & Ni, J. (2007). Fluoride distribution in electrocoagulation defluoridation process. Separation and Purification Technology. https://doi.org/10.1016/j.seppur.2007.01.030

CHAPTER SIX

Conclusions and Recommendations

Conclusion

In the East Africa Rift Valley zone, groundwater is the most important source for community water supply, mainly in rural areas. However, one of the main challenges associated with its utilization is elevated levels of fluoride and arsenic. In these areas, people use bone char and Nalgonda for defluoridation while there is no notable technology for arsenic removal. The methods appear to have shortcomings, due to rejection by some local users due to cultural beliefs. This research work focused on investigating an alternative cost-effective method for remediation of fluoride and/or arsenic from groundwater. The study reports on the efficiency of the optimized operation condition of the hybrid Al-Fe electrocoagulation. The findings of the study can be concluded as follows in alignment with the specific objectives:

- This research demonstrated that both Al and Fe electrodes in electrocoagulation can effectively remove fluoride from groundwater. Al-EC attained higher fluoride removal of 94% compared to the Fe-EC that achieved 92% removal of initial 16 mg/L of fluoride in 50 minutes. As revealed in this report aluminum electrode required higher current density (J) = 18.5 $mAcm^{-2}$ at pH 6.8 for effective dissolution than iron electrode that required J = 6.25 $mAcm^{-2}$ at pH 6.5, however, both electrodes achieved the same amount of coagulant of 0.063 mg/L.
- Moreover, the FTIR and XRD data, revealed that removal of fluoride by Al-EC and Fe-EC occurred through different mechanisms. Fluoride was removed through ionic exchange by replacing hydroxide of $Al(OH)_3$ in Al-EC, while fluoride was adsorbed on the surface of $Fe(OH)_2$ in Fe-EC. It can be ascertained that both electrodes Al and Fe followed Freundlich adsorption model suggesting that the removal of fluoride was through formation of multiple

layers on the surface of $Al(OH)_3$ and $Fe(OH)_2$. The kinetic data fitted well with pseudo second order and that Intraparticle diffusion was not the sole step in the diffusion rate of fluoride through the pores of adsorbents in both cases. Meanwhile, the Al-EC and Fe-EC are found to have adsorption affinity of 981 and 573 L/mg and monolayer adsorption capacity of 131 and 0.08 mg/g, respectively making Al-EC a better choice for defluoridation despite the fact that both attained reduction of fluoride to a permissible WHO standard for drinking purpose (≤ 1.5 mg/L) at optimized operational parameters.

- This research work also revealed that the combination of aluminum and iron electrodes in electrocoagulation, can effectively reduce fluoride and arsenic simultaneously from the water. Under optimized conditions of current density of 9.90 $mAcm^{-2}$, pH 7.5, reaction time of 50 minutes and initial concentration of arsenic 200 µg/L and that of fluoride 16 mg/L, the Al-Fe EC achieved 93% and 95% reduction of fluoride and arsenic, respectively in a reactor of surface area to volume ratio of 0.13 cm^{-1}. Meanwhile, the hybrid Al-Fe EC afforded treatment of groundwater collected from Arusha, Tanzania by reducing initial fluoride concentration of 13.45 mg/L to 1.4 mg/L. The technology also managed to reduce concurrent F (7.6 mg/L) and As (220 µg/L) of the groundwater from Ziway, Ethiopia to 0.7 mg/L and 4.4 µg/L of fluoride and arsenic, respectively satisfying WHO recommended for drinking water for both fluoride and arsenic.
- One of the shortfalls of Nalgonda and bone char which are currently used for defluoridation is the production of high volume of sludge that become difficult for their disposal and may result to secondary hazards to the environment. For example, it may require 800 mg of chemicals for treatment of 10 mg/L of fluoride by Nalgonda technology, which correspond to 80 mg of alum per unit mass of fluoride treated. This study has found that, the application of hybrid Al-Fe EC can produce a minimal amount of sludge of only 27 mg and 2.15 mg of sludge per mass unit of fluoride and arsenic treated, respectively.
- Cost wise the optimized operation parameter of the hybrid Al-Fe EC afforded to treat the water at a cost of 0.99 USD/m^3.
- The effects of co-existing ions on the performance of Al-Fe EC on the other hand, are found to depend on the type and concentration of individual ion except that of carbonates which

had no influence on the removal of fluoride and arsenic. The calcium ion is found to synergize the removal of fluoride possibly by increasing positive surface charge of the Al-Fe oxyhydroxide while at higher concentration > 75 mg/L it has negative effect on the arsenic removal. Sulphate and nitrate on the other hand, tend to reduce the efficiency of Al-Fe EC on arsenic removal which is attributed to the formation of a passive film layer on the anode electrode and reducing corrosion of anode. The effect of magnesium on the removal of both fluoride and arsenic depends on the concentration levels, where it reduces removal efficiency when at higher concentration (>75 mg/L). Generally, in the presence of all co-existing ions the effect is negligible and the removal efficiency is found to be similar as in the absence of co-ions.

- Moreover, this study found that Al-Fe EC achieved the maximum monolayer adsorption capacity of 76.36 mg/g and 1.14 mg/g on fluoride and arsenic, respectively. The adsorption of both fluoride and arsenic were spontaneous and physical in nature with arsenic demonstrated stronger adsorption affinity constant to Al-Fe oxyhydroxide (K_F = 18.18 L/mg) compared to that of fluoride (K_F = 0.12 L/mg). The individual As and F removal obeyed Langmuir adsorption model while in a binary component both extended Langmuir and extended Freundlich can well describe adsorption processes. Moreover, the pseudo second order fitted well to the experimental data of the simultaneous F and As removal. The removal of fluoride and arsenic were through different mechanisms, fluoride was removed through the ion exchange while arsenic removal was dominated by electrostatic attraction which means that the simultaneous removal of arsenic and fluoride can be achieved with less competition for the adsorption sites.
- Despite successful data collection to achieve the objectives of this research, the study encountered some limitations, such as lack of instruments to characterize flocs for surface area and funds to collect different real groundwater samples for hybrid Al-Fe EC technology performance testing.

Recommendations

This study has provided insights of the optimized hybrid Al-Fe electrocoagulation technology for the removal of fluoride and arsenic from groundwater. It also reported the removal mechanisms

associated with the two pollutants as well as the influence of co-existing ions on the performance of the technology.

- ✓ This study indicated the feasibility of the hybrid Al-Fe EC technology for the remediation of fluoride and/or arsenic in a laboratory scale setup. However, for the application of the technology, it's important to scale up the reactor. I recommend that the scale up be done stepwise by starting with a household levels using a bucket of 10 or 20 L as a reactor size. Upon success, the test can be advanced to a larger reactor mainly for small community utilization.
- ✓ This study has provided statistical model equations that allow application of the hybrid Al-Fe EC for treatment of water containing different initial concentration of fluoride (2-30 mg/L) and/or arsenic (15-250 μg/L). Therefore, I recommend that by the use of model equations stipulated herein (Chapter 3, equations 3.5 and 3.6), various sets of optimum operation conditions can be obtained and evaluated for the treatment of different water sources contaminated by fluoride and/or arsenic.
- ✓ The co-existing ions when present together are found to have negligible effects on the performance of Al-Fe EC towards fluoride and arsenic removal. However, further investigation is required to evaluate the removal capability of the hybrid Al-Fe EC technology on various groundwater sources.
- ✓ The cost estimated for the treatment of fluoride and arsenic at the optimized operation parameter of the hybrid Al-Fe EC by this study is 0.99 USD/m^3. This seems to be relatively high and may face competition from other available technologies. However, by the use of statistical model equations developed and shown on page 88, other optimum conditions mainly by adjusting the current density and treatment time that could afford lower treatment cost can be obtained and tested in future studies.
- ✓ This study found that carbonates have no effect on the performance of hybrid Al-Fe EC technology for fluoride and arsenic removal. However, the carbonate range used was lower (100 mg/L) compared to that found in many groundwater sources in the East Africa Rift Valley. Moreover, the study didn't investigate the effects of phosphates on the performance of the technology. Therefore, further investigation using relatively higher

levels of carbonates > 100 mg/L and how phosphates might influence the performance can be done in future studies.